Spring 2013

A generalized approach for compliant mechanism design using the synthesis with compliance method, with experimental validation

Ashish B. Koli

Department:

A GENERALIZED APPROACH FOR COMPLIANT MECHANISM DESIGN USING THE SYNTHESIS WITH COMPLIANCE METHOD, WITH EXPERIMENTAL VALIDATION

by

ASHISH BHARAT KOLI

A THESIS

Presented to the Faculty of the Graduate School of the

MISSOURI UNIVERSITY OF SCIENCE AND TECHNOLOGY

In Partial Fulfillment of the Requirements for the Degree

MASTER OF SCIENCE IN MECHANICAL ENGINEERING

2013

Approved by

Dr. Ashok Midha, Advisor
Dr. K. Chandrashekhara
Dr. Xiaoping Du

ABSTRACT

Compliant mechanisms offer numerous advantages over their rigid-body counterparts. The synthesis with compliance technique synthesizes compliant mechanisms for conventional rigid-body synthesis tasks with energy/torque specifications at precision positions. In spite of its usefulness, the method suffers from some limitations/problems. The purpose of this work is to investigate these sensitivities with the synthesis with compliance technique and improve upon existing method. A new, simple but efficient, method for synthesis with compliance using an optimization approach is proposed, and its usefulness and simplicity demonstrated over the existing method. The strongly and weakly coupled system of kinematic and energy/torque equations in the existing method has been studied, and the new method is made simple by removing the strong coupling between these sets of equations. All synthesis cases are solved by treating them as though they are governed by weakly coupled systems of equations.

Representative examples of different synthesis tasks are presented. The results are verified with finite element analysis software ABAQUS® and ANSYS® by means of coupler curve/precision position comparisons, and stored energy comparisons. An experimental setup has been devised to perform experiments on compliant mechanisms for validation purposes. The results obtained using the Pseudo-Rigid-Body Model (PRBM) for compliant mechanism synthesis match closely with experimental and finite element analysis (FEA) results, and hence reinforce the utility of the synthesis with compliance method using the PRBM in compliant mechanism synthesis.

ACKNOWLEDGMENTS

I would like to express my gratitude to my advisor Dr. Ashok Midha for his guidance, and never ending support both academically and financially during last two years. His optimism and enthusiasm for the research were a constant source of encouragement to me, without which this work would not have been accomplished.

I would also like to thank Dr. K. Chandrashekhara and Dr. Xiaoping Du for their valuable time and effort as members of my thesis committee. I offer special thanks to Dr. Ashok Midha and Dr. K. Chandrashekhara for all that I have learned from them in and out of classes.

Additionally, I would like to thank the Department of Mechanical and Aerospace Engineering at Missouri S&T for providing me with financial support in the form of Graduate Teaching Assistantships. I express my sincere thanks to my friends and research associates Sushrut Bapat, Raghvendra Kuber, Vivekanada Chinta for their support, critique, encouraging thoughts and discussions.

Finally, I would like to thank my parents Mr. Bharat Koli, Mrs. Khashabai Koli, and my sister Mrs. Ashwini Patil, for their never ending support and love, and God Almighty for guiding me throughout my life.

TABLE OF CONTENTS

Page

LIST OF ILLUSTRATIONS

Page

LIST OF TABLES

Page

1. INTRODUCTION

The compliant mechanisms are functionally similar to the rigid-body mechanisms but they gain some or all of their mobility from the deflection of flexible members rather than from movable joints only (Howell 2001).

1.1. DEFINITION

A kinematic mechanism is a mechanical device used to transfer or transform motion, force, or energy (Erdman et al., 1997). The rigid-body mechanisms consist of rigid links joined together by joints or kinematic pairs and they gain their mobility from the movable joints only. A four-bar mechanism is a very well-known example of a rigid-body mechanism. Figure 1.1 shows a crank-rocker mechanism.

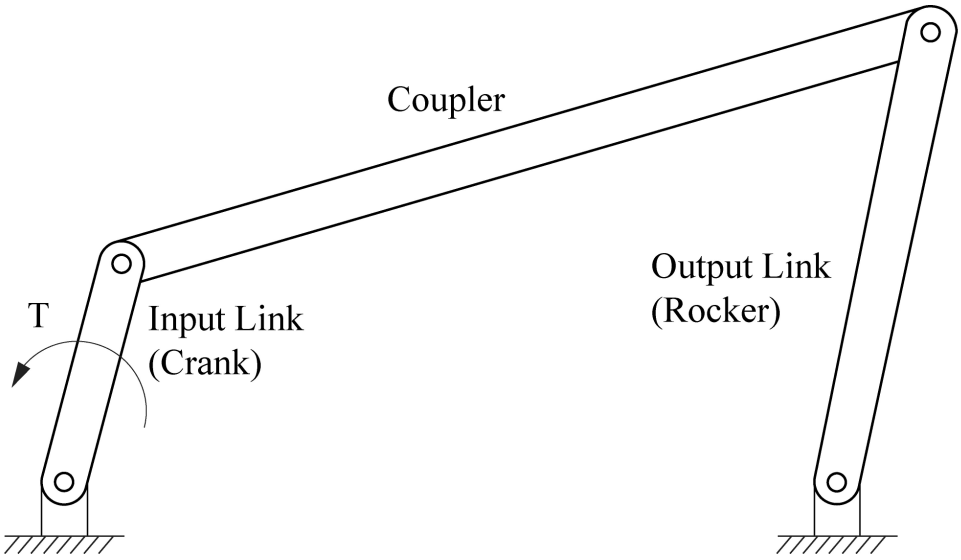

Figure 1.1. A Rigid-Body Four-Bar (Crank-Rocker) Mechanism

It is an inversion of a four-bar mechanism, generally with an input torque T applied at the crank which rotates through 360^0 and serves to oscillate the rocker link. An example of a compliant crimping mechanism developed by AMP Inc. (Her, 1986) is shown in Figure 1.2 with its rigid-body counterpart design. Only one-half of the mechanism is shown because of its symmetry.

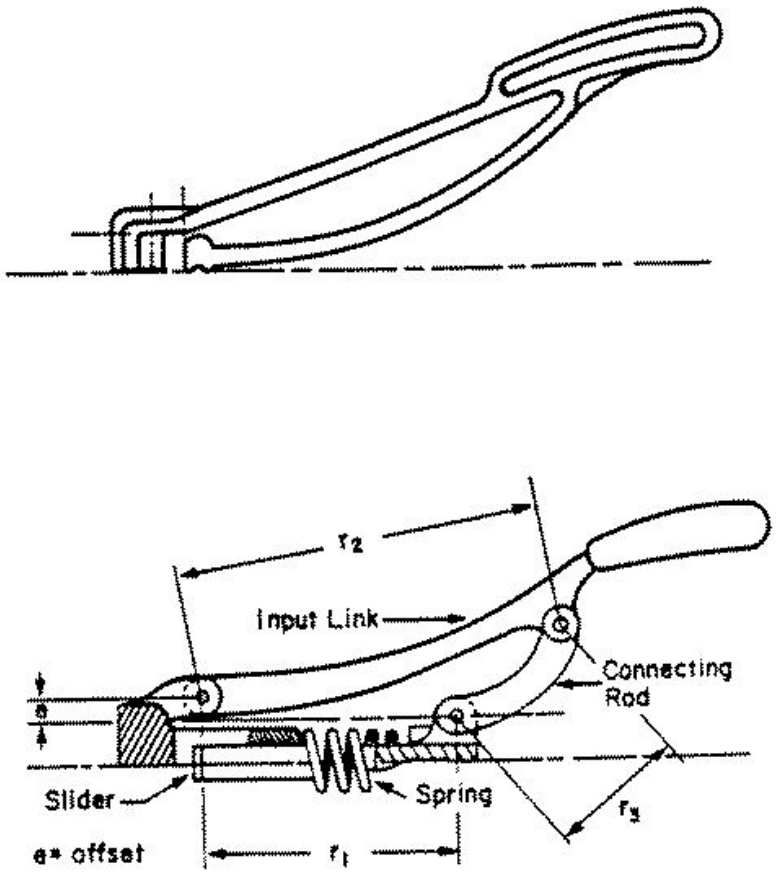

Figure 1.2. A Compliant Crimping Mechanism with its Rigid-Body Counterparts (Her, 1986)

A pseudo-rigid-body model concept (Howell and Midha, 1994) provides a simple way to use the vast rigid-body mechanism knowledge base available to synthesize and analyze compliant mechanisms. It models the large deflections of the flexible segments, reducing them to their rigid-body kinematic counterparts and torsional springs to represent their compliance, their equivalence being maintained in their force-deflection characteristics. The compliant mechanisms can be fully compliant consisting of no rigid links or joints, or can be partially compliant with flexible segments and rigid links and joints. The compliant mechanisms have numerous advantages (Howell, 2001) as follows:

1. The compliant mechanisms may contain fewer parts, or can be manufactured/molded as one-piece resulting in cost reduction due to reduced assembly time, simplified manufacturing processes, and general integration of form and function.
2. With less number of parts, the compliant mechanisms are relatively lighter as compared with rigid-body mechanisms.
3. The compliant mechanisms have fewer movable joints.
    i) This results in reduced wear and reduced need for lubrication
    ii) Lacking lash, it reduces the noise and vibration
4. Less number of joints also helps increase the mechanical precision, making them useful in high-precision instruments.
5. As the compliant mechanisms achieve some of their mobility from the deflection of their flexible members, the stored strain energy may be transferred, transformed or released at a later time in a different manner. They can be used to design mechanisms having specific force-deflection properties, e.g. compliant

constant-force mechanism, which generates a nearly constant output force in response to, say, a linear input displacement.

6. The compliant mechanisms can be easily miniaturized and so they may result in space savings and find useful applications in MEMS devices.

The compliant mechanisms also have few disadvantages, as follows:

1. Due to the large deflections of flexible links, the design and analysis of compliant mechanisms is more difficult than that of rigid-body mechanisms.
2. Fatigue analysis is important in the design of compliant mechanisms, and the choice of material is critical to attain a required fatigue life. The large deflection of a flexible member is limited by its geometric and material properties. The compliant segmentscannot produce continuous rotational motion, as does a rigid-body crank.
3. Flexible segments under stress for long periods of time, or at high temperatures, may experience stress relaxation or creep and may be rendered ineffective in their function.

In spite of the above disadvantages, compliant mechanisms are continuing to findimportant applications (Howell, 2001) in the engineering world and society at large, such as micro-sensors and actuators in micro-electro-mechanical (MEMS) devices, crashworthiness applications in automobiles due to the energy storage characteristics, precision machines, robotics, biomedical devices and prosthetics, surgical tools, adaptive structures, etc. Compliant mechanisms are also widely used in items such as grippers, Compliers®, bicycle brakes, binder clips, staple removers, etc.

1.2. HISTORICAL DEVELOPMENT

Use of flexible members to store energy and create motion has been in use since ages, e.g. in bows and catapults (Howell, 2001). The strain energy stored in the bow is released in the form of kinetic energy of the arrow. A systematic development of compliant mechanisms started in the second half of the twentieth century. Burns (1964) and Burns and Crossley (1968) performed the kinetostatic synthesis of flexible-link mechanisms. They considered a four-bar planar linkage with a flexible coupler and took into account the geometrical behavior of the flexible link along with an applied torque. Sevak and McLarnan (1974) synthesized and analyzed flexible link mechanisms for function generation using finite element analysis and optimization techniques, in particular, Fletcher and Powell's variable metric method. Shoup and Mclarnan (1971) and Shoup (1972) used elliptic integrals to arrive at first approximations of the parameters including forces, elastic properties, dimensions, etc. occurring in the equations of the undulating and nodal elastic describing the static behavior of an end-loaded flexible strip. These first approximations are useful in obtaining iterative solutions of equations for force or motion analysis of flexible-link mechanisms containing members that undergo large elastic deflections. Winter and Shoup (1972) performed displacement analysis of path-generating flexible-link mechanisms using elliptic integrals and obtained their coupler curves.

Bishop and Drucker (1945) obtained a solution for the large-deflection of a cantilever beam using elliptic integrals. Elliptic integrals were used for more complex geometries and loading conditions in later works (e.g. Frish-Fay 1962; Mattiason, 1981; and Zhang, 2012). Numerical techniques like chain algorithm may be found in earlier

works by Harrison (1973) and Miller (1980). The beam is discretized into smaller beam elements and each segment is analyzed in succession. Thus, the small displacements of each element are combined through chain calculation to obtain the large deflection of entire beam. Miller (1980) used the shooting method along with a Newton-type iteration to obtain improved estimates. Her (1986) and Midha et al. (1992) extended the chain algorithm idea with critical improvements, developing a more accurate chain calculation algorithm for use in large deflection, compliant mechanism analysis. A graphical, user-driven Newton-Raphson technique which allows accurate solutions of loads in large deflection problems is presented by Hill (1990). A line search technique is also included to enhance the stability of this numerical method.

Her (1986) and Her and Midha (1987) developed appropriate terminology for the compliant mechanisms, and identified their kinematic properties. The concept of compliance number is also introduced which helps in evaluating the degrees of freedom of compliant mechanisms. Howell (1993) and Howell and Midha (1994) developed a method for designing compliant mechanisms using small-length flexural pivots. Howell (1991), and Howell and Midha (1995) proposed the pseudo-rigid-body concept for initially straight cantilevered flexible segments, subjected to end force or moment loading. Pauly (2002) presented an improved values of pseudo-rigid-body model parameters for compliant beams with nearly axial, tensile end force loads. Dado (2000) presented a variable parametric pseudo-rigid-body model for large-deflection beams with end loads. Norton (1991), Midha et al. (1992a), Midha et al. (1992b) and Midha et al. (1994) outlined the nomenclature and classification of the compliant mechanisms. Norton (1991), Norton et al. (1991),(1993), and Midha et al (2000) used pseudo-rigid-

body model concepts to study kinematic mobility of the compliant mechanisms and to specify the limit positions of compliant mechanisms. Mettlach and Midha (1999) outlined the concept of characteristic deflection domain in compliant mechanism design and analysis. Murphy (1993) used type synthesis technique in compliant mechanisms and represented compliant mechanisms by matrix representation based on kinematics and on compliant segment types and connectivity between the segments.

Howell (1993) used kinematic loop-closure equations along with energy/torque considerations to account for the energy storage in compliant mechanisms to synthesize the compliant mechanisms for specified energy/ torques at precision positions. Mettlach and Midha (1995), (1996) presented graphical techniques and used Burmester theory to synthesize compliant mechanisms for more number of precision positions. Dado (2005) developed a variable parametric pseudo-rigid-body model for limit position synthesis of complaint four-bar mechanism with energy specifications. Annamalai (2003), Midha et al. (2004) used the pseudo-rigid-body model concept to synthesize the compliant four-bar mechanism with energy and torque specifications. Kolachalam (2003), Midha et al. (2011) synthesized the compliant single strip mechanisms for energy, torque and force specifications. Saggere and Kota (2001), synthesized the four-bar mechanism with compliant coupler which requires prescribed shape change along with rigid-body motion for motion generation. Tari and Su (2011) presented a complex solution framework by polynomial approximations of nonlinear the kinematic and energy equations for kinetostatic synthesis of compliant mechanism. Midha et al. (2012) developed a technique using pseudo-rigid-body-model to analyze fixed-guided compliant beam with an inflection point.

1.3. SCOPE OF INVESTIGATION

The objectives of this work are: a) To investigate the sensitivities of the synthesis with compliance technique, and to improve upon the existing method of compliant mechanism synthesis by overcoming the limitations/problems, associated with it. b) Study the effects of strongly coupling and weakly coupling of kinematic and energy/torque equations on the solutions. c) Validate the results obtained from synthesis with compliance technique using pseudo-rigid-body model with commercial FEA software and with the experimental results.

Section 2 reviews three precision positions synthesis of a rigid-body four-bar mechanism, introduces the pseudo-rigid-body model concept and presents the PRBMs for different types of compliant segments in which a compliant segment is represented as combination of rigid-body links joined at pivot points with torsional springs. The synthesis techniques for compliant mechanisms using pseudo-rigid-body model concept are briefly discussed. Section 3 discusses the synthesis with compliance technique applied to generalized synthesis of compliant mechanism with energy/torque specifications. This Section also outlines the limitations/problems associated with the existing method and introduces the use of optimization in synthesis with compliance method.

Section 4 begins with review of optimization concept, and explains the optimization design process, types of optimization. A new method using optimization for solving energy/torque equations is explained. The design tables outlining the number of equations, number of unknowns and number of free choices for different synthesis types and precision positions with different number of torsional springs are presented. The

different cases of synthesis based on energy/torque specifications at the precision positions, different types of compliant segments using type synthesis etc. are given with appropriate examples. This Section also includes a discussion on the energy equivalence between a compliant mechanism and corresponding pseudo-rigid-body model. The results obtained are compared with commercial FEA software ABAQUS® and ANSYS® by means of coupler curve/precision positions comparisons and energy/torque comparisons. The proposed method is applied to synthesize a straight-line generating compliant mechanism, which can be used in a suspension system of small robotic vehicles.

Section 5 discusses the need for the experimental verification of the results and outlines the experimental setup manufactured. A compliant mechanism synthesis example is provided and the results obtained are compared with, FEA software and with experimental results. Section 6 summarizes the current research effort and outlines the recommendations for future study.

2. SYNTHESIS OF RIGID-BODY AND COMPLIANT MECHANISMS

Kinematic synthesis is a process of designing a mechanism for specified functions. Many different techniques are available for synthesis of the rigid-body mechanisms such as graphical methods, analytical methods and optimization methods. The class of the synthesis problem often decides the choice of the proper method. The rigid-body synthesis can be accomplished by considering kinematic considerations only; however to synthesize the compliant mechanisms, one has to take into account the large deflections of the flexible members that arise due to the material and geometric nonlinearities along with the kinematic considerations. A pseudo-rigid-body model (Howell and Midha, 1995) is a technique to model the flexible member, which undergo large deflections using the rigid-body members and torsional springs that reflect the equivalent force-deflection characteristics (Howell 2001). In this way, the available rigid-body synthesis techniques can be applied to synthesize and analyze the compliant mechanisms (Howell and Midha, 1996).

This Section reviews the rigid-body synthesis methods and classification of the synthesis problems. A pseudo-rigid body model concept is discussed for the different types of compliant segments. Synthesis of compliant mechanisms using PRBM is presented followed by the review of compliant mechanism synthesis methods.

2.1. RIGID-BODY FOUR-BAR MECHANISM SYNTHESIS

The two major categories in the area of synthesis (Sandor and Erdman, 1984) are type synthesis which includes finding mechanism type, number of links in the

mechanism, degrees of freedom etc. for given synthesis problem and dimensional synthesis which calculates the dimensions of the mechanisms e.g. link lengths, starting position etc. for a pre-selected mechanism type. Depending on the tasks performed, the kinematic synthesis is classified into three different types (Sandor and Erdman, 1984; Norton, 1999) function generation, path generation and motion generation. They are briefly discussed as follows:

In function generation, the input function (input link 2 position, in Figure 2.1) is correlated with the output function (output link 4 position) at the precision positions. In the path generation, the floating point on the coupler link, called as coupler point is required to traverse a prescribed path. If the position of the coupler point is correlated with the input-link positions or with time, the synthesis is called path generation with prescribed timing. In the motion generation, the position of the coupler point is correlated with the orientation of the coupler link i.e. coupler link is guided through the prescribed sequence. The synthesis methods are discussed herewith for a three precision positions synthesis of a four-bar mechanism. The precision positions are the positions prescribed for successive locations of the output (coupler or rocker) link in the plane (Norton, 1999). In the Figure 2.1, P is the precision position. The number of precision positions for which the mechanism can be synthesized is limited by the number of equations available to get the solution (Norton, 1999). A rigid-body four-bar mechanism can be easily synthesized graphically and analytically for two or three precision positions. A closed form solution for loop-closure equations is possible even for four and five precision positions four-bar synthesis problem (Erdman and Sandor, 1997; Norton, 1999). A Burmester theory is often used for four precision positions rigid-body synthesis (Howell, 2001). Many

researchers have developed solutions for the 5 to 9 precision positions synthesis problems using continuation methods also known as homotopy methods (Norton, 1999).

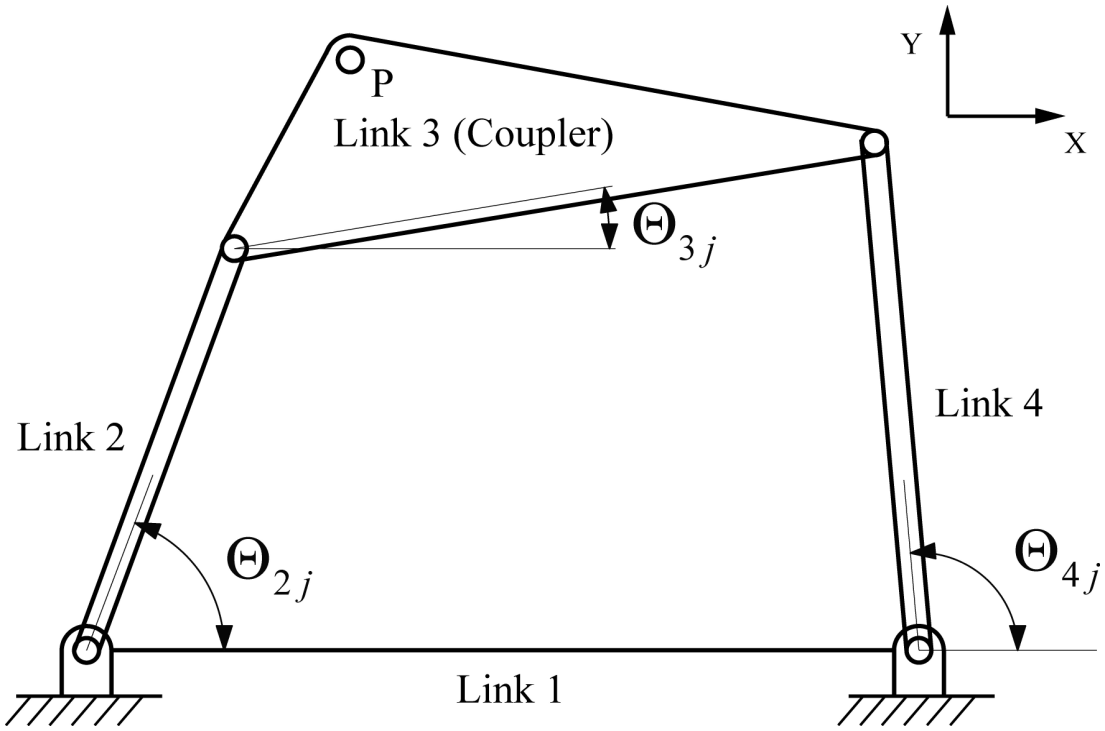

Figure 2.1. Schematic of a Rigid-Body Four-Bar Mechanism

The analytical synthesis method uses the vector dyadic approach. A pair of vectors is called a dyad (Sandor and Erdman 1984; Howell, 2001). The independent closed loops are identified in the mechanism and the loop-closure vector equations are obtained (Mallik et al., 1994). Each such vector equation will give two scalar equations. The solutions of this set of equations will synthesize the mechanism. Generally a four-bar mechanism can be represented by two dyads. The loop-closure equations can be obtained

using two dyads in initial and final position of the mechanism. The solutions to these equations will yield a four-bar mechanism dimensions.

In many cases, it may happen that, the number of equations available is less than number of unknowns to find. In such cases, a user has to make best guesses for some of the unknowns and they are known as free choices so as to solve the system of equations for remaining variables. Again analytical synthesis may yield the infinite number of solutions owing the freedom of assigning values to the free choices. It is a designer's judgment to select the best solution of all the possible solutions and it may require analysis and iterations. In the following sections, the vector loop approach is used for three precision positions rigid-body synthesis of a four-bar mechanism.

2.1.1. Function Generation. As discussed above, in function generation a mechanism is synthesized for relation between input link angle and output link angle at precision positions. In function generation (Midha et al. 1997; Annamalai, 2003) output link angle,ψ_j, is specified as a function of input link angle, ϕ_j , where j represents j^{th} position of the mechanism. The vector schematic of a four-bar mechanism for function generation for any two precision positions is shown in Figure 2.2. Z_2 is the input link and Z_4 is output link, γ_j represents the rotation of the Z_3 coupler link from its initial position to j^{th} position.

Following the loop $[Z_2 \rightarrow Z_3 \rightarrow Z_4 \rightarrow Z_{4j} \rightarrow Z_{3j} \rightarrow Z_{2j}]$ in 1^{st} and j^{th} positions of the mechanism in Figure 2.2**,** the vector loop-closure equation can be written as follows.

$$Z_2 + Z_3 - Z_4 + Z_{4j} - Z_{3j} - Z_{2j} = 0 \qquad (1)$$

where, $Z_{2j} = Z_2 e^{i\phi_j}$; $Z_{3j} = Z_3 e^{i\gamma_j}$; $Z_{4j} = Z_4 e^{i\psi_j}$

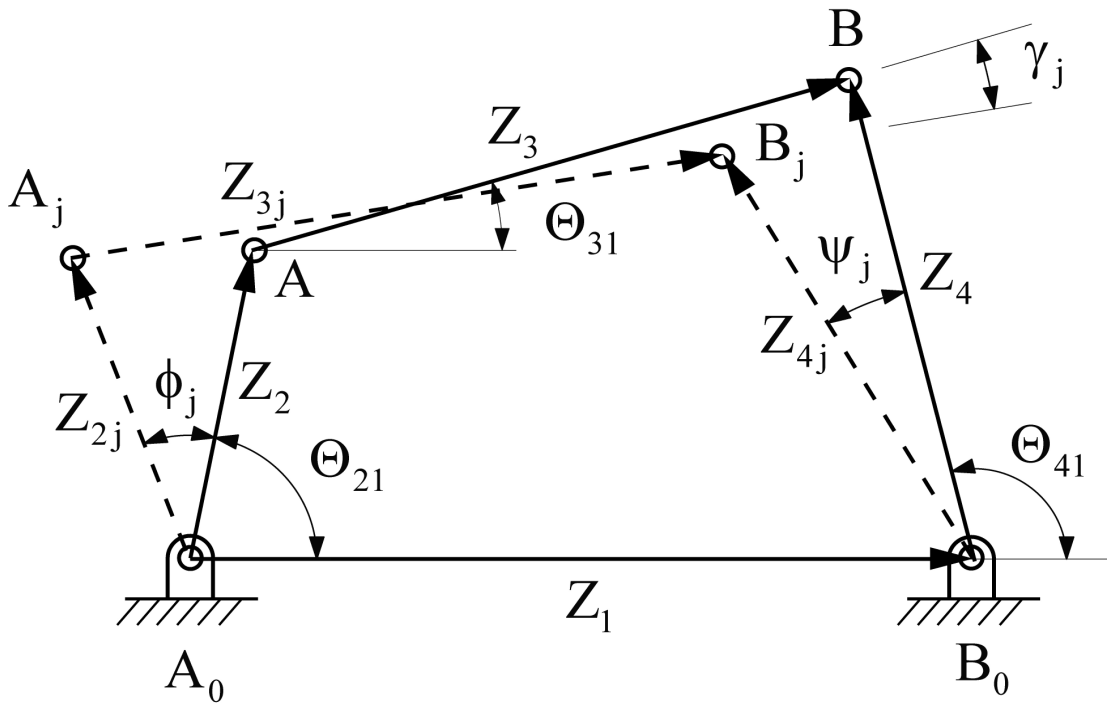

Figure 2.2. Vector Schematic of Four-Bar Mechanism in its 1st and jth Precision Positions for Function Generation

Using above relations equation (1) can be written as follows

$$Z_2\left(1 - e^{i\phi_j}\right) + Z_3\left(1 - e^{i\gamma_j}\right) + Z_4\left(e^{i\psi_j} - 1\right) = 0 \qquad (2)$$

Considering three precision positions synthesis problem the vector loop-closure equation for positions 1 and 2 can be written using equation (2) as

$$Z_2\left(1 - e^{i\phi_2}\right) + Z_3\left(1 - e^{i\gamma_2}\right) + Z_4\left(e^{i\psi_2} - 1\right) = 0 \qquad (3)$$

Similarly, for positions 1 and 3;

$$Z_2\left(1 - e^{i\phi_3}\right) + Z_3\left(1 - e^{i\gamma_3}\right) + Z_4\left(e^{i\psi_3} - 1\right) = 0 \qquad (4)$$

Vector equations (3) and (4) represents 4 scalar equations, let the vector Z_n can be represented in complex number form in its first position as

$$Z_n = R_n e^{i\Theta_{n1}} = R_n(\cos\Theta_{n1} + i\sin\Theta_{n1}) \quad (5)$$

where, R_n = length of the vector

Θ_{n1} = Angle of the n^{th} vector in its first position from right horizontal measured in counterclockwise direction

The four scalar equations are

$$R_2[\cos(\Theta_{21}) - \cos(\Theta_{21} + \phi_2)] + R_3[\cos(\Theta_{31}) - \cos(\Theta_{31} + \gamma_2)] + R_4[\cos(\Theta_{41} + \psi_2) - \cos(\Theta_{41})] = 0 \quad (6a)$$

$$R_2[\sin(\Theta_{21}) - \sin(\Theta_{21} + \phi_2)] + R_3[\sin(\Theta_{31}) - \sin(\Theta_{31} + \gamma_2)] + R_4[\sin(\Theta_{41} + \psi_2) - \sin(\Theta_{41})] = 0 \quad (6b)$$

$$R_2[\cos(\Theta_{21}) - \cos(\Theta_{21} + \phi_3)] + R_3[\cos(\Theta_{31}) - \cos(\Theta_{31} + \gamma_3)] + R_4[\cos(\Theta_{41} + \psi_3) - \cos(\Theta_{41})] = 0 \quad (6c)$$

$$R_2[\sin(\Theta_{21}) - \sin(\Theta_{21} + \phi_3)] + R_3[\sin(\Theta_{31}) - \sin(\Theta_{31} + \gamma_3)] + R_4[\sin(\Theta_{41} + \psi_3) - \sin(\Theta_{41})] = 0 \quad (6d)$$

The values of $\phi_2, \psi_2, \phi_3, \psi_3$ are given as input in the synthesis problem. The unknowns in the above four equations are

$$R_2, \Theta_{21}, R_3, \Theta_{31}, R_4, \Theta_{41}, \gamma_2, \gamma_3$$

Since, there are four nonlinear equations and eight unknowns; in order to solve this system of equations, any four variables are chosen as free choices and the remaining four variables are calculated by solving four equations.

2.1.2. Path Generation. In path generation synthesis, a coupler point is required to pass through the prescribed precision positions (Sandor and Erdman, 1984; Howell, 2001; Kolachalam, 2003). The point P_j is the coupler point of the mechanism in its j^{th} position and path vector δ_j represents the change in position of the coupler point P from

1^{st} position to j^{th} position. The vector loop-closure equations for path generation synthesis can be obtained using two dyads: the input (A_0AP_1) and output (B_0BP_1) dyads from Figure 2.3.

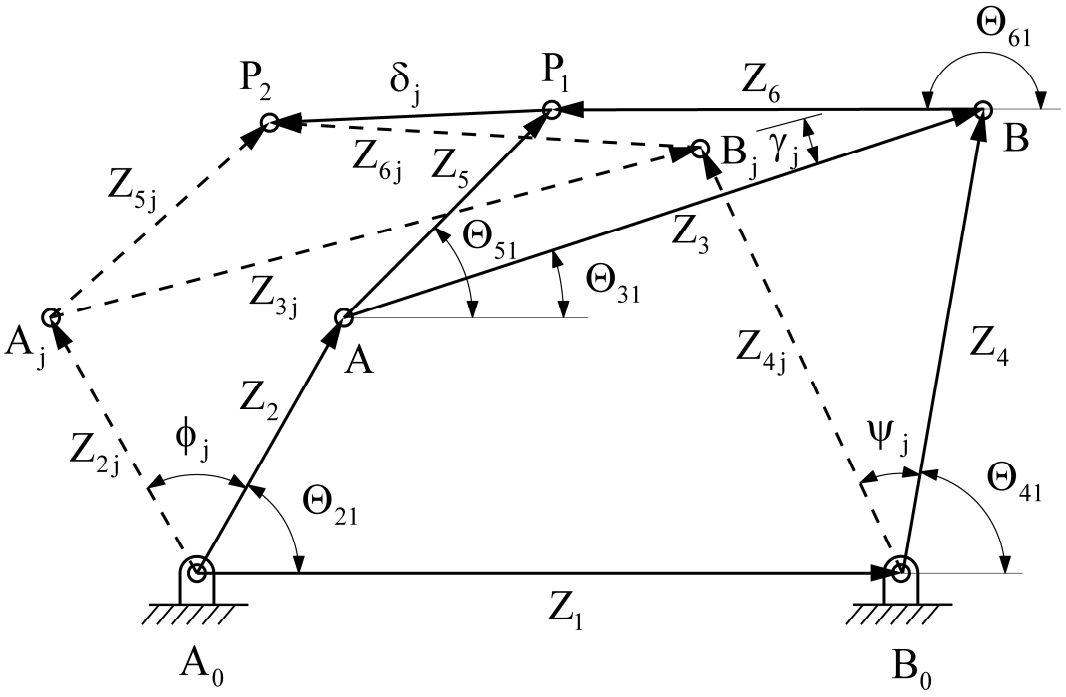

Figure 2.3. Vector Schematic of the Four-Bar Mechanism in its 1^{st} and j^{th} Precision Positions for Path, Motion Generation and Path Generation with Prescribed Timing

Vector Z_2 represents the input link, while vector Z_4 represents the output link. Angles ϕ_j ,ψ_j, γ_j are rotations of the input, output and coupler links from 1^{st} position to j^{th} position. Following the left loop $[Z_2 \rightarrow Z_5 \rightarrow \delta_j \rightarrow Z_{5j} \rightarrow Z_{2j}]$ and right loop $[Z_4 \rightarrow Z_6 \rightarrow \delta_j \rightarrow Z_{6j} \rightarrow Z_{4j}]$ from initial to j^{th} position; two vector loop-closure equations can written as follows:

$$Z_2\left(e^{i\phi_j}-1\right)+Z_5\left(e^{i\gamma_j}-1\right)=\delta_j \tag{7}$$

$$Z_4\left(e^{i\psi_j}-1\right)+Z_6\left(e^{i\gamma_j}-1\right)=\delta_j \tag{8}$$

These two vector equations will yield four scalar equations for two precision positions. For three precision position synthesis case using the equations (7) and (8), four loop-closure equations can be obtained as follows:

For positions 1 and 2;

$$Z_2\left(e^{i\phi_2}-1\right)+Z_5\left(e^{i\gamma_2}-1\right)=\delta_2 \tag{9}$$

$$Z_4\left(e^{i\psi_2}-1\right)+Z_6\left(e^{i\gamma_2}-1\right)=\delta_2 \tag{10}$$

For positions 1 and 3;

$$Z_2\left(e^{i\phi_3}-1\right)+Z_5\left(e^{i\gamma_3}-1\right)=\delta_3 \tag{11}$$

$$Z_4\left(e^{i\psi_3}-1\right)+Z_6\left(e^{i\gamma_3}-1\right)=\delta_3 \tag{12}$$

The above four vector loop-closure equations will yield eight scalar equations using equation (5) and they are as follows:

$$R_2[\cos(\Theta_{21}+\phi_2)-\cos(\Theta_{21})]+R_5[\cos(\Theta_{51}+\gamma_2)-\cos(\Theta_{51})]=\mathrm{Re}(\delta_2) \tag{13a}$$

$$R_2[\sin(\Theta_{21}+\phi_2)-\sin(\Theta_{21})]+R_5[\sin(\Theta_{51}+\gamma_2)-\sin(\Theta_{51})]=\mathrm{Im}(\delta_2) \tag{13b}$$

$$R_4[\cos(\Theta_{41}+\psi_2)-\cos(\Theta_{41})]+R_6[\cos(\Theta_{61}+\gamma_2)-\cos(\Theta_{61})]=\mathrm{Re}(\delta_2) \tag{13c}$$

$$R_4[\sin(\Theta_{41}+\psi_2)-\sin(\Theta_{41})]+R_6[\sin(\Theta_{61}+\gamma_2)-\sin(\Theta_{61})]=\mathrm{Im}(\delta_2) \tag{13d}$$

$$R_2[\cos(\Theta_{21}+\phi_3)-\cos(\Theta_{21})]+R_5[\cos(\Theta_{51}+\gamma_3)-\cos(\Theta_{51})]=\mathrm{Re}(\delta_3) \tag{13e}$$

$$R_2[\sin(\Theta_{21}+\phi_3)-\sin(\Theta_{21})]+R_5[\sin(\Theta_{51}+\gamma_3)-\sin(\Theta_{51})]=\mathrm{Im}(\delta_3) \tag{13f}$$

$$R_4[\cos(\Theta_{41}+\psi_3)-\cos(\Theta_{41})]+R_6[\cos(\Theta_{61}+\gamma_3)-\cos(\Theta_{61})]=\mathrm{Re}(\delta_3) \tag{13g}$$

$$R_4[\sin(\Theta_{41}+\psi_3)-\sin(\Theta_{41})]+R_6[\sin(\Theta_{61}+\gamma_3)-\sin(\Theta_{61})]=\mathrm{Im}(\delta_3) \tag{13h}$$

where, $\mathrm{Re}(\delta_2)$ and $\mathrm{Im}(\delta_2)$ represents the real and imaginary parts of the path vector δ_2 and the same applies for vector δ_3. For the path generation synthesis δ_2 and δ_3 are specified as input while the unknowns in the above equations are

$$R_2, \Theta_{21}, R_5, \Theta_{51}, R_4, \Theta_{41}, R_6, \Theta_{61}, \phi_2, \phi_3, \psi_2, \psi_3, \gamma_2, \gamma_3$$

Since, there are 8 non-linear equations and 14 unknowns, in order to solve this system of equations any of the 6 variables are chosen as free choices and the remaining eight variables are calculated by solving eight equations.

2.1.3. Motion Generation. In motion generation synthesis (Sandor and Erdman, 1984; Howell, 2001; Kolachalam, 2003) in addition to the precision positions, the coupler orientations are also specified at each precision position (Figure 2.3). The governing loop-closure equations for three precision positions motion generation synthesis case are the same as those for the path generation synthesis case but the number of unknowns gets reduced by two due to specification of couple link angle (γ_j) at precision positions. The unknowns are

$$R_2, \Theta_{21}, R_5, \Theta_{51}, R_4, \Theta_{41}, R_6, \Theta_{61}, \phi_2, \phi_3, \psi_2, \psi_3$$

There are 8 non-linear equations and 12 unknowns, any four variables are considered as free choices so as to solve the above system of equations for 8 unknown variables.

2.1.4. Path Generation with Prescribed Timing. In path generation with prescribed timing synthesis (Sandor and Erdman, 1984; Howell, 2001; Kolachalam, 2003) the precision positions are correlated with input link angles. This is similar to the motion generation expect instead of coupler link angles (γ_j), input link angles (ϕ_j) are specified at precision positions (Figure 2.3). The governing loop-closure equations for

three precision positions path generation with prescribed timing synthesis case are the same as those for the path generation or motion generation synthesis case.

Here, the unknowns are

$$R_2, \Theta_{21}, R_5, \Theta_{51}, R_4, \Theta_{41}, R_6, \Theta_{61}, \psi_2, \psi_3, \gamma_{2,}\gamma_3$$

In this case also, there are 8 non-linear equations and 12 unknowns, any four variables are considered as free choices so as to solve the above system of equations for 8 unknown variables.

2.2. COMPLIANT MECHANISM DESIGN

Compliant mechanisms involve the large nonlinear deflections, so the conventional linear equations are not applicable to the compliant mechanisms design. These large deflections cause geometric nonlinearities in the compliant mechanisms. Bisshopp and Drucker (1945), developed elliptic integrals for analysis of large-deflection analysis problems. Elliptic integrals are the functions like trigonometric functions where an input is given and result is calculated by series of expansion (Howell, 2001).

e.g. cosine trigonometric function where angle can be an input and result will be obtained by cosine series expansion. One difference in analogy between the trigonometric function and elliptic integrals is the trigonometric functions have only one independent function, while elliptic integrals may require two or three independent variables. The use of elliptic integrals is limited to the relatively simple geometries and simple loading cases due to several simplifying assumptions such as linear material properties, inextensible materials (Howell, 2001).

A nonlinear finite element analysis and chain algorithm (Her et al., 1992) can be used for analysis of more complicated geometries and loadings problems (Howell, 2001). These methods can be useful in analyzing the compliant mechanisms obtained using pseudo-rigid-body model concept technique. These methods can also be used to analyze the complex geometry problems which will be difficult to model using pseudo-rigid-body models. However, it will be still wise decision to use pseudo-rigid-body models in the preliminary design stages to obtain the general understanding of the behavior and characteristics of the mechanism and then use above methods to improve the design obtained.

2.2.1. Pseudo-Rigid-Body Model Concept. A pseudo-rigid-body model concept is used to model the large deflections of flexible members using rigid-body members and torsional springs having equivalent force-deflections characteristics (Howell and Midha, 1996; Howell 2001). It can be shown that free end of the flexible cantilever beam with force at the free end follows a nearly circular path, having some radius of curvature along the beam's length (Howell, 2001). This idea is used to develop the parametric approximations for the beam's deflection path, wherein it is assumed that nearly circular path travel of beam's end can be modeled by two rigid links joined at characteristic pivot (Howell, 1991) along the beam (Howell and Midha, 1995; Howell, 2001). The characteristic pivot location on the beam is measured as a fraction of beam length from the beam end. This fractional distance is known as characteristic radius,γl, where γ is called as characteristic radius factor. The average value of the characteristic radius factor γ is found to be 0.85. For most of the pseudo-rigid-body models of the various beam types, this value can be taken as the preliminary estimate. The characteristic radius,γl,

represents the radius of circular deflection path traversed by the end of pseudo-rigid-body link. The torsional spring at the characteristic pivot is used to model the force-deflection characteristics of the flexible beam and represents the beam's resistance to the deflection and this resistance can be modeled by the stiffness coefficient,K_Θ, which represents torsional spring property of the beam. The average value of K_Θ is taken as 2.65 for $0.5 < n < 1.0$ (Howell, 2001).

Figure 2.4 shows the initially straight cantilever beam of length L which undergoes the large deflection due to applied transverse and axial end forces P and nP respectively. θ_0, is the beam end angle of the cantilever beam. Figure 2.5 shows the equivalent pseudo-rigid-body model of the cantilever beam with two rigid links and torsional spring at the characteristic pivot. The angle by which the characteristic radius or the longer pseudo-rigid-body link rotates is referred as pseudo-rigid-body angle Θ. The nearly linear relationship is approximated between θ_0 and Θ (Howell and Midha, 1995; Howell, 2001) by

$$\theta_0 = c_\theta \Theta \tag{14}$$

where, c_θ is the parametric angle coefficient. More explanation on pseudo-rigid-body models can be found in *Compliant Mechanisms*, Howell 2001.

2.2.2. Types of Compliant Segments and Equivalent PRBMs. The compliant mechanisms can have compliant segments as well as rigid links and joints. Depending on the types of links and joints in the mechanism, compliant mechanisms are classified as fully compliant mechanisms or partially compliant mechanisms. The mechanism shown in Figure 2.6 has no traditional joints and so zero links. These mechanisms obtain all of their motions from deflections of flexible members and termed as fully compliant

mechanisms (Howell, 2001). The compliant mechanisms that contain one or more kinematic pairs along with compliant segments are termed as partially compliant mechanisms (Howell, 2001). The compliant mechanisms may contain different types of compliant segments such as fixed-pinned (Howell and Midha, 1995; Howell, 2001) compliant segments, fixed-guided compliant segments and small-length flexural pivots. These different types of compliant segments with their equivalent PRBMs are discussed in the subsequent sections.

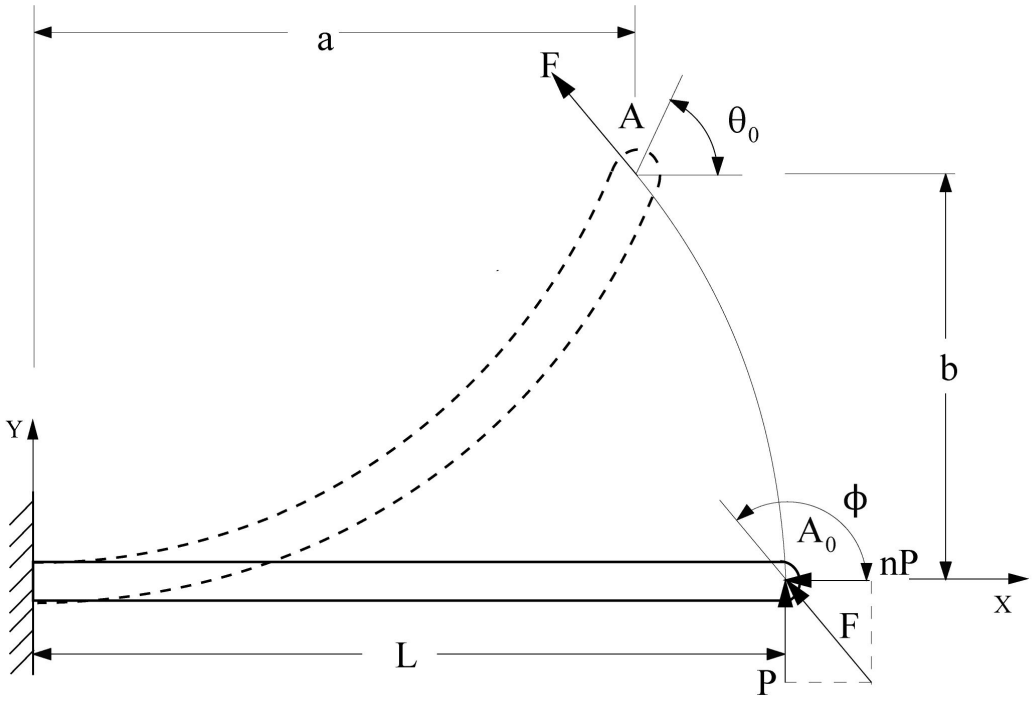

Figure 2.4. A Compliant Cantilever Beam with Large-Deflection

2.2.2.1. Fixed-pinned compliant segment. Consider a flexible cantilever beam of length L having constant cross-sectional area and linear material properties shown in Figure 2.4. Large deflection elliptic integrals show that free end of the cantilever beam

follows the nearly circular path with a force at free end (Howell, 2001). This deflection path is modeled by two rigid links connected at characteristic pivot and force-deflection characteristic of the beam are modeled by the torsional spring at the characteristic pivot. The equivalent pseudo-rigid-body model for the fixed-pinned beam with force at the free end is shown in Figure 2.5.

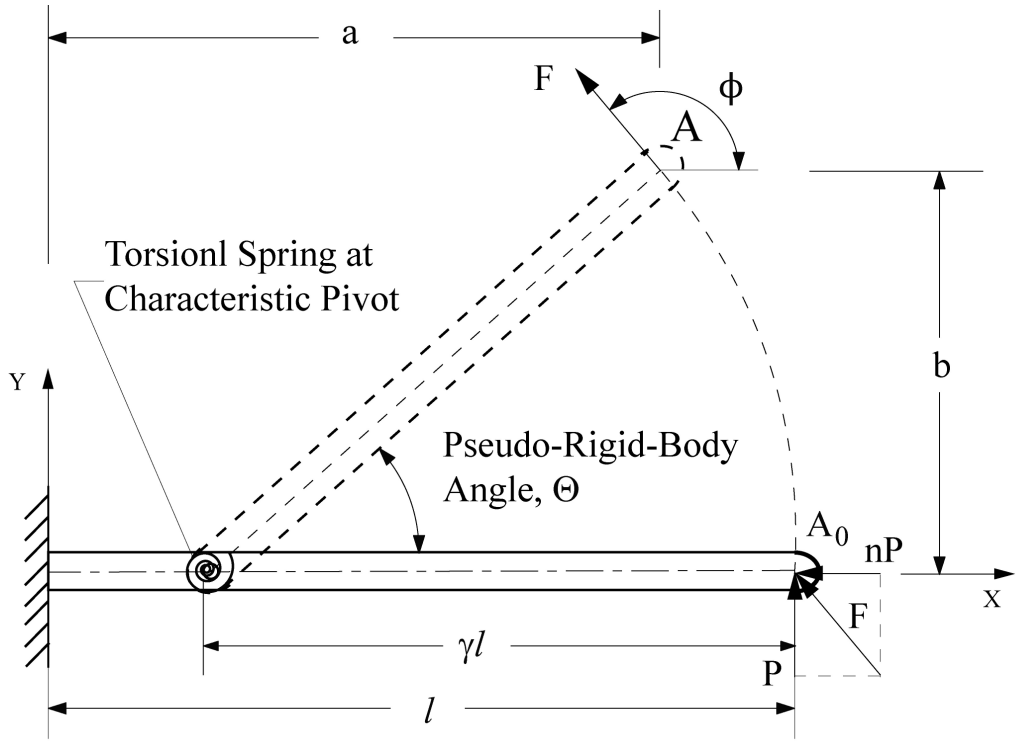

Figure 2.5. A Pseudo-Rigid-Body Model of Compliant Cantilever Beam with Large-Deflection

The characteristic pivot is located at $(1-\gamma)$L distance from the fixed end of the beam. The value of γ can be taken as 0.85 as a preliminary estimate. The equivalent

spring constant,K_t, of the torsional spring attached at the characteristic pivot, can be determined using the equation (Howell, 2001):

$$K_t = \gamma K_\Theta \frac{EI}{L} \tag{15}$$

where, $K_\Theta \equiv$ Stiffness coefficient (average value of K_Θ can be taken as 2.65)

$E \equiv$ Elastic modulus

$I \equiv$ Moment of inertia

2.2.2.2. Fixed-guided compliant segment. Consider a cantilever flexible beam with loadings as shown in Figure 2.7. The one end of the beam is fixed while the other end is to be maintained at constant angle and in order to have a constant beam-end angle, the resultant moment M_0 must be present at the free end with the force P. The resulting deflected shape of the beam is anti-symmetric at its centerline, where the curvature becomes zero (Howell, 2001). Moment also becomes zero at the mid-length as it is proportional to the curvature according the Euler-Bernoulli principle.

Considering only the one-half of the beam, it will have force P at its end and it will have same pseudo-rigid-body model as discussed for the fixed-pinned segment. The pseudo-rigid-body model for the whole beam can be obtained by combining the two anti-symmetric one-half beam models as shown in Figure 2.8. Thus, PRBM consists of three rigid links joined at two characteristic pivots as shown in Figure 2.8 with two torsional springs; one at each characteristic pivot. The characteristic pivot is located at the distance $(1-\gamma)\frac{L}{2}$ from each end. The value of γ can be taken as 0.85.

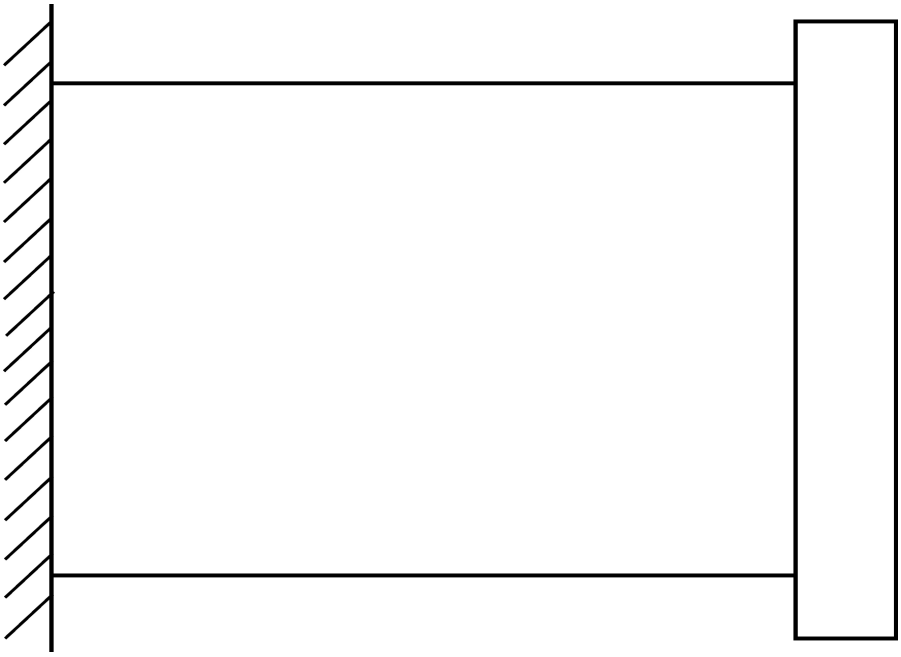

Figure 2.6. A Fully Compliant Mechanism (Howell, 2001)

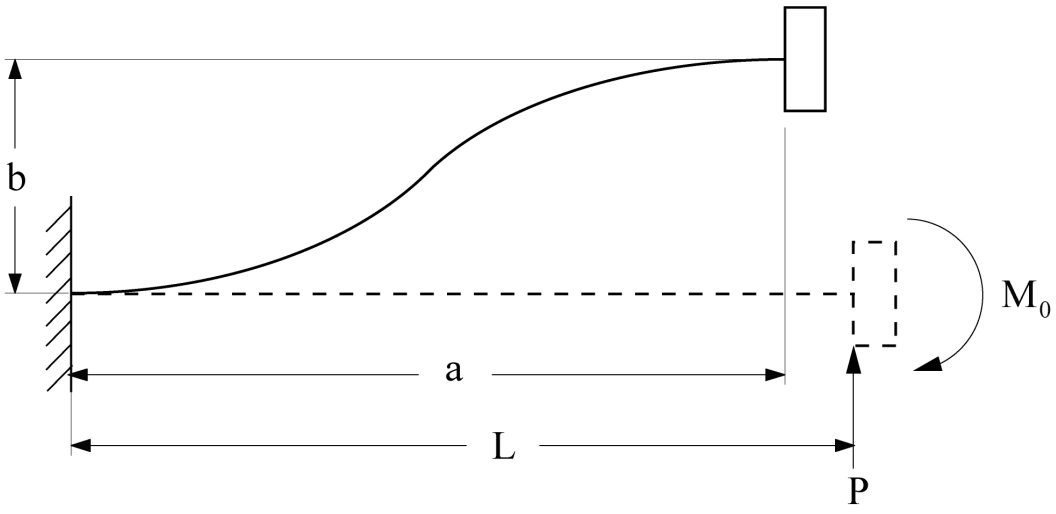

Figure 2.7. A Fixed-Guided Compliant Beam with Constant Beam-End Angle

The torsional spring constant, K_t, of the each spring can be determined by the following the expression (Howell, 2001):

$$K_t = 2\gamma K_\Theta \frac{EI}{L} \tag{16}$$

2.2.2.3. Small-length flexural pivot. Consider a cantilever beam shown in Figure 2.9. The beam is composed of two segments; a short flexible segment and long rigid segment. If the small flexible segment is significantly shorter and flexible than longer rigid segment, $(l << L)$ or $\left((El) << (EL)\right)$ then smaller segment is known as small-length flexural pivot. Usually length of the longer segment(L), is 10 times more than length of smaller segment (l) (Howell, 2001).

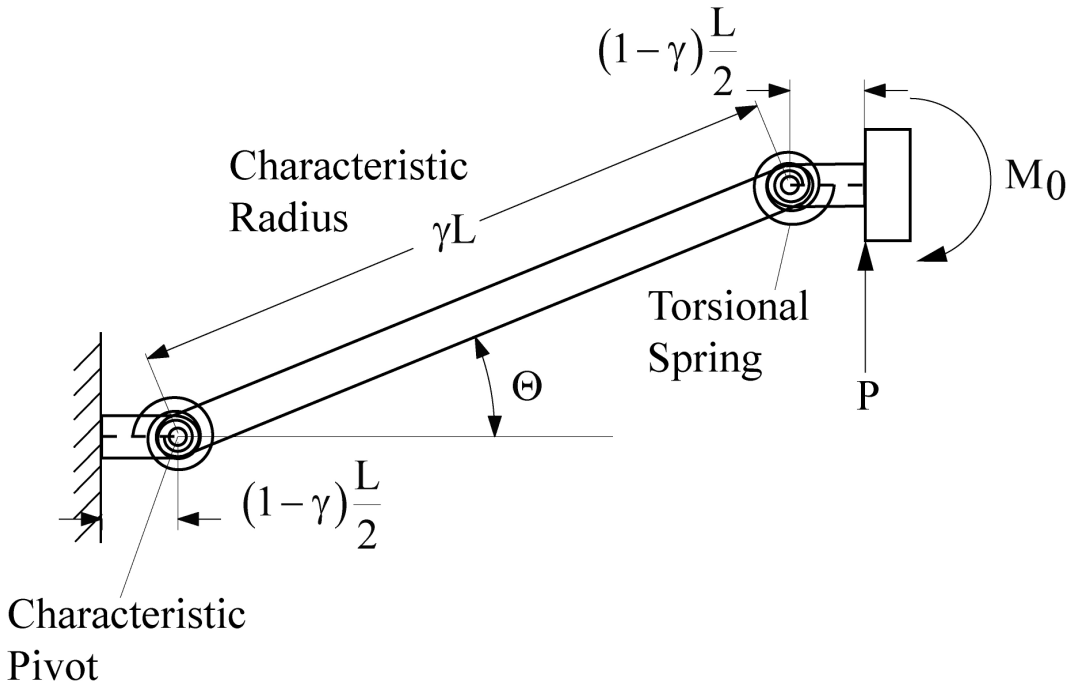

Figure 2.8. A Pseudo-Rigid-Body Model of Fixed-Guided Compliant Beam with Constant Beam-End Angle

As the flexible segment is much shorter than rigid segment, the motion of the system can be modeled as two rigid links joined at pin joint called as characteristic pivot as shown in Figure 2.10. The characteristic pivot can be assumed at the center of the flexible segment as the deflection occurs at the flexible segment and is much smaller than length of the rigid segment (Howell, 2001).

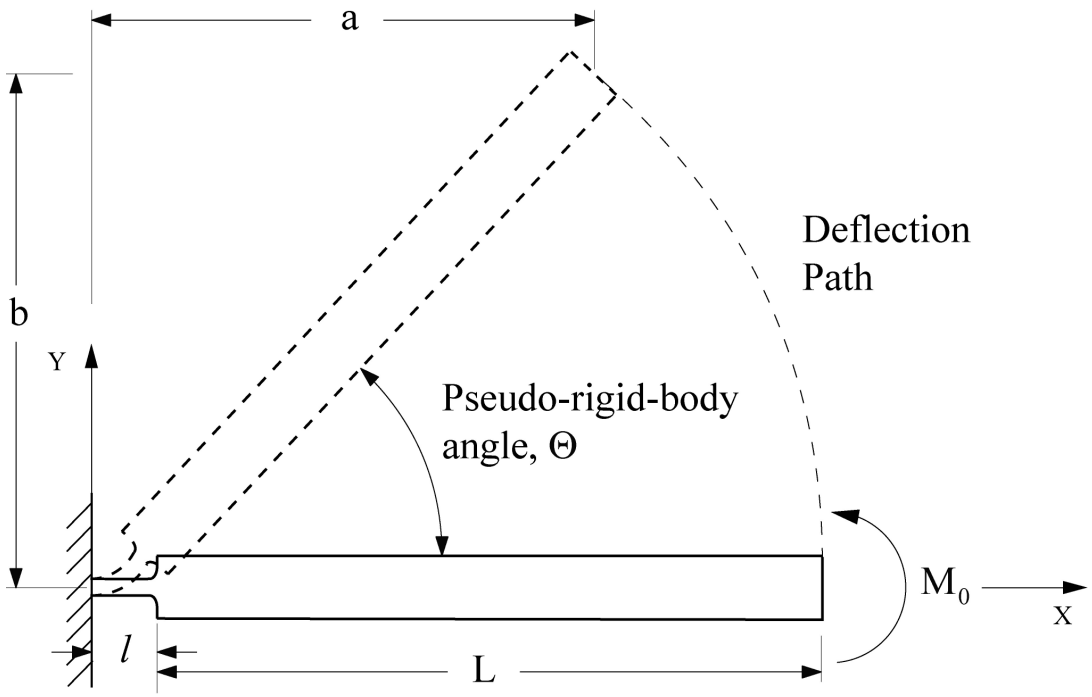

Figure 2.9. A Small-Length Flexural Pivot

The equivalent spring constant, K_t of the torsional spring attached at the characteristic pivot is given by expression (Howell, 1991, 2003).

$$K_t = \frac{EI}{l} \tag{17}$$

where, E is the modulus of elasticity, I is the moment of inertia and l is the length of the flexible segment.

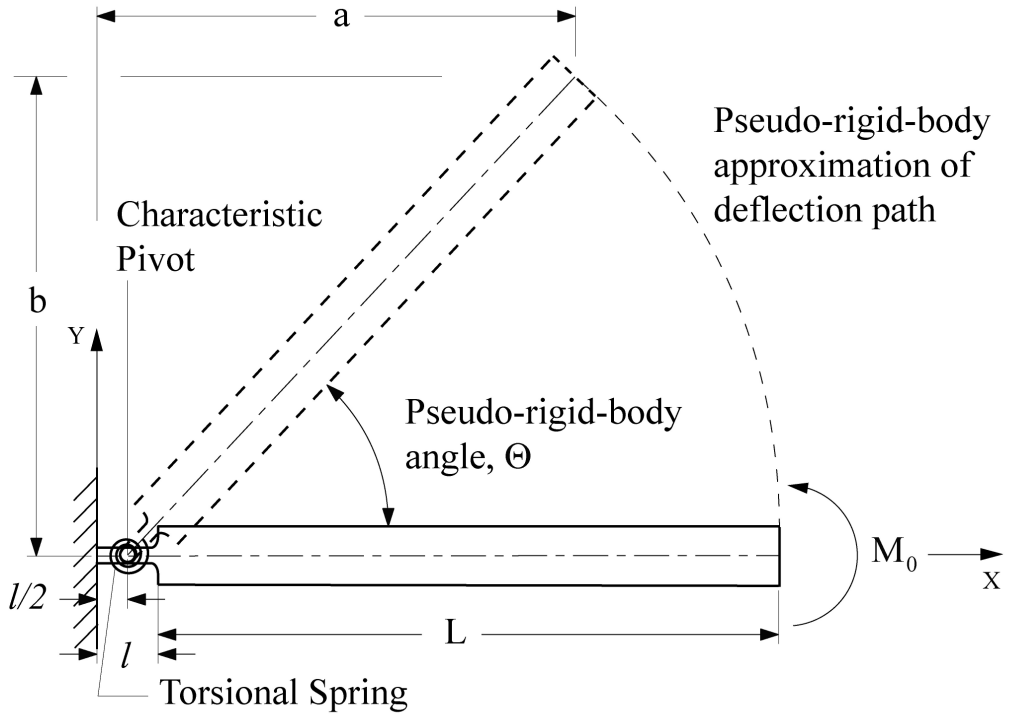

Figure 2.10. A Pseudo-Rigid-Body Model of a Small-Length Flexural Pivot

2.3. COMPLIANT MECHANISM SYNTHESIS.

As opposed to the rigid-body mechanism synthesis much less work has been done in the area of compliant mechanism synthesis. Earlier efforts in the compliant mechanism synthesis were done by (Burns, 1964; Burns and Crossley, 1968) and developed the kinetostatic synthesis of four-bar mechanism with flexible coupler link. In 1980, Ashok Midha pioneered work in compliant mechanism design methods with the concentrated

compliance. Howell and Midha (1994) developed the pseudo-rigid-body model, which modeled the flexible segments by equivalent rigid links and torsional springs and made the compliant mechanism synthesis much easier using available rigid-body mechanism theories. Mettlach and Midha (1995) presented a graphical synthesis technique using Burmester theory to design the compliant mechanisms for more number of precision positions. Murphy et al. (1996) developed the method based in graph theory to design the different topologies of the compliant mechanisms employing type synthesis techniques. Annamalai (2003), Midha et al. (2004) used the pseudo-rigid-body model concept to synthesize the pseudo-rigid-body four-bar mechanism with energy/torque specifications. Kolachalam (2003), Midha et al. (2011) synthesized the compliant single strip mechanisms for energy, torque and force specifications. Dado (2005) developed a variable parametric pseudo-rigid-body model for limit position synthesis of complaint four-bar mechanism with energy specifications.

Design methodologies for the distributed compliance first appeared in the works of Ananthsuresh (1994). In this case, continuum solid mechanics methods are used instead of rigid-body kinematics. Ananthsuresh (1994) used the structural optimization technique to design the compliant mechanisms with distributed compliance by using homogenization method and using the displacement of one point as objective function. Another structural optimization method using mechanism deformation energy as objective function is developed by Frecker et al. (1997). Saggere and Kota (2001) synthesized the four-bar mechanism with compliant coupler which requires prescribed shape change along with rigid-body motion for motion generation. In the recent times, Lu and Kota (2003) used load-path methodology and genetic algorithms in designing the

shape morphing compliant mechanisms. Krovi et al. (2002) studied the kinetostatic synthesis of planar-coupled serial chain mechanisms by combining precision point synthesis and optimization.

Su and McCarthy (2007) synthesized the bi-stable four-bar compliant mechanism using polynomial homotopy technique. Tari and Su (2011) presented a complex solution framework for kinetostatic synthesis of compliant four-bar mechanism. There are other design methods for compliant mechanisms known as inverse design methods that allow designer to determine the initial shape such that it attains the desired shape under applied loads (Albanesi et al. 2010).

2.3.1. Compliant Mechanism Synthesis Methods Using PRBM Concept. Compliant mechanism synthesis poses many challenges that are not found in rigid-body synthesis. Unlike the rigid-body mechanism, motion of the compliant mechanism depends on the location, direction and magnitude of the applied forces. The compliant mechanisms inherently have limits on geometry. e.g. the compliant segments such as small-length flexural pivots can't fully rotate. For motion, the compliant segments have to deform, this induces stresses in them. So, stress and fatigue are of major concern while designing compliant mechanisms etc. The compliant mechanism synthesis using pseudo-rigid-body model can be divided into two major classes (Howell, 2001) rigid-body-replacement synthesis and synthesis with compliance. These methods are discussed in detail in following sections.

2.3.1.1. Rigid-body replacement (kinematic) synthesis. The synthesis of compliant mechanisms in which rigid-body equations are directly applied to the pseudo-rigid-body model without any concern for energy storage characteristics of the

mechanism, is called as rigid-body replacement synthesis. As only kinematic equations are considered only for synthesis, this is also known as kinematic synthesis. In this approach, pseudo-rigid-body model is obtained for compliant mechanism and using rigid-body kinematic equations, link lengths are obtained. Once the kinematic geometry is obtained, structural properties of the mechanism are determined according to the allowable stresses or the input requirements. This synthesis approach is particularly useful when a compliant mechanism is to be used for conventional rigid body tasks like function generation, path generation etc. without considering energy storage in the mechanism.

The major task in this synthesis method is determining and evaluating the pseudo-rigid-body model for the compliant mechanism as the synthesis may yield number of solutions that may be valid for rigid-body mechanism but not for the compliant mechanism due to some practical limits on the geometry, e.g. small-length flexural pivots can't rotate fully. So, the iterative approach will be more useful in this compliant mechanism synthesis method.

2.3.1.2. Synthesis with compliance (kinetostatic synthesis). The compliant mechanism synthesis technique, which considers energy storage characteristics in the flexible segments in addition to the rigid-body kinematic equations, is termed as synthesis with compliance (Howell and Midha, 1994; Howell, 2001). As both kinematic equations and static force equations are considered for the synthesis, this is also known as kinetostatic synthesis. The synthesis includes loop-closure equations for the pseudo-rigid-body model and energy equations. The energy storage characteristics of the mechanism can be considered as energy stored in the system as function of input, required input

torque or force and required input and output force or torque at each precision position (Howell, 2001). The example of synthesis with compliance can be a mechanism designed for path generation with energies or torques or forces specified at the precision positions. As discussed in the rigid-body replacement synthesis, in this method also an appropriate pseudo-rigid-body model for the compliant mechanism is obtained using kinematic equations. The structural properties of the flexible segments are then determined according to the allowable stresses or the input requirements using the energy equations.

The energy is stored in the form of strain energy in the flexible members of compliant mechanisms. This energy can be accounted using the torsional springs of appropriate stiffness values at characteristic pivots in the pseudo-rigid-body model. The consideration of energy equations along with kinematic equations for the synthesis results in two sets of unknowns in the system of equations. i) kinematic variables includes link lengths, angles of the pseudo-rigid-body model links ii) energy variables consists of spring constants, K_t, related to the stiffness coefficient, $K_{\Theta,}$ and undeflected spring parameters, β_0, related to the initial pseudo-rigid-body model, Θ_0. Figure 2.11 shows the four-bar mechanism with four torsional springs attached at pin joints.

2.3.2. Energy Considerations. In designing compliant mechanism using synthesis with compliance technique, energies are specified at precision positions in addition to the kinematic variable specifications depending synthesis type e.g. for the motion generation synthesis case, coupler link angles (γ_s) are specified along with precision positions. Considering the pseudo-rigid-body four-bar mechanism, a maximum of four torsional springs can be attached at the four pin joints.

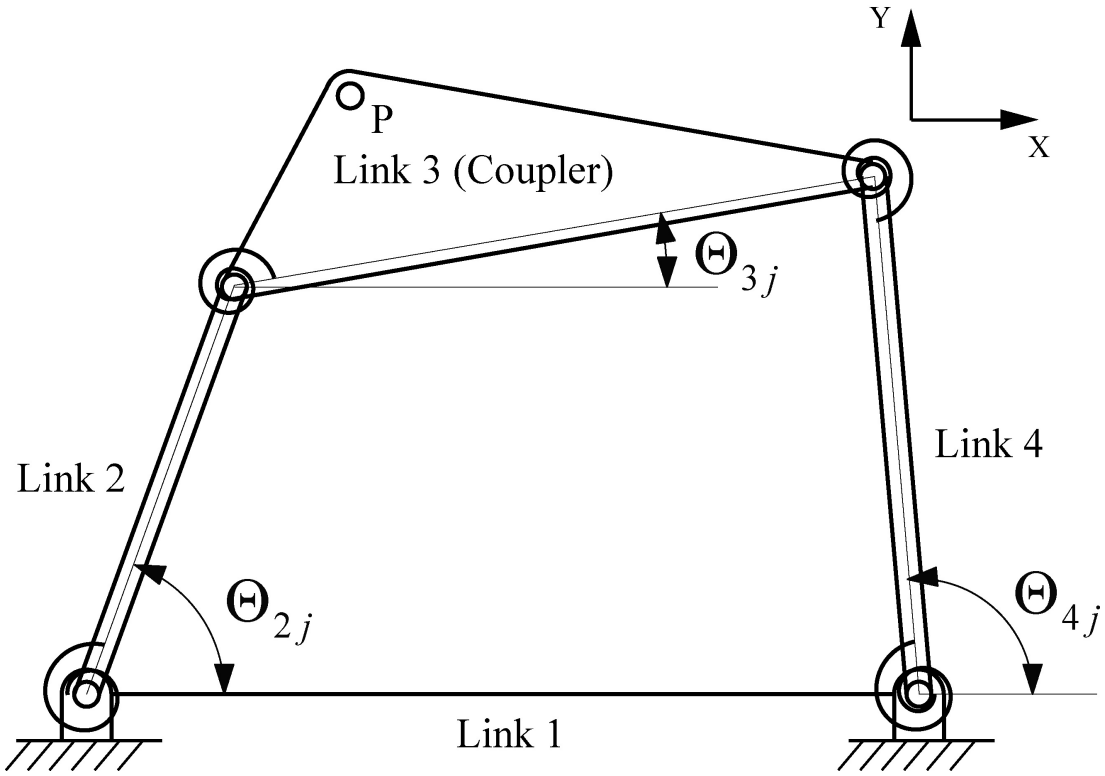

Figure 2.11. A Four-Bar Mechanism with Four Torsional Springs at the Pivots

Thus, the synthesis problem mainly becomes determination of these spring constants which contribute the same energy stored in the mechanism as specified. The total energy stored in the compliant mechanism at j^{th} precision position, E_j is calculated (Howell 1993; Annamalai, 2003) by potential energies stored in each torsional spring as

$$E_j = \frac{1}{2}\sum_{i=1}^{m} K_i\left(\beta_{ij} - \beta_{i0}\right)^2; \qquad 1 \le m \le 4 \qquad (18)$$

where, K_i is the spring constant of the i^{th} spring, β_{ij} is the j^{th} angular position of the i^{th} spring, β_{i0} is undeflected angular position of the i^{th} torsional spring and m is the number

of torsional springs in the mechanism. The angle β_{ij} can be expressed in terms of pseudo-rigid-body model angle, Θ_0 (Howell, 1993; Annamalai, 2003) as follows:

$$\beta_{1j} = \Theta_{2j} \tag{19a}$$

$$\beta_{2j} = 180^0 - \left(\Theta_{2j} - \Theta_{3j}\right) \tag{19b}$$

$$\beta_{3j} = \Theta_{4j} - \Theta_{3j} \tag{19c}$$

$$\beta_{4j} = \Theta_{4j} \tag{19d}$$

where, Θ_{ij} is the angle of the i^{th} link in the j^{th} position. Using equations (19), the mechanism total energy, E_j in j^{th} position can be written as follows:

$$\begin{aligned} E_j = \frac{1}{2}\Big[K_1\left(\Theta_{2j} - \Theta_{20}\right)^2 + K_2\Big[\left(\Theta_{3j} - \Theta_{30}\right) - \left(\Theta_{2j} - \Theta_{20}\right)\Big]^2 \\ + K_3\Big[\left(\Theta_{4j} - \Theta_{40}\right) - \left(\Theta_{3j} - \Theta_{30}\right)\Big]^2 + K_4\left(\Theta_{4j} - \Theta_{40}\right)^2\Big] \end{aligned} \tag{20}$$

Considering three precision positions synthesis problem, equation (20) can be written for each precision position as follows:

$$\begin{aligned} E_1 = \frac{1}{2}[K_1(\Theta_{21} - \Theta_{20})^2 + K_2[(\Theta_{31} - \Theta_{30}) - (\Theta_{21} - \Theta_{20})]^2 \\ + K_3[(\Theta_{41} - \Theta_{40}) - (\Theta_{31} - \Theta_{30})]^2 + K_4(\Theta_{41} - \Theta_{40})^2] \end{aligned} \tag{21a}$$

$$\begin{aligned} E_2 = \frac{1}{2}[K_1(\Theta_{21} + \phi_2 - \Theta_{20})^2 \\ + K_2[(\Theta_{31} + \gamma_2 - \Theta_{30}) - (\Theta_{21} + \phi_2 - \Theta_{20})]^2 \\ + K_3[(\Theta_{41} + \psi_2 - \Theta_{40}) - (\Theta_{31} + \gamma_2 - \Theta_{30})]^2 \\ + K_4(\Theta_{41} + \psi_2 - \Theta_{40})^2] \end{aligned} \tag{21b}$$

$$E_3 = \frac{1}{2}[K_1(\Theta_{21} + \phi_3 - \Theta_{20})^2 + K_2[(\Theta_{31} + \gamma_3 - \Theta_{30}) - (\Theta_{21} + \phi_3 - \Theta_{20})]^2 + K_3[(\Theta_{41} + \psi_3 - \Theta_{40}) - (\Theta_{31} + \gamma_3 - \Theta_{30})]^2 + K_4(\Theta_{41} + \psi_3 - \Theta_{40})^2] \quad (21c)$$

These three energy equations can be solved for four unknown spring constants. i.e. K_1, K_2, K_3, K_4. If the first precision position of the mechanism is considered to be an undeflected position i.e. zero-energy position of the mechanism, then the system of reduced equations is used and is given below:

$$E_1 = 0 \quad (22a)$$

$$E_2 = \frac{1}{2}[K_1(\phi_2)^2 + K_2(\phi_2 - \gamma_2)^2 + K_3(\psi_2 - \gamma_2)^2 + K_4(\psi_2)^2] \quad (22b)$$

$$E_2 = \frac{1}{2}[K_1(\phi_3)^2 + K_2(\phi_3 - \gamma_3)^2 + K_3(\psi_3 - \gamma_3)^2 + K_4(\psi_3)^2] \quad (22c)$$

In this particular case, first energy equation is trivial and may be neglected. Other two energy equations can solved for four unknowns K_1, K_2, K_3, K_4. Once the pseudo-rigid-body four-bar mechanism has been synthesized, the next step is to determine the dimensions of the flexible members. In this work, rectangular sections of compliant members have been assumed.

2.4. COMPLIANT SEGMENT DESIGN

Depending on the type of the compliant segments i.e. fixed-pinned segment, fixed-guided segment, small-length flexural pivot considered in the compliant

mechanism, dimensions of compliant segments can be determined as discussed in the following sections.

2.4.1. Fixed-Pinned Segment. The equivalent pseudo-rigid-body model for the fixed-pinned compliant segment is shown in Figure 2.5. After determining all the pseudo-rigid-body link lengths from the synthesis; if a fixed-pinned segment is selected as a flexible member, the distance of the characteristic pivot from the fixed end of the compliant beam is taken as $(1-\gamma)\mathrm{L}$, where, γ can be taken as 0.85 and the stiffness coefficient is assumed to be 2.65. It is assured that the pin joint of the pseudo-rigid-body link and characteristic pivot coincides with each other. Thus, pseudo-rigid-body link lengths obtained are used to find the characteristic radius, $\gamma\mathrm{L}$. The total link length of compliant fixed-pinned segment L can be obtained as:

$$\gamma\mathrm{L} = |\mathrm{Z}| \;\Rightarrow \mathrm{L} = |\mathrm{Z}|/\gamma \tag{23}$$

where, $|\mathrm{Z}| = \mathrm{R} =$ length of the pseudo-rigid-body link

Once the spring constants are known, the equation (15) and equation (23) is used to determine the either width or thickness of the segment by assuming an appropriate value for the other as follows:

$$\mathrm{I} = \frac{\mathrm{bh}^3}{12} \tag{24}$$

$$\mathrm{b} = \frac{12\mathrm{KL}}{\gamma \mathrm{K}_\Theta \mathrm{Eh}^3} \tag{25}$$

$$\mathrm{h} = \left(\frac{12\mathrm{KL}}{\gamma \mathrm{K}_\Theta \mathrm{Eb}}\right)^{\frac{1}{3}} \tag{26}$$

2.4.2. Fixed-Guided Compliant Segment. The equivalent pseudo-rigid-body model for the fixed-guided compliant segment with constant beam-end angle is shown in Figure 2.8. This model assumes that one end of the compliant segment is maintained at constant angle. For the compliant mechanism motions considered here, it will be difficult to enforce this assumption, so this model is used as a possible approximation.

If a fixed-guided compliant segment is selected, the distance to the characteristic pivot from the either end is given by$(1-\gamma)\frac{L}{2}$, the value of γ is assumed to be 0.85 and stiffness coefficient to be 2.65. While using fixed-guided compliant segment in the mechanism, it is reasonable to assume two same spring constants on the one pseudo-rigid-body link. It is assured that the pin joints of the pseudo-rigid-body link and characteristic pivots coincide with each other. Thus, pseudo-rigid-body link lengths obtained are used to find the characteristic radius, γL. The total link length of compliant fixed-guided segment L, can be obtained using equation (23). Once the spring constants are known, the equation (16) is used to determine the either width or thickness of the segment by assuming an appropriate value for the other as follows:

$$b = \frac{6KL}{\gamma K_{\Theta} E h^3} \tag{27}$$

$$h = \left(\frac{6KL}{\gamma K_{\Theta} E b}\right)^{\frac{1}{3}} \tag{28}$$

2.4.3. Small-Length Flexural Pivot. The equivalent pseudo-rigid-body model of the small-length flexural pivot is shown in Figure 2.10. The compliant mechanisms with flexure pivots, utilizes the small-length flexural pivots assumption. If the small length flexural pivot is selected as a compliant segment, the characteristic pivot is located at its

center. The length of small-length flexural pivot is assumed to $\left(\frac{1}{10}\right)^{\text{th}}$ of the pseudo-rigid-body link length.

$$l = \frac{\mathrm{L}}{10} \tag{29}$$

Once the length of the small-length flexural pivot and spring constant of torsional spring are known, equation (17) is used to determine the either width or thickness by assuming an appropriate value for the other as follows:

$$\mathrm{b} = \frac{12\mathrm{K}l}{\mathrm{E}\mathrm{h}^3} \tag{30}$$

$$\mathrm{h} = \left(\frac{12\mathrm{K}l}{\mathrm{E}\mathrm{b}}\right)^{\frac{1}{3}} \tag{31}$$

2.5. SUMMARY

In this Section, the rigid-body synthesis methods for three-precision positions synthesis of a four-bar mechanism are reviewed. A pseudo-rigid-body concept is discussed and pseudo-rigid-body models are presented for three types of compliant segments. The compliant mechanism synthesis methods are reviewed. The two synthesis methods for compliant mechanism synthesis using pseudo-rigid-body model concept are discussed and energy considerations for compliant mechanism synthesis are introduced. The different types of compliant segments such small-length flexural pivots, full-length compliant segments are designed.

3. SYNTHESIS WITH COMPLIANCE FOR ENERGY AND TORQUE SPECIFICATIONS AND NEED FOR OPTIMIZATION APPROACH TO SOLVE ENERGY/TORQUE EQUATIONS

Synthesis with compliance technique (Howell and Midha, 1996; Howell, 2001) synthesizes the compliant mechanisms considering both loop-closure kinematic equations and energy/toque equations. This concept was introduced briefly in Section 2 applied to synthesis of a pseudo-rigid-body four-bar mechanism for three precision positions with energy specified at each position and a particular case where first precision position is energy-free position of the mechanism i.e. energy is zero at the first precision position. This Section reviews the general synthesis with compliance technique applied to different synthesis problems such as function generation, path generation etc. with more than three precision positions and torque specifications problems also. The Section also enlists the design tables, which gives an easy tool for the user to determine the number of equations and number of unknowns required to synthesize the pseudo-rigid-body four-bar mechanism for energy and torque specifications. The limitations/problems with synthesis with compliance technique are presented in subsequent sections. The new approach to solve the system of energy/torque equations using optimization is introduced at the end of the Section.

3.1. SYNTHESIS WITH COMPLIANCE

The synthesis with compliance technique uses pseudo-rigid-body model concept for compliant mechanism synthesis. This method provides multiplicity of solutions along with expediency and accuracy of the solutions (Annamalai, 2003). The pseudo-rigid-body links and their orientations in precision positions constitute the kinematic equations i.e.

loop-closure equations, while the spring constants and deflections of springs attached at the characteristic pivots in pseudo-rigid-body model constitutes energy equations and results in two different sets of unknowns.

i. Kinematic variables consisting of pseudo-rigid-body link lengths and their angles corresponding to precision positions, and
ii. Energy variables consisting of spring constants and undeflected torsional spring positions.

Thus, the loop-closure equations represent kinematic mobility of the mechanism, while the energy/torque equations represent the mechanism compliance. The compliant mechanisms can be reduced to pseudo-rigid-body model with rigid links and torsional springs. Consider the basic four-bar mechanism with its pin joints representing characteristic pivots and torsional springs at the characteristic pivots representing the segment compliances as shown in Figure 3.1. Depending on the number of springs in the system, the number of unknowns i.e. kinematic variables and energy variables introduced in the system changes. The variables common in both the kinematic equations and energy equations cause coupling in them.

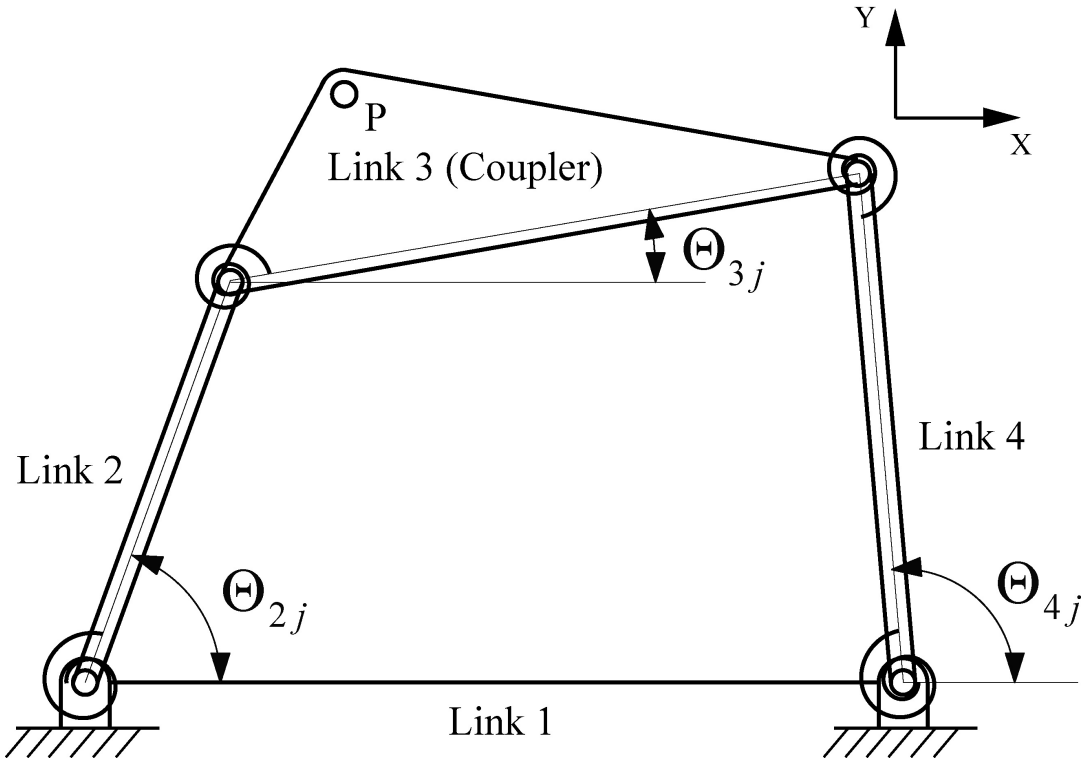

Figure 3.1. A Four-Bar Mechanism with Four Torsional Springs at the Pivots

Let, the energy equations for n- precision positions problem add n equations and 2m unknowns to the system. If the kinematic equations could be solved independent of energy equations, the system is said to be weakly coupled system (Howell, 2001). The system can be made weakly coupled only if

$$2m \geq n \tag{32}$$

But if the more equations than number of unknowns are introduced into the systems, then the kinematic and energy/torque equations are solved simultaneously and system becomes strongly coupled. It is usually useful and will reduce the efforts required to obtain the solution if the kinematic and energy equations, which are nonlinear, could be solved separately (Howell, 2001).

The inclusion of different types of compliant segments in the mechanism gives wide range of solutions to the design problems (Howell, 2001). For a pseudo-rigid-body four-bar mechanism, with different types of compliant segments such as small-length flexural pivots, full-length compliant segments, all possible 18 configurations depending on the number of springs used are presented in Figure 3.2 (Midha et al., 1997; Annamalai, 2003). Using different compliant segment types for pseudo-rigid-body links and starting with four torsional springs in the mechanism, three compliant mechanism configurations (Figure 3.2 A-C) are possible. Similarly, five compliant mechanism configurations (Figure 3.2 D-H) with three springs, eight configurations (Figure 3.2 I-P) with two springs and two configurations (Figure 3.2 Q,R) with one spring are possible, resulting in total of 18 configurations. It is the user's decision to choose the suitable configuration for particular task considering design and manufacturing constraints.

3.1.1. Kinematic Considerations. The kinematic synthesis of pseudo-rigid-body mechanism is discussed in Section 2.1. It is reviewed quickly here for the sake of continuity. In function generation, the vector loop $[Z_2 \rightarrow Z_3 \rightarrow Z_4 \rightarrow Z_{4j} \rightarrow Z_{3j} \rightarrow Z_{2j}]$ in 1^{st} and j^{th} positions of the mechanism in Figure 2.2**,** gives following loop-closure equation:

$$Z_2\left(1 - e^{i\phi_j}\right) + Z_3\left(1 - e^{i\gamma_j}\right) + Z_4\left(e^{i\psi_j} - 1\right) = 0 \qquad (2)$$

In path generation, motion generation and path generation with prescribed timing, left loop $[Z_2 \rightarrow Z_5 \rightarrow \delta_j \rightarrow Z_{5j} \rightarrow Z_{2j}]$ and right loop $[Z_4 \rightarrow Z_6 \rightarrow \delta_j \rightarrow Z_{6j} \rightarrow Z_{4j}]$ from initial to j^{th} position of the mechanism in Figure 2.3; give following two vector loop-closure equations:

$$Z_2\left(e^{i\phi_j}-1\right)+Z_5\left(e^{i\gamma_j}-1\right)=\delta_j \tag{7}$$

$$Z_4\left(e^{i\psi_j}-1\right)+Z_6\left(e^{i\gamma_j}-1\right)=\delta_j \tag{8}$$

3.1.2. Energy/Torque Considerations. The total energy stored in the compliant mechanism at j^{th} precision position,E_j, is calculated (Howell, 1993; Annamalai, 2003) by the potential energies stored in each torsional spring of the corresponding pseudo-rigid-body model as

$$E_j=\frac{1}{2}\sum_{i=1}^{m}K_i\left(\beta_{ij}-\beta_{i0}\right)^2;\qquad 1\le m\le 4 \tag{18}$$

where, K_i is the spring constant of the i^{th} spring, β_{ij} is the j^{th} angular position of the i^{th} spring, β_{i0} is the undeflected angular position of the i^{th} torsional spring and m is the number of torsional springs in the mechanism. The corresponding torque equation (Howell, 1993; Mettlach 1996; Annamalai, 2003) is given as

$$T_{2j}=\sum_{i=1}^{m}K_i\left(\beta_{ij}-\beta_{i0}\right)\frac{d\beta_{ij}}{dS}\qquad 1\le m\le 4 \tag{33}$$

where, S represents the input variable for the mechanism. The angle β_{ij} is related to pseudo-rigid-body angles as given in equations (19) as follows:

$$\beta_{1j}=\Theta_{2j} \tag{19a}$$

$$\beta_{2j}=180^0-\left(\Theta_{2j}-\Theta_{3j}\right) \tag{19b}$$

$$\beta_{3j}=\Theta_{4j}-\Theta_{3j} \tag{19c}$$

$$\beta_{4j}=\Theta_{4j} \tag{19d}$$

where, Θ_{ij} is the angle of the i^{th} link in the j^{th} position. If Θ_2 is the input, then $\frac{d\beta_{ij}}{dS}$ may be expressed as:

$$\left(\frac{d\beta_1}{d\Theta_2}\right)_j = 1 \tag{34a}$$

$$\left(\frac{d\beta_2}{d\Theta_2}\right)_j = \left(\frac{d\Theta_3}{d\Theta_2}\right)_j - 1 = h_{3j} - 1 \tag{34b}$$

$$\left(\frac{d\beta_3}{d\Theta_2}\right)_j = \left(\frac{d\Theta_4}{d\Theta_2}\right)_j - \left(\frac{d\Theta_3}{d\Theta_2}\right)_j = h_{4j} - h_{3j} \tag{34c}$$

$$\left(\frac{d\beta_4}{d\Theta_2}\right)_j = \left(\frac{d\Theta_4}{d\Theta_2}\right)_j = h_{4j} \tag{34d}$$

where, h_{ij} represents the first-order kinematic coefficient of the i^{th} link at the j^{th} position, and is defined (Hall, 1981) as follows:

$$h_{3j} = \frac{R_2 \sin(\Theta_{4j} - \Theta_{2j})}{R_3 \sin(\Theta_{3j} - \Theta_{4j})} \tag{35a}$$

$$h_{4j} = \frac{R_2 \sin(\Theta_{3j} - \Theta_{2j})}{R_4 \sin(\Theta_{3j} - \Theta_{4j})} \tag{35b}$$

Using equations (19) in equation (18), energy at the j^{th} position can be written as:

$$\begin{aligned} E_j = \frac{1}{2}\Big[K_1(\Theta_{2j} - \Theta_{20})^2 + K_2\big[(\Theta_{3j} - \Theta_{30}) - (\Theta_{2j} - \Theta_{20})\big]^2 \\ + K_3\big[(\Theta_{4j} - \Theta_{40}) - (\Theta_{3j} - \Theta_{30})\big]^2 + K_4(\Theta_{4j} - \Theta_{40})^2\Big] \end{aligned} \tag{20}$$

Using equations (19), (33) and (34) in equation (32), the torque at the j^{th} position can be written as:

$$
\begin{aligned}
T_{2j} = {} & K_1(\Theta_{2j} - \Theta_{20}) \\
& + K_2\left[(\Theta_{3j} - \Theta_{30}) - (\Theta_{2j} - \Theta_{20})\right]\left(\frac{R_2 \sin(\Theta_{4j} - \Theta_{2j})}{R_3 \sin(\Theta_{3j} - \Theta_{4j})} - 1\right) \\
& + K_3\left[(\Theta_{4j} - \Theta_{40}) - (\Theta_{3j} - \Theta_{30})\right]\left(\frac{R_2 \sin(\Theta_{3j} - \Theta_{2j})}{R_4 \sin(\Theta_{3j} - \Theta_{4j})}\right. \\
& \left. - \frac{R_2 \sin(\Theta_{4j} - \Theta_{2j})}{R_3 \sin(\Theta_{3j} - \Theta_{4j})}\right) + K_4(\Theta_{4j} - \Theta_{40})\frac{R_2 \sin(\Theta_{3j} - \Theta_{2j})}{R_4 \sin(\Theta_{3j} - \Theta_{4j})}
\end{aligned} \tag{36}
$$

where, Θ_{n0} represents the angular position of the n^{th} link in the energy-free state.

The number of equations, number of unknowns and number of free choices for function generation, path, and motion generation and path generation with prescribed timing for given number of torsional springs (m) are summarized in the Tables 3.1-3.4 respectively (Annamalai, 2003). For example, for a function generation synthesis of four-bar mechanism for three precision positions with one torsional spring, there are 7 equations comprised of 4 loop-closure equations and 3 energy/torque equations and 10 unknowns, and hence 3 free choices yielding the solutions in the order of $(\infty)^3$. In the last column of the table, notations s.c. and w.c. represents strongly coupled and weakly coupled cases respectively.

For function generation synthesis case for five precision positions with one spring, the number of equations become more than unknowns, hence over-constraining the system and so not included in the Table 3.1 (Annamalai, 2003).

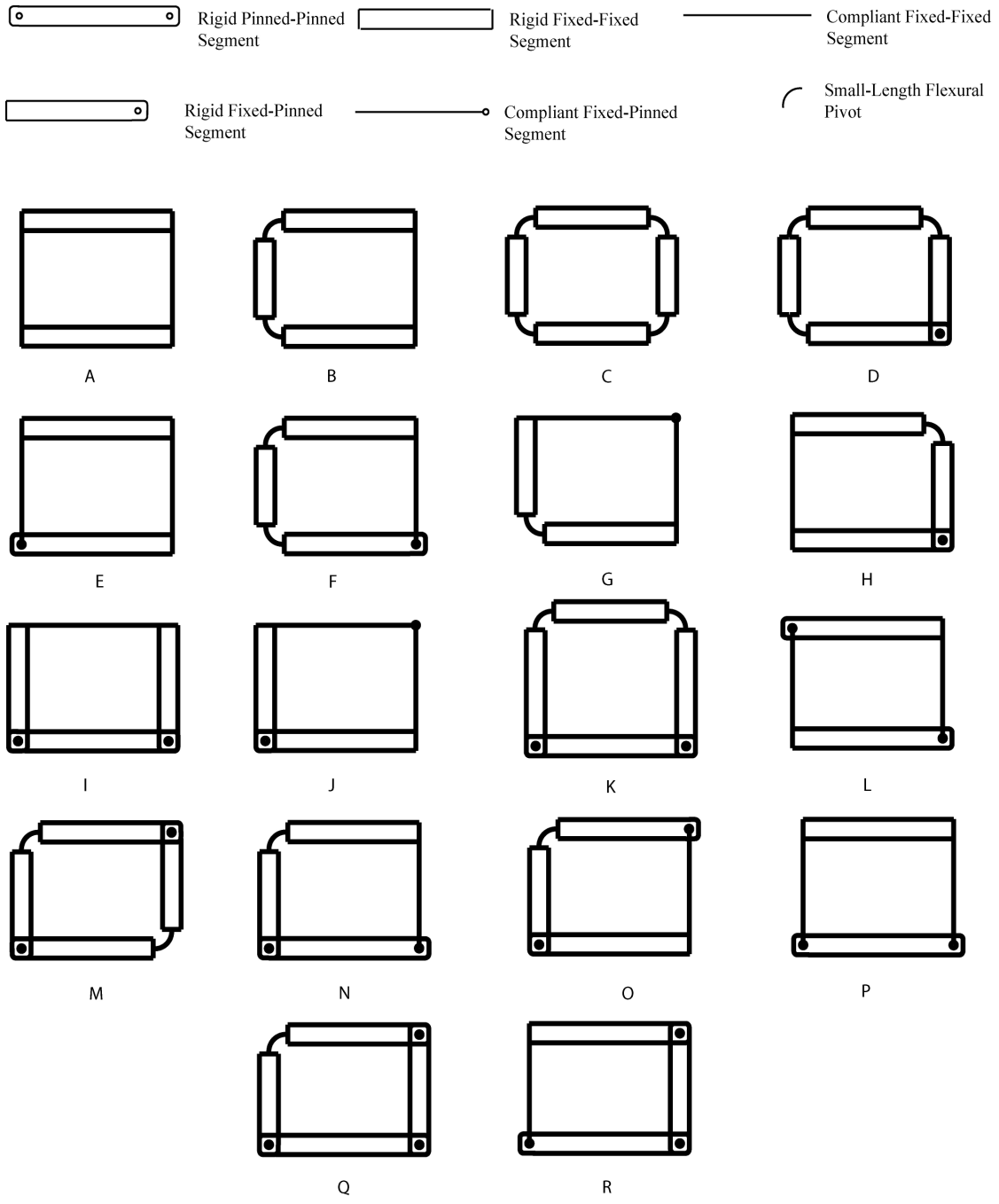

Figure 3.2. 18 Possible Configurations of Compliant Mechanism Types from Pseudo-Rigid-Body Four-Bar Mechanism

3.2. NEED OF COUPLER EQUATION FOR STRONGLY COUPLED SYSTEM

The torque equation (36) involving first-order kinematic coefficients, adds two additional unknowns to the system R_3 and Θ_{3j}, where j represents j^{th} precision position. In pseudo-rigid-body synthesis for three-precision positions with one spring for torque specifications (e.g. refer to Table 3.3) when $j > 1$, Θ_{3j} is given by $(\Theta_{31} + \gamma_j)$, where γ_j is the angle of coupler in j^{th} precision position relative to the first precision position. Hence, if Θ_{31} is determined, then Θ_{3j} can be easily calculated. For function generation synthesis case, this may be free choice or can be solved for from kinematic equations. However, for the other synthesis cases requiring use of dyads such as motion generation Θ_{31} is not readily available.

For weakly coupled system of equations, Θ_{31} can be determined separately from kinematic equations after solving loop-closure equations. However, for strongly coupled system, it needs to be solved simultaneously and can be easily obtained from use of coupler equation as follows (Figure 2.3):

$$Z_3 - Z_5 + Z_6 = 0 \tag{37}$$

Accordingly, for strongly coupled, torque specification case, except for the function generation, the number of equations and number of unknowns are increased by two and are indicated within brackets in Tables 3.2-3.4.

3.3. SYNTHESIS CASE WITH NON-PRESCRIBED ENERGY-FREE STATE

Consider a synthesis case, where energy-free state of the compliant mechanism is different from prescribed positions.

Table 3.1. Design Choices Based on Number of Torsional Springs for Function Generation Synthesis with Compliance

Number of Torsional Springs	Number of Equations	Number of Unknowns	Number of Free Choices
Three Precision Positions			
1	7	$Z_2,\ Z_3,\ Z_4, \gamma_2, \gamma_3, K_1, \beta_{10}$ (10)	3 (s.c.)
2	9*	$Z_2, Z_3, Z_4, \gamma_2, \gamma_3, K_1, K_2, \Theta_{20}, \Theta_{30}, \Theta_{40}$ (13)	4 (w.c.)
3	9*	" $+ K_3$ (14)	5 (w.c.)
4	9*	" $+ K_4$ (15)	6 (w.c.)
Four Precision Positions			
1	10	$Z_2, Z_3, Z_4, \gamma_2, \gamma_3, \gamma_4, K_1, \beta_{10}$ 11)	1 (s.c.)
2	14*	$Z_1, Z_2, Z_3, Z_4, \gamma_2, \gamma_3, \gamma_4, K_1, K_2, \Theta_{20}, \Theta_{30}, \Theta_{40}$ (16)	2 (s.c.)
3	12	$Z_2, Z_3, Z_4, \gamma_2, \gamma_3, \gamma_4, K_1, K_2, K_3, \Theta_{20}, \Theta_{30}, \Theta_{40}$ (15)	3 (w.c.)
4	12	" $+ K_4$ (16)	4 (w.c.)
Five Precision Positions			
2	17*	$Z_2, Z_3, Z_4, \gamma_2, \gamma_3, \gamma_4, \gamma_5, K_1, K_2, \Theta_{20}, \Theta_{30}, \Theta_{40}$ (17)	0 (s.c.)
4	17*	$Z_2, Z_3, Z_4, \gamma_2, \gamma_3, \gamma_4, \gamma_5, K_1, K_2, K_3, \Theta_{20}, \Theta_{30}, \Theta_{40}$ (18)	1 (s.c.)
5	15	" $+ K_4$ (17)	2 (w.c.)

* Equation (38) gives two more scalar equations. s.c. and w.c. denotes the strongly and weakly coupled system.

For a pseudo-rigid-body four-bar mechanism with more than one spring, the deflection-free state of the one spring doesn't govern the deflection-free state of the other springs. But for the monolithic compliant mechanism, the energy-free state of the one compliant segment implies the energy-free state of the all compliant segments in the

mechanism at that position. Thus, while synthesizing the compliant mechanism, the deflection-free state of all springs in pseudo-rigid-body mechanism should be related with each other. Even if the resulting mechanism may be valid pseudo-rigid-body mechanism with independent springs, it cannot be a valid one-piece compliant mechanism until the deflection-free states of the torsional springs are not related with each other. These additional constraints need to relate the deflection-free state angles (Θ_{n0}) of the springs with one another. At the energy-free state of the mechanism i.e. at the zero-energy position of the mechanism, β_{i0} of the springs are related to the pseudo-rigid-body link angles Θ_{n0} by equation (19). Since, Θ_{n0} are the part of designed pseudo-rigid-body mechanism, they need to satisfy the following four-bar loop-closure equation in energy-free position of the mechanism, where, the subscript '0' refers to the energy-free state of the mechanism.

$$Z_{20} + Z_{30} = Z_1 + Z_{40} \tag{38}$$

This equation provides additional constraints to the deflection-free state of the springs in the mechanism. The equation (38) would suffice to satisfactorily synthesize the weakly coupled system. However for a strongly coupled system, few additional equations are needed for satisfactory solution. For example, for strongly coupled function generation synthesis case with non-prescribed energy-free state, the equations (2), (18) or (36), and (38), adds Z_1 as an additional unknown. To accommodate these two new unknowns, first-precision position four-bar loop-closure equation as below is used.

Table 3.2. Design Choices Based on Number of Torsional Springs for Path Generation Synthesis with Compliance

Number of Torsional Springs	Number of Equations	Number of Unknowns	Number of Free Choices
Three Precision Positions			
1	11[+2*]	$Z_2, Z_4, Z_5, Z_6, \phi_2, \phi_3, \gamma_2, \gamma_3, \psi_2, \psi_3, K_1, \beta_{10}$ (16)[+2**]	5 (s.c.)
2	13	$Z_2, Z_4, Z_5, Z_6, \phi_2, \phi_3, \gamma_2, \gamma_3, \psi_2, \psi_3, K_1, K_2, \Theta_{20}, \Theta_{30}, \Theta_{40}$ (19)	6 (w.c.)
3	13	" $+ K_3$ (20)	7 (w.c.)
4	13	" $+ K_4$ (21)	8 (w.c.)
Four Precision Positions			
1	16[+2*]	$Z_2, Z_4, Z_5, Z_6, \phi_2, \phi_3, \phi_4, \gamma_2, \gamma_3, \gamma_4, \psi_2, \psi_3, \psi_4, K_1, \beta_{10}$ (19)[2**]	3 (s.c.)
2	22$	$Z_1, Z_2, Z_3, Z_4, Z_5, Z_6, \phi_2, \phi_3, \phi_4, \gamma_2, \gamma_3, \gamma_4, \psi_2, \psi_3, \psi_4, K_1, K_2, \Theta_{20}, \Theta_{30}, \Theta_{40}$ (26)	4 (s.c.)
3	18	$Z_2, Z_4, Z_5, Z_6, \phi_2, \phi_3, \phi_4, \gamma_2, \gamma_3, \gamma_4, \psi_2, \psi_3, \psi_4, K_1, K_2, K_3, \Theta_{40}$ (23)	5 (w.c.)
4	18	" $+ K_4$ (14)	4 (w.c.)
Five Precision Positions			
1	21[+2*]	$Z_2, Z_4, Z_5, Z_6, \phi_2, \phi_3, \phi_4, \phi_5, \psi_2, \psi_3, \psi_4, \psi_5, K_1, \beta_{10}$ (22)[+2**]	3 (s.c.)
2	27$	$Z_1, Z_2, Z_3, Z_4, Z_5, Z_6, \phi_2, \phi_3, \phi_4, \phi_5, \gamma_2, \gamma_3, \gamma_4, \gamma_5, \psi_2, \psi_3, \psi_4, \psi_5, K_1, K_2, \Theta_{20}, \Theta_{30}, \Theta_{40}$ (29)	2 (s.c.)
3	27$	" $+ K_3$ (30)	3 (s.c.)
4	23	$Z_2, Z_4, Z_5, Z_6, \phi_2, \phi_3, \phi_4, \phi_5, \gamma_2, \gamma_3, \gamma_4, \gamma_5, \psi_2, \psi_3, \psi_4, \psi_5, K_1, K_2, K_3, K_4, \Theta_{20}, \Theta_{30}, \Theta_{40}$ (27)	4 (w.c.)

* Equation (39) gives two more scalar equations. $ Equation (38) gives two more scalar equations. ** Z_3 adds two unknowns. s.c. and w.c. denotes the strongly and weakly coupled system

Table 3.3. Design Choices Based on Number of Torsional Springs for Motion Generation Synthesis with Compliance

Number of Torsional Springs	Number of Equations	Number of Unknowns	Number of Free Choices
Three Precision Positions			
1	11[+2*]	$Z_2, Z_4, Z_5, Z_6, \phi_2, \phi_3, \psi_2, \psi_3, K_1, \beta_{10}$ (14)[+2**]	3 (s.c.)
2	13	$Z_2, Z_4, Z_5, Z_6, \phi_2, \phi_3, \psi_2, \psi_3, K_1, K_2, \Theta_{20}, \Theta_{30}, \Theta_{40}$ (17)	4 (w.c.)
3	13	$" + K_3$ (18)	5 (w.c.)
4	13	$" + K_4$ (19)	6 (w.c.)
Four Precision Positions			
1	16[+2*]	$Z_2, Z_4, Z_5, Z_6, \phi_2, \phi_3, \phi_4, \psi_2, \psi_3, \psi_4, K_1, \beta_{10}$ (16)[2**]	0 (s.c.)
2	22[$]	$Z_1, Z_2, Z_3, Z_4, Z_5, Z_6, \phi_2, \phi_3, \phi_4, \psi_2, \psi_3, \psi_4, K_1, K_2, \Theta_{20}, \Theta_{30}, \Theta_{40}$ (23)	1 (s.c.)
3	18	$Z_2, Z_4, Z_5, Z_6, \phi_2, \phi_3, \phi_4, \psi_2, \psi_3, \psi_4, K_1, K_2, K_3, \Theta_{20}, \Theta_{30}, \Theta_{40}$ (23)	2 (w.c.)
4	18	$" + K_4$ (24)	3 (w.c.)
Five Precision Positions			
4	23	$Z_2, Z_4, Z_5, Z_6, \phi_2, \phi_3, \phi_4, \phi_5, \psi_2, \psi_3, \psi_4, \psi_5, K_1, K_2, K_3, K_4, \Theta_{20}, \Theta_{30}, \Theta_{40}$ (23)	0 (w.c.)

[*] Equation (39) gives two more scalar equations. [$] Equation (38) gives two more scalar equations. ** Z_3 adds two unknowns. s.c. and w.c. denotes the strongly and weakly coupled system.

Table 3.4. Design Choices Based on Number of Torsional Springs for Path Generation with Prescribed Timing Synthesis with Compliance

Number of Torsional Springs	Number of Equations	Number of Unknowns	Number of Free Choices
Three Precision Positions			
1	11[+2*]	$Z_2,\ Z_4,\ Z_5,\ Z_6, \gamma_2, \gamma_3, \psi_2, \psi_3, K_1, \beta_{10}$ (14)[+2**]	3 (s.c.)
2	13	$Z_2,\ Z_4,\ Z_5,\ Z_6, \gamma_2, \gamma_3, \psi_2, \psi_3, K_1, K_2, \Theta_{20}, \Theta_{30}, \Theta_{40}$ (17)	4 (w.c.)
3	13	" $+ K_3$ (18)	5 (w.c.)
4	13	" $+ K_4$ (19)	6 (w.c.)
Four Precision Positions			
1	16[+2*]	$Z_2,\ Z_4,\ Z_5,\ Z_6, \gamma_2, \gamma_3, \gamma_4, \psi_2, \psi_3, \psi_4, K_1, \beta_{10}$ (16)[2**]	0 (s.c.)
2	22[$]	$Z_1, Z_2, Z_3, Z_4, Z_5, Z_6, \gamma_2, \gamma_3, \gamma_4, \psi_2, \psi_3, \psi_4, K_1, K_2, \Theta_{20}, \Theta_{30}, \Theta_{40}$ (23)	1 (s.c.)
3	18	$Z_2,\ Z_4,\ Z_5,\ Z_6, \gamma_2, \gamma_3, \gamma_4, \psi_2, \psi_3, \psi_4, K_1, K_2, K_3, \Theta_{20}, \Theta_{30}, \Theta_{40}$ (23)	2 (w.c.)
4	18	" $+ K_4$ (24)	3 (w.c.)
Five Precision Positions			
4	23	$Z_2,\ Z_4,\ Z_5,\ Z_6, \gamma_2, \gamma_3, \gamma_4, \gamma_5, \psi_2, \psi_3, \psi_4, \psi_5, K_1, K_2, K_3, K_4, \Theta_{20}, \Theta_{30}, \Theta_{40}$ (23)	0 (w.c.)

[*] Equation (38) gives two more scalar equations. [$] Equation (37) gives two more scalar equations. ** Z_3 adds two unknowns. s.c. and w.c. denotes the strongly and weakly coupled system

$$Z_2 + Z_3 = Z_1 + Z_4 \tag{39}$$

For the remaining synthesis cases; Z_1 and Z_3 become additional unknowns. In order to accommodate these, the coupler equation (37) is used in addition to the equation (39). Thus, the system accumulates the four more scalar equations. The above discussion is applicable to the four-bar synthesis case with two or more springs. For pseudo-rigid-body four-bar mechanism with one spring, the energy-free state of that spring will be the energy-free state of the mechanism and so no additional constraints are required.

As mentioned before, above discussion assumes the energy-free state of the mechanism is different from the prescribed positions of the mechanism. If the energy-free state of the mechanism is assumed to be one of the prescribed positions, then reduced system of equations can be used for synthesis. In Tables 3.3 and 3.4, for five precision positions synthesis, the cases with one, two and three springs are not included due to over-constraining of the system with more number of equations than more number of unknowns. In Tables 3.2-3.4, the numbers in the brackets refer to additional equations or unknowns arising, when the torque is specified at the precision positions instead of energies. The synthesis with compliance method using strongly coupled and weakly coupled system of equations can be represented as flowchart shown Figure 3.3.

3.4. LIMITATIONS/PROBLEMS WITH SYNTHESIS WITH COMPLIANCE TECHNIQUE

Though the synthesis with compliant technique is useful to synthesize compliant mechanisms for specified energy/torques at precision positions, it has some limitations/problems. In next section, these limitations/problems are presented.

- The synthesis with compliance technique solves the kinematic and energy/torque equations using strongly coupled and weakly coupled system approach depending on the number of unknowns in common (condition given by the equation (32)). The kinematic and energy/torque equations are nonlinear equations and generally solving nonlinear equations by coupling increases the complexity of the system and computational time also. It will be advantageous if the coupling between kinematic and energy/torque equations can be reduced and equations can be solved separately.
- The variables involved in the system include kinematic and energy variables. They are generally more than number of equations. In order to solve the equations, the user has to assign reasonable values to selected free choices and initial guesses to the remaining unknowns. In the strongly coupled system of equations, kinematic and energy/torque equations are solved simultaneously and numbers of variables are more. It becomes cumbersome to assign the reasonable values to large number of variables.

  e.g. from Table 3.3, for three precision positions motion generation synthesis with one spring for energy specification, which is strongly coupled case, the number of equations involved are 11 and number of variables are 14, giving 3 free choices. It is little more cumbersome to assign reasonable values to all of 14 different variables in order to get reasonable solution.
- In weakly coupled system of equations, kinematic equations are solved separately and kinematic configuration is solved for, before solving the energy/torque equations; as a result the latter system frequently yields negative solutions for

spring stiffness values, which cannot be currently controlled. It has been observed that specification of energy values at all the precision positions tends to over-constrain the energy equations and yield negative values for the spring stiffness values (Annamalai, 2003).

e.g. A compliant mechanism with fully-compliant segment is to be designed for three precision positions, path generation with prescribed timing synthesis for energy specifications as follows (Annamalai,2003):

$\delta_2 = 0.822 - 0.076\mathrm{i}$ $\delta_3 = 1.802 - 0.24\mathrm{i}$

$\phi_2 = -4°$ $\phi_3 = -9°$

$E_1 = 3.14\ \mathrm{in} - \mathrm{lb}$ $E_2 = 8.0\ \mathrm{in} - \mathrm{lb}$ $E_3 = 16.5\ \mathrm{in} - \mathrm{lb}$

Assuming four torsional springs in pseudo-rigid-body mechanism resulting system is weakly coupled with 13 equations and 19 unknowns, thus 6 free choices. Selecting $R_2, \Theta_{21}, R_4, \Theta_{41}$ as free choices for solving kinematic equations yield following solution.

$Z_1 = 4.384 + 0.177\mathrm{i}$ $Z_2 = 1.885 + 9.815\mathrm{i}$

$Z_3 = 2.231 - 1.092\mathrm{i}$ $Z_4 = -0.268 + 8.546\mathrm{i}$

K_2, K_3 are selected as remaining two free choices $(= 42\mathrm{lb} - \mathrm{in})$ to solve energy equations and following solution is obtained:

$K_1 = -30.67\ \mathrm{lb} - \mathrm{in/rad}$ $K_4 = 85.98\ \mathrm{lb} - \mathrm{in/rad}$

This is not a satisfactory solution as spring stiffness K_1 is negative.

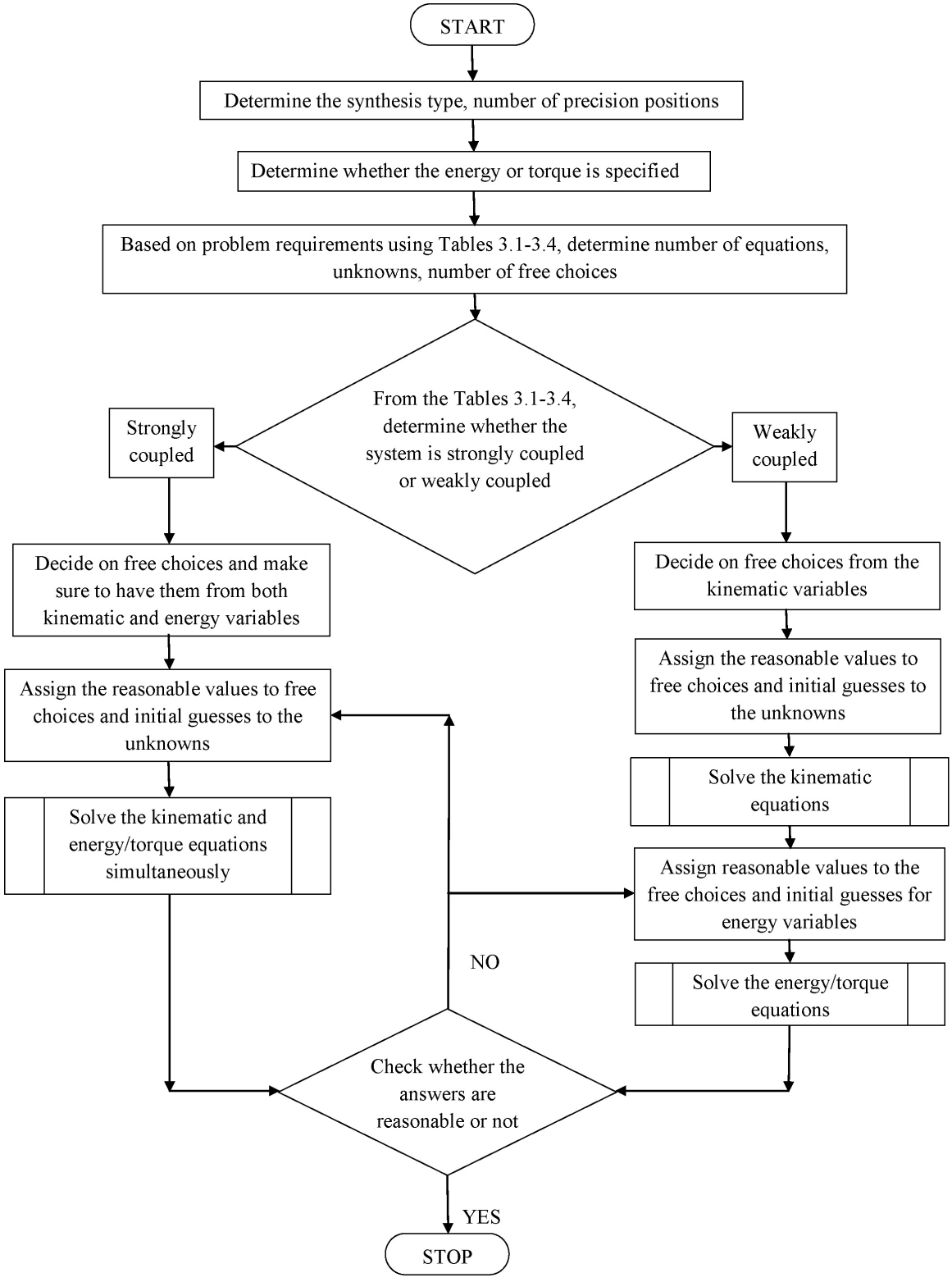

Figure 3.3. A Flowchart Showing Synthesis with Compliance Technique

- Because of the nonlinearity of the equations involved in the system, the solutions are very sensitive to the values assigned to the free choices and initial guesses. Even the slight change in their values won't give solutions or may give unreasonable solutions.

  e.g. In the above example, while solving the energy equations we have 3 energy equations and 2 zero-energy state loop-closure equations with 7 unknowns: 4 spring constants, $K_1,\ K_2\ ,\ K_3,\ K_4$ and 3 zero-energy position link angles, $\Theta_{20},\ \Theta_{30},\ \Theta_{40}$. In order to solve this system, two variables let $K_2 = 50\ \text{lb} - \text{in/rad}$ and $K_3 = 50\ \text{lb} - \text{in/rad}$ are selected as free choices and initial guesses are assigned to the remaining the 5 variables as follows:

  $K_1 = 40\ \text{lb} - \text{in/rad}, \quad K_4 = 40\ \text{lb} - \text{in/rad}, \quad \Theta_{20} = \Theta_{21} = 79.129°,$

  $\Theta_{30} = \Theta_{31} = -26.071°,$ and $\Theta_{40} = \Theta_{41} = 91.798°$

  The energies specified at three precision positions are

  $E_1 = 3.14\ \text{in} - \text{lb} \quad E_2 = 8.0\ \text{in} - \text{lb} \quad E_3 = 16.5\ \text{in} - \text{lb}$

  With these values, the solution is obtained as follows:

  $K_1 = 32.664\ \text{lb} - \text{in/rad} \qquad K_4 = 2.434\ \text{lb} - \text{in/rad}$

  However, if energy value at first precision position is changed slightly from $3.14\ \text{in} - \text{lb}$ to $3.15\ \text{in} - \text{lb}$, following solution is obtained with one spring constant negative which is not acceptable.

  $K_1 = 65.718\ \text{lb} - \text{in/rad} \qquad K_4 = -20.154\ \text{lb} - \text{in/rad}$

- If the system of equations yields the negative or the unrealistic solutions, one approach is to change free choices until a reasonable solution is achieved (Howell, 2001); but this may require many iterations to get the desired solution,

especially for a strongly coupled system and there is no way for the user to assist in assigning values to free choices and initial guesses so as to achieve the realistic solutions easily.

Some efforts have been done to overcome some of above-mentioned problems. In order, not to over-constrain the energy equations which may yield negative spring stiffness values in weakly coupled system of equations, (Annamalai, 2003) suggested to solve the energy equations by taking energy at one of the precision positions to be unknown instead of specifying all the energies.

e.g. The example presented above (Annamalai, 2003) has one of spring constant negative, in order to overcome this problem, E_1 is treated as unknown and K_1, K_2, K_3 are selected as free choices and solution obtained is

$E_1 = 3.16 \text{ in} - \text{lb}$ $K_4 = 37.682 \text{ in} - \text{lb/rad}$

Even for the strongly coupled system of equations, wherein all the kinematic and energy/torque unknowns would be simultaneously solved for, it has been suggested to take care while selecting free choices so as not to nearly completely define kinematic configuration and this may give unrealistic solutions.

In order to get multiple solutions, which includes realistic and unrealistic solutions, Tari and Su (2011) developed polynomial solver based framework for solving kinetostatic synthesis equations. They approximated the nonlinear energy equations into polynomials using numerical approximations and generated multiple solutions using polynomial homotopy technique and then sifted out the solutions with negative spring stiffness values.

3.5. OPTIMIZATION APPROACH IN SYNTHESIS WITH COMPLIANCE TECHNIQUE

A new, simple way to solve kinematic and energy/torque equations is proposed using optimization approach that overcomes some of the above-mentioned limitations/problems with synthesis with compliance technique. This method is briefly introduced in the following paragraphs and it will be explained in detail in Section 4.

In the new approach, instead of solving kinematic and energy/torque equations as strongly coupled and weakly coupled system, they are solved as weakly coupled system only. The kinematic loop-closure equations are solved using conventional nonlinear equations solving algorithms such as Newton-Raphson algorithm; while energy/torque equations are solved by using constrained optimization technique. This solves many of above-mentioned limitations/problems associated with the existing method.

In this method, the coupling between kinematic and energy/torque equations is reduced and the equations are solved as weakly coupled system, thus making the method computationally simple and fast.

Due to weakly coupled system of equations, kinematic and energy variables are separated from each other and so user has to assign reasonable values to the relatively less number of variables (for kinematic variables only). Due to the use of optimization for solving energy/torque equations, the user is not required to make free choices for solving these equations.

Thus, the sensitivity of solutions to the values assigned to the free choices and initial guesses is somewhat reduced. e.g. In the example presented in above section, the solutions are very sensitive to the values assigned to the free choices and initial guesses. When the same energy equations are solved by new approach using optimization, the

solutions are not changed much with the little changes in values assigned to the variables. Here, the zero-energy position loop-closure equations are solved separately. So there will be 3 energy equations and 4 unknown spring constants. In the previous method, user has to select two of the spring constants as free choices but in optimization approach user is not required to make free choices. The initial values are assigned 4 spring constants as follows with same energies as in the above example.

$K_1 = 40\ \text{lb} - \text{in/rad}$, $K_2 = 50\ \text{lb} - \text{in/rad}$,

$K_3 = 50\ \text{lb} - \text{in/rad}$, $K_4 = 40\ \text{lb} - \text{in/rad}$

$E_1 = 3.14\ \text{in} - \text{lb}$ $E_2 = 8.0\ \text{in} - \text{lb}$ $E_3 = 16.5\ \text{in} - \text{lb}$

The solution obtained is as follows

$K_1 = 38.5034\ \text{lb} - \text{in/rad}$, $K_2 = 44.0435\ \text{lb} - \text{in/rad}$,

$K_3 = 42.3228\ \text{lb} - \text{in/rad}$, $K_4 = 37.5872\ \text{lb} - \text{in/rad}$

When the energy value at first precision position is changed from $3.14\ \text{in} - \text{lb}$ to $3.15\ \text{in} - \text{lb}$, the solution is not changed much and it is still acceptable.

$K_1 = 38.5042\ \text{lb} - \text{in/rad}$, $K_2 = 44.0473\ \text{lb} - \text{in/rad}$,

$K_3 = 42.3279\ \text{lb} - \text{in/rad}$, $K_4 = 37.5886\ \text{lb} - \text{in/rad}$

One of the main problems with synthesis of compliance technique is negative or unreasonable values of the spring constants in the solution of weakly coupled system. This is overcome by applying lower and upper bounds to the solutions in the optimization for solving energy/torque equations. e.g. the example presented above shows that synthesis with compliance technique gives negative answer for one of spring constant but with new approach, the solutions are positive and acceptable.

While solving the energy/torque equations using constrained optimization technique, the objective function is evaluated at each solution point. This value gives a way to the user, to decide the direction, in which the values assigned to the initial guesses or energy specifications should change, if required, to get an acceptable solution. This will significantly reduce the number of iterations to get the solution.

3.6. SUMMARY

The synthesis with compliance method is explained in detail. The energy and torque considerations for synthesis are presented along with kinematic equations. The tables giving information about number of equations, number of unknowns and number of free choices for different synthesis cases with varying number of springs in four-bar pseudo-rigid-body model are enlisted. The limitations/problems with the current synthesis with compliance technique are explained with suitable examples. At the end of the Section, new method for solving kinematic and energy/torque equations using optimization approach, which overcomes limitations/problems with existing method is introduced.

4. SYNTHESIS WITH COMPLIANCE TECHNIQUE WITH OPTIMIZATION APPROACH AND DIFFERENT CASES

The synthesis with compliance technique suffers from some limitations/problems as discussed previous Section. To overcome these problems, a new approach for synthesis with compliance technique using optimization is introduced in Section 3. In this Section, the optimization concept is briefly reviewed at the beginning followed by explanation of use of optimization in the synthesis with compliance technique. The optimization routine developed for energy equations is discussed later along with suitable examples. The different cases of synthesis like use of type synthesis i.e. use of small-length flexural pivots or full-length compliant segments to replace the springs in the pseudo-rigid-body model, and other cases like undeflected position of the mechanism to be one of the precision positions etc. are presented with examples. The energy equivalence of pseudo-rigid-body model and corresponding compliant mechanism is discussed and comparison between the solutions obtained using pseudo-rigid-body models and commercial finite element software ABAQUS® and ANSYS® is presented. Finally, few recommendations for energy/torque to be specified at the precision positions are suggested.

4.1. INTRODUCTION TO OPTIMIZATION

Optimization is a design tool which helps user automatically to identify the optimal design from number of available design solutions or even from the infinite number of design solutions (Rao, 2009). The use of optimization is increasing in the industry to select optimal designs as it provides a designer with cheap and efficient way

to identify the optimal solution before physical deployment. Even the optimization is used in day-to-day life regularly. e.g. one may want to minimize the monthly expenditure for resources maintaining certain level of living or while buying a car, one may want to meet certain exceptions like fuel economy, maintenance costs etc. with a maximum limit for the price. Engineering designs also work in the same way, where objectives are met or optimized satisfying some design constraints.

The first step in the optimization is creating the optimization model in mathematical formulations known as optimization modeling (Nocedal and Wright, 2000). The modeling involves deciding the objective, a quantitative measure for the performance of a system under study. e.g. the objective of the study could be maximizing profit, minimizing expenditure etc. The objective depends on the certain characteristics of the system known as design variables or unknowns. These variables are often constrained in some way but they may be unconstrained at times. The goal of the optimization problem is finding the values of these variables which optimize the objective. The modeling is the first and the most important step in the optimization process. If the model is too simplistic, it may not give useful insights into the practical problem; and if it is too complex, it may be difficult to solve (Nocedal and Wright, 2000).

After creating the model, the second step in the optimization process is the solving the model. Three methods are generally used and they are analytical method, graphical method and numerical method (Rao, 2009). The use of analytical and graphical methods is limited to the simple problems such as problems with simple objective function. Usually engineering design problems are complex and include too many design variables with complicated objective functions and constraints (Rao, 2009). In such cases,

numerical methods are used to solve the optimization models. With numerical method, the optimal design starts from initial design point. The numerical optimizer evaluates the objective function, constraints and their derivatives at the design point. Based on the function value and derivatives, the solver decides the search direction along which the objective function is likely to descend. The step size along the descent direction is decided, so that the value of objective function decreases to the lowest possible value without violating any constraints. The current design point moves in the descent direction by the step size to the new design point in the next iteration. The solver evaluates the objective function, constraints and derivatives at the new design point and check for the convergence of the solution. If the solution does not converge, then solver finds new search direction and step size to obtain new design point and continues to do so until it finds the optimal solution.

The last step in the optimization process is the posterior analysis in which the user performs some analyses tasks on the optimal solution to determine whether the solution is optimal, whether it is reasonable etc. The optimal solution obtained depends on where optimization search process starts; when multiple local optimal points exist. So in order to obtain the global optimal solution different starting points should be used.

4.1.1. Optimization Design Process and Mathematical Modeling. The above discussed steps in the optimization design process can be shown in flowchart as shown in Figure 4.1. Mathematically, optimization is the minimization or maximization of an objective function subject to constraints of the variables.

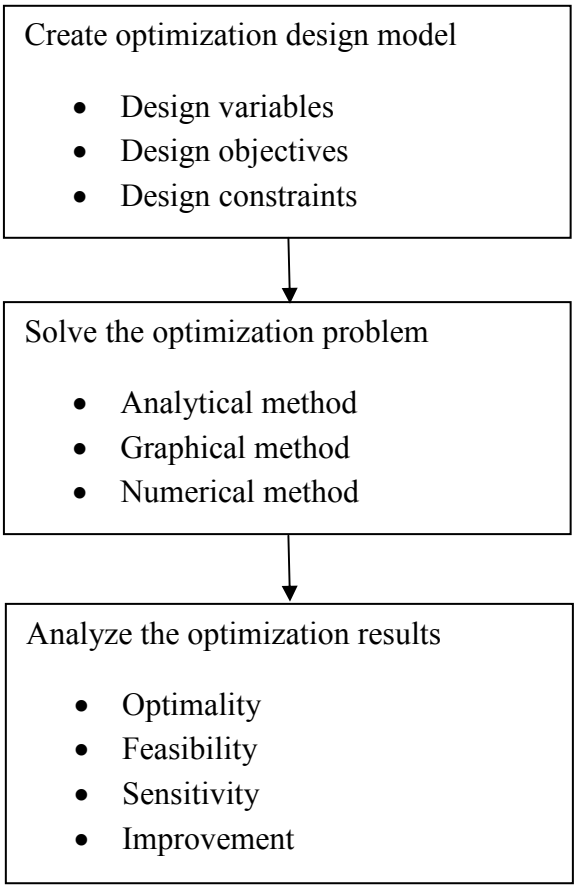

Figure 4.1. A Flowchart Showing Optimization Design Process

A standard optimization model (Rao, 2009) can be written as follows:

$$\min_{x} f(x_1, x_2, \ldots x_n)$$

subject to

$$c_i(x_1, x_2, \ldots x_n) \leq 0, \quad i = 1,2, \ldots n_i$$

$$ceq_j(x_1, x_2, \ldots x_n) = 0, \quad j = 1,2, \ldots n_e$$

$$lb_k \leq x_k \leq ub_k, \quad k = 1,2, \ldots n$$

where, $x = (x_1, x_2, \ldots x_n)$ is the vector of design variables that is to be determined during the process, $f(x_1, x_2, \ldots x_n)$is the objective function that is to be minimized,

$c_i(x_1, x_2, \ldots x_n)$ is the inequality constraint function, $ceq_j(x_1, x_2, \ldots x_n)$ is the equality constraint function, lb_k and ub_k are the lower and the upper bounds of the design variable respectively. If the designer wishes to maximize the objective function; $f(x_1, x_2, \ldots x_n)$ is changed to $-f(x_1, x_2, \ldots x_n)$

Different software can be used to solve the optimization problems such as Microsoft Excel, MATLAB® etc. In this work, MATLAB® is used to solve the optimization problems, as it is easier to write the three separate files for objective function file containing objective function, constraints file containing equality and inequality constraints & lower and upper bounds and main file that calls the objective function, constraints functions and solves the problem. They can be edited easily if they are written separately.

4.2. TYPES OF OPTIMIZATION.

The optimization problems can be classified according to the nature of the objective function, constraints (e.g. linear, nonlinear, convex), the nature of the variables (e.g. small, large), the smoothness of the functions (e.g. differentiable, or non-differentiable) and so on (Nocedal and Wright, 2000). One of the important classifications of the optimization problems is according to the constraints on the variables i.e. unconstrained optimization which has no constraints and constrained optimization in which the variables are constrained in some way.

4.2.1. Unconstrained Optimization. In this type of optimization, the variables are unconstrained. Sometimes for the problems with the natural constraints, it may be safe to disregard the constraints on the variables as they do not affect the solution or the

do not interfere with the solution (Nocedal and Wright, 2000). In the unconstrained optimization, the objective function is minimized that depends upon real variables and without restrictions. There are many algorithms available for the unconstrained optimization of smooth functions. All of them require the user to give a starting point. It will be easy for the user who has knowledge of the application and data set of the problem to give a reasonable initial starting point. Most of the algorithms use two strategies to move to the next design point from the starting point i) Line search methods and ii) Trust region methods. More information about these strategies and unconstrained optimization can be found in *Numerical Optimization* Nocedal and Wright, 2000.
The mathematical formulation for this kind of optimization is as follows:

$$\min_{x} f(x)$$

with no restrictions on variables.

The MATLAB® provides many different solvers for the unconstrained optimization such as fminunc, fminsearch etc. It is the user's responsibility to choose the right solver of the optimization problem depending on type of objective function and constraint functions. More information on choosing right type of optimization solver can be found in HELP in MATLAB®.

4.2.2. Constrained Optimization. In this type of optimization, there are some constraints on the variables e.g. size or shape constraint in design problem or expenditure constraints on the profitability problem etc. These constraints may be simple bounds on the variables like $0 \leq x_1 \leq 100$ or some linear unequality constraints such as $x_1 + x_2 < 500$ or linear equality constraints $x_1 - x_2 = 50$ or it may be some complex nonlinear

relationships among the variables. A mathematical formulation of these optimization problems is (Nocedal and Wright, 2000) as follows:

$$\min_{x} f(x)$$

$$\text{subject to}$$

$$c_i(x) \leq 0, \qquad i = 1,2, \dots n_i$$

$$ceq_j(x) = 0, \qquad j = 1,2, \dots n_e$$

$$lb_k \leq x_k \leq ub_k, \quad k = 1,2, \dots n$$

where, $f(x)$ is a objective function, $c_i(x)$ are the unequality constraints, $ceq_j(x)$ are the equality constraints and lb_k, & ub_k represents the lower and upper bounds for the design variable x respectively.

For the constrained optimization, MATLAB® has many different solvers, such as fmincon, fminbnd, fseminf etc. Each solver is used to solve particular type of problems, e.g. fminbnd is used to find the minimum of a single-variable function on a fixed interval, fseminf is used to find semi-infinitely constrained multivariable nonlinear function and fmincon is used to minimum of constrained nonlinear multivariable function. In this work, the MATLAB® optimization solver, fmincon is used to solve the optimization problem.

4.3. OPTIMIZATION ROUTINE FOR SOLVING ENERGY/TORQUE EQUATIONS IN SYNTHESIS WITH COMPLIANCE TECHNIQUE

In the synthesis with compliance technique, the kinematic and energy/torque equations are solved either strongly coupled or weakly coupled depending on the number on the equations and unknowns introduced in the system due to energy/torque

considerations using conventional nonlinear equations solver algorithm. A new way is proposed to solve the kinematic equations by conventional algorithm and energy/torque equations by optimization approach separately.

The optimization design process involves the three steps as shown in Figure 4.1. The first step is creating optimization design model which includes objective function and constraint functions. The energy/torque considerations introduce number of energy/torque equations in the system in addition to the kinematic equations depending on the number of precision positions and energy/torque specified at the precision positions. Let us consider a general synthesis case: A four-bar mechanism with four torsional springs at the pivots is to be synthesized for three precision positions with energy specifications for motion generation. The system has 8 loop-closure kinematic equations given by equations (13), 3 energy equations at three precision positions given by equations (21) and 2 scalar loop-closure equations at the energy-free state of the mechanism given by equation (38). The loop-closure kinematic equations are as follows:

$$R_2[\cos(\Theta_{21}+\phi_2)-\cos(\Theta_{21})]+R_5[\cos(\Theta_{51}+\gamma_2)-\cos(\Theta_{51})]=\mathrm{Re}(\delta_2) \quad (13a)$$

$$R_2[\sin(\Theta_{21}+\phi_2)-\sin(\Theta_{21})]+R_5[\sin(\Theta_{51}+\gamma_2)-\sin(\Theta_{51})]=\mathrm{Im}(\delta_2) \quad (13b)$$

$$R_4[\cos(\Theta_{41}+\psi_2)-\cos(\Theta_{41})]+R_6[\cos(\Theta_{61}+\gamma_2)-\cos(\Theta_{61})]=\mathrm{Re}(\delta_2) \quad (13c)$$

$$R_4[\sin(\Theta_{41}+\psi_2)-\sin(\Theta_{41})]+R_6[\sin(\Theta_{61}+\gamma_2)-\sin(\Theta_{61})]=\mathrm{Im}(\delta_2) \quad (13d)$$

$$R_2[\cos(\Theta_{21}+\phi_3)-\cos(\Theta_{21})]+R_5[\cos(\Theta_{51}+\gamma_3)-\cos(\Theta_{51})]=\mathrm{Re}(\delta_3) \quad (13e)$$

$$R_2[\sin(\Theta_{21}+\phi_3)-\sin(\Theta_{21})]+R_5[\sin(\Theta_{51}+\gamma_3)-\sin(\Theta_{51})]=\mathrm{Im}(\delta_3) \quad (13f)$$

$$R_4[\cos(\Theta_{41}+\psi_3)-\cos(\Theta_{41})]+R_6[\cos(\Theta_{61}+\gamma_3)-\cos(\Theta_{61})]=\mathrm{Re}(\delta_3) \quad (13g)$$

$$R_4[\sin(\Theta_{41}+\psi_3)-\sin(\Theta_{41})]+R_6[\sin(\Theta_{61}+\gamma_3)-\sin(\Theta_{61})]=\mathrm{Im}(\delta_3) \quad (13h)$$

Thus, there are 8 equations and 12 unknowns for the motion generation synthesis. So, 4 free choices are required to solve the above equations and to obtain the kinematic configuration. The 3 energy equations and vector loop-closure equation for zero-energy position are as follows:

$$E_1 = \frac{1}{2}[K_1(\Theta_{21} - \Theta_{20})^2 + K_2[(\Theta_{31} - \Theta_{30}) - (\Theta_{21} - \Theta_{20})]^2 + K_3[(\Theta_{41} - \Theta_{40}) - (\Theta_{31} - \Theta_{30})]^2 + K_4(\Theta_{41} - \Theta_{40})^2] \tag{21a}$$

$$E_2 = \frac{1}{2}[K_1(\Theta_{21} + \phi_2 - \Theta_{20})^2 + K_2[(\Theta_{31} + \gamma_2 - \Theta_{30}) - (\Theta_{21} + \phi_2 - \Theta_{20})]^2 + K_3[(\Theta_{41} + \psi_2 - \Theta_{40}) - (\Theta_{31} + \gamma_2 - \Theta_{30})]^2 + K_4(\Theta_{41} + \psi_2 - \Theta_{40})^2] \tag{21b}$$

$$E_3 = \frac{1}{2}[K_1(\Theta_{21} + \phi_3 - \Theta_{20})^2 + K_2[(\Theta_{31} + \gamma_3 - \Theta_{30}) - (\Theta_{21} + \phi_3 - \Theta_{20})]^2 + K_3[(\Theta_{41} + \psi_3 - \Theta_{40}) - (\Theta_{31} + \gamma_3 - \Theta_{30})]^2 + K_4(\Theta_{41} + \psi_3 - \Theta_{40})^2] \tag{21c}$$

$$Z_{20} + Z_{30} = Z_{10} + Z_{40} \tag{38}$$

The equation (38) will give 2 scalar equations and has 3 unknowns. These 2 equations are solved simultaneously with energy equations in the existing method. In the new approach, these 2 equations are separated from energy equations and solved by making one free choice. Thus, 3 energy equations have 4 spring stiffness as unknowns and all other variables are known from kinematic equations and from zero-energy loop-closure equations. The energy equations are solved using optimization. One of the main

problems with the synthesis with compliance technique is the solutions yielding negative and unrealistic spring stiffness values. This is overcome by constraining the spring stiffness values i.e. by applying the lower and upper bounds. The optimization problem is created as below:

$$f_1(K_1, K_2, K_3, K_4) = E_1 - \left\{\frac{1}{2}[K_1(\Theta_{21} - \Theta_{20})^2 + K_2[(\Theta_{31} - \Theta_{30}) - (\Theta_{21} - \Theta_{20})]^2 + K_3[(\Theta_{41} - \Theta_{40}) - (\Theta_{31} - \Theta_{30})]^2 + K_4(\Theta_{41} - \Theta_{40})^2]\right\}$$

$$f_2(K_1, K_2, K_3, K_4) = E_2 - \left\{\frac{1}{2}[K_1(\Theta_{21} + \phi_2 - \Theta_{20})^2 + K_2[(\Theta_{31} + \gamma_2 - \Theta_{30}) - (\Theta_{21} + \phi_2 - \Theta_{20})]^2 + K_3[(\Theta_{41} + \psi_2 - \Theta_{40}) - (\Theta_{31} + \gamma_2 - \Theta_{30})]^2 + K_4(\Theta_{41} + \psi_2 - \Theta_{40})^2]\right\}$$

$$f_3(K_1, K_2, K_3, K_4) = E_3 - \frac{1}{2}[K_1(\Theta_{21} + \phi_3 - \Theta_{20})^2 + K_2[(\Theta_{31} + \gamma_3 - \Theta_{30}) - (\Theta_{21} + \phi_3 - \Theta_{20})]^2 + K_3[(\Theta_{41} + \psi_3 - \Theta_{40}) - (\Theta_{31} + \gamma_3 - \Theta_{30})]^2 + K_4(\Theta_{41} + \psi_3 - \Theta_{40})^2]$$

$$f = f_1^2 + f_2^2 + f_3^2$$

Minimize f

Above equations form the objective function of the optimization problem. The upper and lower bounds are applied to the spring stiffness, K values, as per the user's requirement. The constraint function includes any restrictions on the design variables i.e. spring stiffness e.g. all spring stiffness are equal or a fixed-guided compliant segment has two torsional springs at the characteristic pivots in pseudo-rigid-body model. It will be convenient to size the compliant segment if two spring constants are same. This restriction on spring stiffness values should be put in the constraint function.

In MATLAB®, fmincon optimization solver is used for the constrained optimization. The same optimization routine can also be used for torque specifications instead of energy specifications at the precision positions. The equation for the torque at the j^{th} position of the mechanism is given by equation (36).

$$\begin{aligned} T_{2j} = {} & K_1(\Theta_{2j} - \Theta_{20}) \\ & + K_2\left[(\Theta_{3j} - \Theta_{30}) - (\Theta_{2j} - \Theta_{20})\right]\left(\frac{R_2 \sin(\Theta_{4j} - \Theta_{2j})}{R_3 \sin(\Theta_{3j} - \Theta_{4j})} - 1\right) \\ & + K_3\left[(\Theta_{4j} - \Theta_{40}) - (\Theta_{3j} - \Theta_{30})\right]\left(\frac{R_2 \sin(\Theta_{3j} - \Theta_{2j})}{R_4 \sin(\Theta_{3j} - \Theta_{4j})}\right. \\ & \left. - \frac{R_2 \sin(\Theta_{4j} - \Theta_{2j})}{R_3 \sin(\Theta_{3j} - \Theta_{4j})}\right) + K_4(\Theta_{4j} - \Theta_{40})\frac{R_2 \sin(\Theta_{3j} - \Theta_{2j})}{R_4 \sin(\Theta_{3j} - \Theta_{4j})} \end{aligned} \tag{36}$$

The objective function for torque specification case is formed in the same way as that for energy specification case. Using equation (36), the torque equations for three precision positions can be written as shown in equations (40). The Section 4.5 shows different cases/examples of compliant mechanism synthesis such as undeflected position of the mechanism to be different form precision positions, one precision position to be undeflected position of the mechanism etc.

4.3.1. Recommendations for Energy/Toque Specifications. The energy/torque specifications at the precision positions are input to the problem. As the kinematic loop-closure equations and energy/torque equations are nonlinear equations, specification of energy/torque values significantly affect the solution.

$$
\begin{aligned}
T_{21} = {} & K_1(\Theta_{21} - \Theta_{20}) \\
& + K_2[(\Theta_{31} - \Theta_{30}) - (\Theta_{21} - \Theta_{20})]\left(\frac{R_2 \sin(\Theta_{41} - \Theta_{21})}{R_3 \sin(\Theta_{31} - \Theta_{41})}\right. \\
& \left. - 1\right) \\
& + K_3[(\Theta_{41} - \Theta_{40}) - (\Theta_{31} - \Theta_{30})]\left(\frac{R_2 \sin(\Theta_{31} - \Theta_{21})}{R_4 \sin(\Theta_{31} - \Theta_{41})}\right. \\
& \left. - \frac{R_2 \sin(\Theta_{41} - \Theta_{21})}{R_3 \sin(\Theta_{31} - \Theta_{41})}\right) + K_4(\Theta_{41} - \Theta_{40})\frac{R_2 \sin(\Theta_{31} - \Theta_{21})}{R_4 \sin(\Theta_{31} - \Theta_{41})}
\end{aligned}
\tag{40a}
$$

$$
\begin{aligned}
T_{22} = {} & K_1\big((\Theta_{21} + \phi_2) - \Theta_{20}\big) \\
& + K_2\big[\big((\Theta_{31} + \gamma_2) - \Theta_{30}\big) \\
& - \big((\Theta_{21} + \phi_2) - \Theta_{20}\big)\big]\left(\frac{R_2 \sin\big((\Theta_{41} + \psi_2) - (\Theta_{21} + \phi_2)\big)}{R_3 \sin\big((\Theta_{31} + \gamma_2) - (\Theta_{41} + \psi_2)\big)}\right. \\
& \left. - 1\right) \\
& + K_3\big[\big((\Theta_{41} + \psi_2) - \Theta_{40}\big) \\
& - \big((\Theta_{31} + \gamma_2) - \Theta_{30}\big)\big]\left(\frac{R_2 \sin\big((\Theta_{31} + \gamma_2) - (\Theta_{21} + \phi_2)\big)}{R_4 \sin\big((\Theta_{31} + \gamma_2) - (\Theta_{41} + \psi_2)\big)}\right. \\
& \left. - \frac{R_2 \sin\big((\Theta_{41} + \psi_2) - (\Theta_{21} + \phi_2)\big)}{R_3 \sin\big((\Theta_{31} + \gamma_2) - (\Theta_{41} + \psi_2)\big)}\right) \\
& + K_4\big((\Theta_{41} + \psi_2) - \Theta_{40}\big)\frac{R_2 \sin\big((\Theta_{31} + \gamma_2) - (\Theta_{21} + \phi_2)\big)}{R_4 \sin\big((\Theta_{31} + \gamma_2) - (\Theta_{41} + \psi_2)\big)}
\end{aligned}
\tag{40b}
$$

$$
\begin{aligned}
T_{23} = {} & K_1\left((\Theta_{21} + \phi_3) - \Theta_{20}\right) \\
& + K_2\Big[\left((\Theta_{31} + \gamma_3) - \Theta_{30}\right) \\
& - \left((\Theta_{21} + \phi_3) - \Theta_{20}\right)\Big]\left(\frac{R_2 \sin\left((\Theta_{41} + \psi_3) - (\Theta_{21} + \phi_3)\right)}{R_3 \sin\left((\Theta_{31} + \gamma_3) - (\Theta_{41} + \psi_3)\right)}\right. \\
& \left. - 1\right) \\
& + K_3\Big[\left((\Theta_{41} + \psi_3) - \Theta_{40}\right) \\
& - \left((\Theta_{31} + \gamma_3) - \Theta_{30}\right)\Big]\left(\frac{R_2 \sin\left((\Theta_{31} + \gamma_3) - (\Theta_{21} + \phi_3)\right)}{R_4 \sin\left((\Theta_{31} + \gamma_3) - (\Theta_{41} + \psi_3)\right)}\right. \\
& \left. - \frac{R_2 \sin\left((\Theta_{41} + \psi_3) - (\Theta_{21} + \phi_3)\right)}{R_3 \sin\left((\Theta_{31} + \gamma_3) - (\Theta_{41} + \psi_3)\right)}\right) \\
& + K_4\left((\Theta_{41} + \psi_3) - \Theta_{40}\right)\frac{R_2 \sin\left((\Theta_{31} + \gamma_3) - (\Theta_{21} + \phi_3)\right)}{R_4 \sin\left((\Theta_{31} + \gamma_3) - (\Theta_{41} + \psi_3)\right)}
\end{aligned}
\tag{40c}
$$

In the synthesis with compliance technique, the random specifications of energies/torques may not yield the solution or may yield the negative or unrealistic solution such as with negative K values.

With the optimization approach, if the energies are specified randomly, there is chance that you may not get the solution or you may get the solution with all the spring stiffness values either at their lower or upper limits and with function value not close to zero at that solution point. But with this approach the answers will non-negative and within the bounds specified, so user will have control over the spring stiffness values. So, while specifying energies/torques at the precision positions care should to be taken. Instead of specifying values randomly, they should be related with the angles through

which the pseudo-rigid-body links with torsional springs are moving from one precision position to other. The function value at the solution is an indicator of the correctness of the solution. As the objective function is minimized for solving energy equations by optimization approach, its value at the solution point should be very close to zero. The synthesis with compliance method using optimization approach is shown as flowchart in Figure 4.2.

4.3.2. Notions on Energy Equivalence. The pseudo-rigid-body four-bar mechanism is a rigid-body four-bar mechanism with torsional springs at the pivot points, and the compliant mechanism represents the single continuum, where the some or all segments deflect and gives desired motion to the mechanism and stores energy in flexible segments. The synthesis with compliance technique initially helps in designing a pseudo-rigid-body mechanism and then using a pseudo-rigid-body model concept, the compliant mechanism is obtained.

The total energy stored in the pseudo-rigid-body mechanism is obtained by summing up the energies stored in the individual torsional springs at that precision position. The energy stored in the compliant segment has been calculated by chain algorithm assuming the bending energy to be predominant in planar compliant mechanism (Annamalai, 2003). In this work, the energy stored in the compliant mechanism is calculated using commercial finite element software ABAQUS® and/or ANSYS® as strain energy stored in the mechanism. Thus, the compliant mechanism designed for energy specifications, ensures the energy equivalence between compliant mechanism and its pseudo-rigid-body model.

In general, for any compliant mechanism synthesized using synthesis with compliance technique, it can be assured that energy stored in the compliant mechanism is of the same order of that of stored in pseudo-rigid-body model from which the compliant mechanism is obtained (Annamalai, 2003).

However, this energy equivalence does not necessarily ascertain the same the dynamic properties of the two mechanisms. The kinematics of the compliant mechanism is expected to vary in different degrees under different circumstances from that of corresponding pseudo-rigid-body model.

4.4. STRONGLY COUPLED VS. WEAKLY COUPLED SYSTEM

In the synthesis with compliance technique, the kinematic equations and energy/torque equations are solved as either strongly coupled or weakly coupled system of equations depending on the number of equations and number of unknowns introduced in the system by energy/torque considerations. The condition for the system to be solved as weakly coupled is given by equation (32). In the weakly coupled system, the kinematic equations and energy/torque equations are solved separately while in strongly coupled system, kinematic and energy/torque equations are solved simultaneously. However, as the kinematic and energy/torque equations are generally nonlinear, coupling between them increases the complexity of the system.

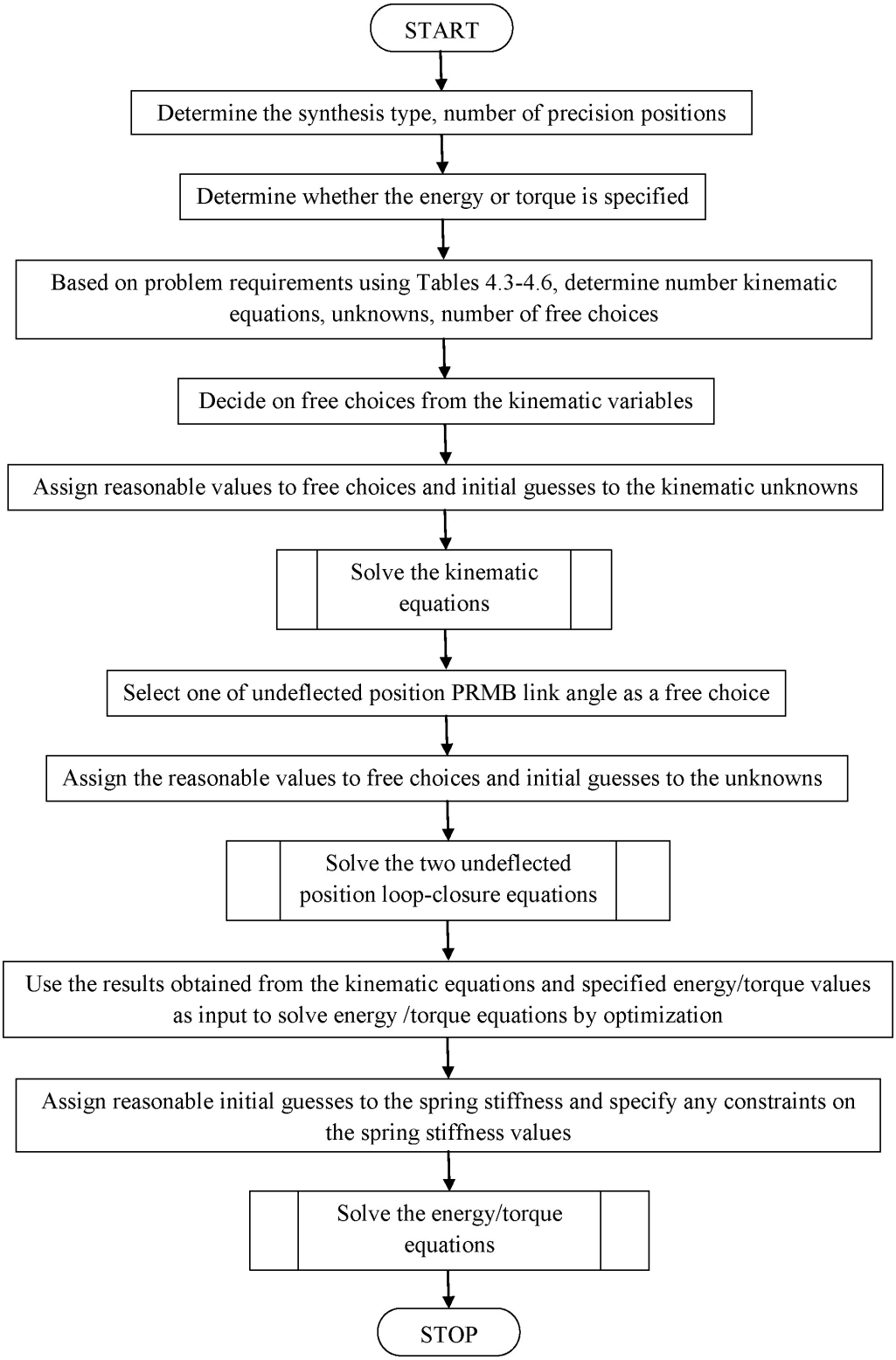

Figure 4.2. A Flowchart Showing Synthesis with Compliance Technique using Optimization Approach

In order to find the effects of strongly coupled and weakly coupled system of equations, for the strongly coupled case of synthesis; the two strategies are proposed for to study the effects.

- Treated as a strongly coupled system: kinematic and energy equations are solved simultaneously
- Treated as a weakly coupled system: kinematic equations are solved by a nonlinear equations solver and then the energy/torque equations are solved by optimization

e.g. It is desired to synthesize a compliant mechanism for three precision positions motion generation synthesis, energy specified at these points as follows:

$\delta_2 = -2 + \mathrm{i}$ $\delta_3 = -4 + 0.75\mathrm{i}$

$\gamma_2 = -7°$ $\gamma_3 = -14°$

$\mathrm{E}_1 = 1.16\mathrm{in} - \mathrm{lb}$ $\mathrm{E}_2 = 28.45\ \mathrm{in} - \mathrm{lb}$ $\mathrm{E}_3 = 95.80\ \mathrm{in} - \mathrm{lb}$

Assuming one torsional spring in the pseudo-rigid-body model four-bar mechanism, there are 11 equations, 14 unknowns and 3 free choices, resulting in strongly coupled system (Table 3.3). Hence, kinematic and energy equations have to be solved simultaneously. A compliant mechanism with one fixed-free segment as shown in Figure 3.2 (R) is selected for synthesis. R_2, R_4 and θ_{21} are selected as free choices. Reasonable initial estimates have assigned to remaining 11 variables. The energy-free state loop-closure equation (38) is not really needed for this case as it has only one spring. But in order to know the mechanism configuration in energy-free state, these two scalar equations are added. This adds 2 more equations and 3 unknowns. The coupler equation (37) and first precision position loop-closure equation (39) are considered to determine

remaining link lengths and angles. These add 4 scalar equations and 4 unknowns. Using equations (6), (21), (37), (38) and (39), the following solution is obtained:

$Z_1 = 11.852 + 2.472i$ $Z_2 = 4.596 + 2.571i$

$Z_3 = 9.26 + 2.077i$ $Z_4 = 2.004 + 3.362i$

$Z_5 = 5.425 + 2.689i$ $Z_6 = -3.835 + 0.612i$

$\phi_2 = 27.367\ ^\circ$ $\phi_3 = 48.979^\circ$

$\psi_2 = 31.488^\circ$ $\psi_3 = 64.433^\circ$

$K_4 = 119.996\ \text{in} - \text{lb/rad}$ $\Theta_{40} = 51.961^\circ$

$\Theta_{20} = 29.999^\circ$ $\Theta_{30} = 16.043^\circ$

In the second technique, the kinematic and energy equations are solved separately i.e. as weakly coupled system. The kinematic equations are solved by conventional nonlinear equations solver and energy equations are solved by constrained optimization approach. In the above example, we have 8 kinematic loop-closure equations and 12 unknowns, giving 4 free choices and solution obtained for kinematic configuration is as below:

$Z_2 = 4.496 + 3.857i$ $Z_4 = 2 + 1.732i$

$Z_5 = 5.425 + 2.689i$ $Z_6 = -3.856 + 0.608i$

$\phi_2 = 27.367^\circ$ $\phi_3 = 48.979$

$\psi_2 = 31.473^\circ$ $\psi_3 = 64.43^\circ$

The coupler equation (37) and first-precision position loop-closure equation (39) are solved separately and solution obtained is follows:

$Z_1 = 11.877 + 2.474i$ $Z_3 = 9.282 + 2.081i$

The energy-free state loop-closure equation results in two scalar equations and has 3 unknowns, giving one free choice. $\Theta_{20} = 30°$ is selected as free choice and the equations are solved for other two unknowns which give following solutions:

$\Theta_{30} = 16.032°$ $\Theta_{40} = 52.029°$

Using the values obtained above, three energy equations are solved by optimization approach and value of K_4 is obtained as $K_4 = 119.9955 \text{ in} - \text{lb/rad}$.

If the solutions obtained from the new technique of solving equations by weakly coupled system using optimization approach are compared with those from strongly coupled system, it has been observed that, the solutions are almost similar with little differences in some values and that is because of the value of Θ_{41} is taken as free choice while solving equations by weakly coupled and in strongly coupled it is regarded as unknown, which changes value of Θ_{41} from $60°$ to $59.9279°$. Thus, it can be concluded that solutions is obtained by using both the strategies and it is believed that, the latter strategy, which uncouples the equation sets, yields the solution from an entire set of possible solutions. As in the latter case, as the kinematic and energy equations are solved separately, the system becomes much simpler than strongly coupled one.

The length of the fixed-pinned segment is determined by using the following equation:

$$\gamma L = |Z| \Rightarrow L = |Z|/\gamma \quad (23)$$

where, γ is the characteristic radius factor with average value 0.85, $|Z|$ is the length of the corresponding pseudo-rigid-body link and L is the length of compliant segment. Selecting output link R_4 as pseudo-rigid-body link the compliant link length L_4 comes out as 4.7059 in. Using the equation, (15) as given below, the moment of inertia is obtained.

$$K_t = \gamma K_\Theta \frac{EI}{L} \quad (15)$$

where, E is the modulus of elasticity, I is the moment of inertia, L is the length of the compliant segment, γ is the characteristic radius factor, K_Θ is the stiffness coefficient, K_t is torsional spring stiffness. Using the thermoplastic polymer Polypropylene, material, moment of inertia I comes out as $I = 1.2535 \times 10^{-3}$ in^4. Selecting the rectangular cross-section for the compliant segment and assuming the width of 0.5 in, the thickness of the compliant segment is obtained by following equation (24).

$$I = \frac{bh^3}{12} \quad (24)$$

where, b is the width and h is the thickness of the segment. The value of thickness obtained is 0.3110 in. The resulting compliant mechanism is shown in Figure 4.3. The precisions positions from PRBM and from the corresponding compliant mechanism are compared. In order to obtain the precision positions in ABAQUS®, the X displacements are given to the coupler point of the compliant mechanism for each precision position and the Y displacements are obtained. This comparison is shown in Table 4.1.

Table 4.1. Precision Positions Comparison PRBM vs. Compliant Mechanism (FEA)

Pseudo-rigid-body four-bar mechanism		Compliant mechanism (ABAQUS®)		% Relative error in Y displacement
X displacement	Y displacement	X displacement	Y displacement	
-0.431	0.54	-0.431	0.5395	0.0727
-2.4312	1.5403	-2.4312	1.5288	0.4012
-4.4312	1.2906	-4.4312	1.2699	0.4479

The coupler curve is plotted for a pseudo-rigid body model with precision points marked on it. The precision positions obtained from corresponding compliant mechanism in ABAQUS® are also shown on it. The coupler curve for this example is shown in Figure 4.4. An energy comparison between pseudo-rigid-body model and compliant mechanism, using commercial finite element software ABAQUS® is done to verify the equivalence of the design and validate the solution. The results are shown in Table 4.2.

Figure 4.3. Solid Model of a Compliant Mechanism with One Fixed-Free Segment

Table 4.2. Energy Comparison PRBM vs. Compliant Mechanism (FEA)

	Pseudo-rigid-body four-bar mechanism	Compliant mechanism (FEA software)	% Error in Energy
E_1	1.16	1.1096	4.35
E_2	28.45	27.5763	3.07
E_3	95.8	96.8233	1.07

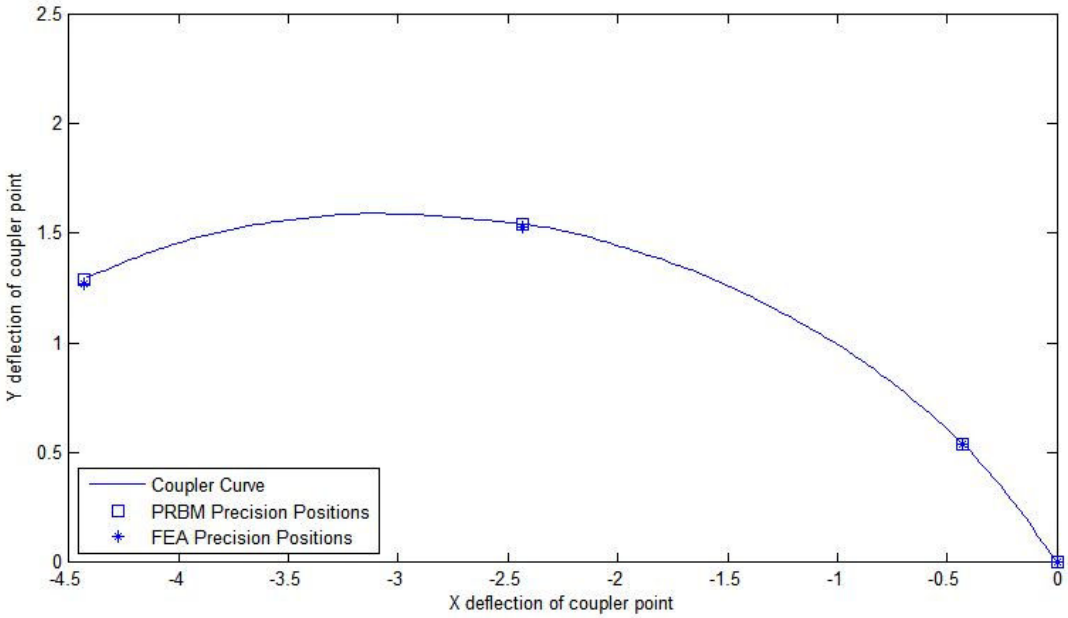

Figure 4.4. Coupler Curve Obtained from PRBM with Precision Positions

Table 4.3-4.6 shows the number of equations, number of unknowns and number of free choices for function, path, motion generation and path generation with prescribed timing depending on number on springs in pseudo-rigid body four-bar mechanism for varying number of precision positions synthesis. In the new technique, the equations are solved separately. The kinematic equations are solved by conventional method so free choices are needed to solve the loop-closure equations. The energy-free state loop-closure

equation gives two scalar equations and three unknowns, requiring one free choice there. As the energy equations are solved by the optimization method, no free choices are needed. In the tables, the number of equations is shown as addition of number kinematic equations, energy-free state loop-closure equations and energy/torque equations. The last column indicates the number of free choices and it includes the free choices for solving the kinematic equations and one free choice of energy-free state loop-closure equations. e.g. from Table 4.4, for three precision positions path generation synthesis with four springs has 8+2+3=13 equations, 12 kinematic unknowns and 7 energy unknowns giving 5 free choices.

From Tables 3.1-3.4, it can be seen that with the synthesis with compliance technique due to strongly coupling of kinematic equations and energy/torque equations, few synthesis cases can't be solved due to over-constraining of the system as number of equations are more than number of variables. Those cases are listed below:

1) Function generation synthesis for five precision positions with one torsional spring in pseudo-rigid-body four-bar mechanism.

2) Motion generation synthesis for five precision positions with one, two, three torsional springs in pseudo-rigid-body four-bar mechanism.

3) Path generation with prescribed timing synthesis for five precision positions with one, two, three torsional springs in pseudo-rigid-body four-bar mechanism.

Table 4.3. Design Choices Based on Number of Torsional Springs for Function Generation Synthesis with Compliance Technique Using Optimization Approach

Number of Torsional Springs	Number of Equations	Number of Kinematic Unknowns	Number of Energy Unknowns	Number of Free Choices
Three Precision Positions				
1	4+2+3=9	$Z_2, Z_3, Z_4, \gamma_2, \gamma_3$ (8)	$K_1, \Theta_{20}, \Theta_{30}, \Theta_{40}$ (4)	5
2	4+2+3=9	$Z_2, Z_3, Z_4, \gamma_2, \gamma_3$ (8)	$K_1, K_2, \Theta_{20}, \Theta_{30}, \Theta_{40}$ (5)	5
3	4+2+3=9	$Z_2, Z_3, Z_4, \gamma_2, \gamma_3$ (8)	$" + K_3$ (6)	5
4	4+2+3=9	$Z_2, Z_3, Z_4, \gamma_2, \gamma_3$ (8)	$" + K_4$ (7)	5
Four Precision Positions				
1	6+2+4=12	$Z_2, Z_3, Z_4, \gamma_2, \gamma_3, \gamma_4$, (9)	$K_1, \Theta_{20}, \Theta_{30}, \Theta_{40}$ (4)	4
2	6+2+4=12	$Z_2, Z_3, Z_4, \gamma_2, \gamma_3, \gamma_4$, (9)	$K_1, K_2, \Theta_{20}, \Theta_{30}, \Theta_{40}$ (5)	4
3	6+2+4=12	$Z_2, Z_3, Z_4, \gamma_2, \gamma_3, \gamma_4$, (9)	$" + K_3$ (6)	4
4	6+2+4=12	$Z_2, Z_3, Z_4, \gamma_2, \gamma_3, \gamma_4$, (9)	$" + K_4$ (7)	4
Five Precision Positions				
1	8+2+5=15	$Z_2, Z_3, Z_4, \gamma_2, \gamma_3, \gamma_4, \gamma_5$ (10)	$K_1, \Theta_{20}, \Theta_{30}, \Theta_{40}$ (4)	3
2	8+2+5=15	$Z_2, Z_3, Z_4, \gamma_2, \gamma_3, \gamma_4, \gamma_5$ (10)	$K_1, K_2, \Theta_{20}, \Theta_{30}, \Theta_{40}$ (5)	3
3	8+2+5=15	$Z_2, Z_3, Z_4, \gamma_2, \gamma_3, \gamma_4, \gamma_5$ (10)	$" + K_3$ (6)	3
4	8+2+5=15	$Z_2, Z_3, Z_4, \gamma_2, \gamma_3, \gamma_4, \gamma_5$ (10)	$" + K_4$ (7)	3

From Tables 4.3-4.6, obtained using new method using optimization approach, as the kinematic and energy/torque equations are solved separately, all of synthesis cases mentioned above which couldn't be solved by existing method are solvable by new approach.

4.5. DIFFERENT CASES

This section shows different cases/examples of compliant mechanism synthesis such as undeflected position of the mechanism different from precision positions, undeflected position of the mechanism to be one of the precision positions etc. Examples are shown for compliant mechanisms with different types of complaint segments such as full length compliant segments, small length flexural pivots etc. All the cases/examples presented herewith are for the pseudo-rigid-body four-bar mechanism synthesis for three precision positions. The kinematic loop-closure equations for the function generation synthesis are given by equations (6). For motion or path generation, the loop-closure equations are given by equations (13). The energy and torque equations for three precision positions are given by equations (21) and equations (40) respectively.

4.5.1. Case 1: Undeflected Position of the Mechanism Different from the Specified Positions.

In this case, the energies are specified at the three precision positions and energy-free state of the mechanism happens to be different from the specified precision positions. Thus, the energy-free state loop-closure equation given by equation (38) needs to be included in the system of equations.

e.g. It is desired to synthesize a compliant mechanism for three precision positions path generation with prescribed timing synthesis, energy specified at these points as follows:

$\delta_2 = -3 + 0.5\mathrm{i}$ $\delta_3 = -5 + 0.25\mathrm{i}$

$E_1 = 6.3\ \text{in} - \text{lb}$ $E_2 = 28\ \text{in} - \text{lb}$ $E_3 = 51.6\ \text{in} - \text{lb}$

$\phi_2 = 20°$ $\phi_3 = 35°$

Assuming two torsional springs in the pseudo-rigid-body model four-bar mechanism, there are 8 kinematic loop-closure equations, 3 energy equations and 2

energy-free state loop-closure equations, having 17 unknowns giving 5 free choices (Table 4.6). A compliant mechanism with one fixed-guided segment as shown in Figure 3.2 (I) is selected for synthesis. As the two springs in pseudo-rigid-body model link generate one fixed-guided segment, two same spring constants will be useful for sizing the compliant segment. This restriction is added in the constraint function of optimization code for energy equations.

$R_2, R_4, \theta_{21}, \theta_{41}$ are selected as free choices as given below for solving loop-closure equations.

$R_2 = 5.5$ in $\quad R_4 = 7$ in

$\theta_{21} = 85°$ $\quad \theta_{41} = 65°$

$\Theta_{20} = 70°$

Two undeflected state loop-closure equations are solved by selecting Θ_{20} as free choice. The solutions obtained from these two sets of equations are used as input to solve 3 energy equations by optimization approach. The coupler equation (37) and first precision position loop-closure equation (39) are considered to determine remaining link lengths and angles. These add 4 scalar equations and 4 unknowns.

Table 4.4. Design Choices Based on Number of Torsional Springs for Path Generation Synthesis with Compliance Technique Using Optimization Approach

Number of Torsional Springs	Number of Equations	Number of Kinematic Unknowns	Number of Energy Unknowns	Number of Free Choices
Three Precision Positions				
1	8+2+3=13	$Z_2, Z_4, Z_5, Z_6, \phi_2, \phi_3, \gamma_2, \gamma_3, \psi_2, \psi_3$ (14)	$K_1, \Theta_{20}, \Theta_{30}, \Theta_{40}$ (4)	7
2	8+2+3=13	$Z_2, Z_4, Z_5, Z_6, \phi_2, \phi_3, \gamma_2, \gamma_3, \psi_2, \psi_3$ (14)	$K_1, K_2, \Theta_{20}, \Theta_{30}, \Theta_{40}$ (5)	7
3	8+2+3=13	$Z_2, Z_4, Z_5, Z_6, \phi_2, \phi_3, \gamma_2, \gamma_3, \psi_2, \psi_3$ (14)	$" + K_3$ (6)	7
4	8+2+3=13	$Z_2, Z_4, Z_5, Z_6, \phi_2, \phi_3, \gamma_2, \gamma_3, \psi_2, \psi_3$ (14)	$" + K_4$ (7)	7
Four Precision Positions				
1	12+2+4=18	$Z_2, Z_4, Z_5, Z_6, \phi_2, \phi_3, \phi_4, \gamma_2, \gamma_3, \gamma_4, \psi_2, \psi_3, \psi_4,$ (17)	$K_1, \Theta_{20}, \Theta_{30}, \Theta_{40}$ (4)	6
2	12+2+4=18	$Z_2, Z_4, Z_5, Z_6, \phi_2, \phi_3, \phi_4, \gamma_2, \gamma_3, \gamma_4, \psi_2, \psi_3, \psi_4,$ (17)	$K_1, K_2, \Theta_{20}, \Theta_{30}, \Theta_{40}$ (5)	6
3	12+2+4=18	$Z_2, Z_4, Z_5, Z_6, \phi_2, \phi_3, \phi_4, \gamma_2, \gamma_3, \gamma_4, \psi_2, \psi_3, \psi_4,$ (17)	$K_1, K_2, K_3, \Theta_{20}, \Theta_{30}, \Theta_{40}$ (6)	6
4	12+2+4=18	$Z_2, Z_4, Z_5, Z_6, \phi_2, \phi_3, \phi_4, \gamma_2, \gamma_3, \gamma_4, \psi_2, \psi_3, \psi_4,$ (17)	$K_1, K_2, K_3, K_4, \Theta_{20}, \Theta_{30}, \Theta_{40}$ (7)	6
Five Precision Positions				
1	16+2+5=23	$Z_2, Z_4, Z_5, Z_6, \phi_2, \phi_3, \phi_4, \phi_5, \gamma_2, \gamma_3, \gamma_4, \gamma_5, \psi_2, \psi_3, \psi_4, \psi_5,$ (20)	$K_1, \Theta_{20}, \Theta_{30}, \Theta_{40}$ (4)	5
2	16+2+5=23	$Z_2, Z_4, Z_5, Z_6, \phi_2, \phi_3, \phi_4, \phi_5, \gamma_2, \gamma_3, \gamma_4, \gamma_5, \psi_2, \psi_3, \psi_4, \psi_5,$ (20)	$K_1, K_2, \Theta_{20}, \Theta_{30}, \Theta_{40}$ (5)	5
3	16+2+5=23	$Z_2, Z_4, Z_5, Z_6, \phi_2, \phi_3, \phi_4, \phi_5, \gamma_2, \gamma_3, \gamma_4, \gamma_5, \psi_2, \psi_3, \psi_4, \psi_5,$ (20)	$K_1, K_2, K_3, \Theta_{20}, \Theta_{30}, \Theta_{40}$ (6)	5
4	16+2+5=23	$Z_2, Z_4, Z_5, Z_6, \phi_2, \phi_3, \phi_4, \phi_5, \gamma_2, \gamma_3, \gamma_4, \gamma_5, \psi_2, \psi_3, \psi_4, \psi_5,$ (20)	$K_1, K_2, K_3, K_4, \Theta_{20}, \Theta_{30}, \Theta_{40}$ (7)	5

Table 4.5. Design Choices Based on Number of Torsional Springs for Motion Generation Synthesis with Compliance Technique Using Optimization Approach

Number of Torsional Springs	Number of Equations	Number of Kinematic Unknowns	Number of Energy Unknowns	Number of Free Choices
Three Precision Positions				
1	8+2+3=13	$Z_2, Z_4, Z_5, Z_6, \phi_2, \phi_3, \psi_2, \psi_3$ (12)	$K_1, \Theta_{20}, \Theta_{30}, \Theta_{40}$ (4)	5
2	8+2+3=13	$Z_2, Z_4, Z_5, Z_6, \phi_2, \phi_3, \psi_2, \psi_3$ (12)	$K_1, K_2, \Theta_{20}, \Theta_{30}, \Theta_{40}$ (5)	5
3	8+2+3=13	$Z_2, Z_4, Z_5, Z_6, \phi_2, \phi_3, \psi_2, \psi_3$ (12)	$" + K_3$ (6)	5
4	8+2+3=13	$Z_2, Z_4, Z_5, Z_6, \phi_2, \phi_3, \psi_2, \psi_3$ (12)	$" + K_4$ (7)	5
Four Precision Positions				
1	12+2+4=18	$Z_2, Z_4, Z_5, Z_6, \phi_2, \phi_3, \phi_4, \psi_2, \psi_3, \psi_4,$ (14)	$K_1, \Theta_{20}, \Theta_{30}, \Theta_{40}$ (4)	3
2	12+2+4=18	$Z_2, Z_4, Z_5, Z_6, \phi_2, \phi_3, \phi_4, \psi_2, \psi_3, \psi_4,$ (14)	$K_1, K_2, \Theta_{20}, \Theta_{30}, \Theta_{40}$ (5)	3
3	12+2+4=18	$Z_2, Z_4, Z_5, Z_6, \phi_2, \phi_3, \phi_4, \psi_2, \psi_3, \psi_4,$ (14)	$" + K_3$ (6)	3
4	12+2+4=18	$Z_2, Z_4, Z_5, Z_6, \phi_2, \phi_3, \phi_4, \psi_2, \psi_3, \psi_4,$ (14)	$" + K_4$ (7)	3
Five Precision Positions				
1	16+2+5=23	$Z_2, Z_4, Z_5, Z_6, \phi_2, \phi_3, \phi_4, \phi_5, \psi_2, \psi_3, \psi_4, \psi_5,$ (16)	$K_1, \Theta_{20}, \Theta_{30}, \Theta_{40}$ (4)	1
2	16+2+5=23	$Z_2, Z_4, Z_5, Z_6, \phi_2, \phi_3, \phi_4, \phi_5, \psi_2, \psi_3, \psi_4, \psi_5,$ (16)	$K_1, K_2, \Theta_{20}, \Theta_{30}, \Theta_{40}$ (5)	1
3	16+2+5=23	$Z_2, Z_4, Z_5, Z_6, \phi_2, \phi_3, \phi_4, \phi_5, \psi_2, \psi_3, \psi_4, \psi_5,$ (16)	$" + K_3$ (6)	1
4	16+2+5=23	$Z_2, Z_4, Z_5, Z_6, \phi_2, \phi_3, \phi_4, \phi_5, \psi_2, \psi_3, \psi_4, \psi_5,$ (16)	$" + K_4$ (7)	1

Table 4.6. Design Choices Based on Number of Torsional Springs for Path Generation with Prescribed Timing Synthesis with Compliance Technique Using Optimization Approach

Number of Torsional Springs	Number of Equations	Number of Kinematic Unknowns	Number of Energy Unknowns	Number of Free Choices
Three Precision Positions				
1	8+2+3=13	$Z_2, Z_4, Z_5, Z_6, \gamma_2, \gamma_3, \psi_2, \psi_3$ (12)	$K_1, \Theta_{20}, \Theta_{30}, \Theta_{40}$ (4)	5
2	8+2+3=13	$Z_2, Z_4, Z_5, Z_6, \gamma_2, \gamma_3, \psi_2, \psi_3$ (12)	$K_1, K_2, \Theta_{20}, \Theta_{30}, \Theta_{40}$ (5)	5
3	8+2+3=13	$Z_2, Z_4, Z_5, Z_6, \gamma_2, \gamma_3, \psi_2, \psi_3$ (12)	$" + K_3$ (6)	5
4	8+2+3=13	$Z_2, Z_4, Z_5, Z_6, \gamma_2, \gamma_3, \psi_2, \psi_3$ (12)	$" + K_4$ (7)	5
Four Precision Positions				
1	12+2+4=18	$Z_2, Z_4, Z_5, Z_6, \gamma_2, \gamma_3, \gamma_4, \psi_2, \psi_3, \psi_4$ (14)	$K_1, \Theta_{20}, \Theta_{30}, \Theta_{40}$ (4)	3
2	12+2+4=18	$Z_2, Z_4, Z_5, Z_6, \gamma_2, \gamma_3, \gamma_4, \psi_2, \psi_3, \psi_4,$ (14)	$K_1, K_2, \Theta_{20}, \Theta_{30}, \Theta_{40}$ (5)	3
3	12+2+4=18	$Z_2, Z_4, Z_5, Z_6, \gamma_2, \gamma_3, \gamma_4, \psi_2, \psi_3, \psi_4,$ (14)	$" + K_3$ (6)	3
4	12+2+4=18	$Z_2, Z_4, Z_5, Z_6, \gamma_2, \gamma_3, \gamma_4, \psi_2, \psi_3, \psi_4$ (14)	$" + K_4$ (7)	3
Five Precision Positions				
1	16+2+5=23	$Z_2, Z_4, Z_5, Z_6, \gamma_2, \gamma_3, \gamma_4, \gamma_5, \psi_2, \psi_3, \psi_4, \psi_5$ (16)	$K_1, \Theta_{20}, \Theta_{30}, \Theta_{40}$ (4)	1
2	16+2+5=23	$Z_2, Z_4, Z_5, Z_6, \gamma_2, \gamma_3, \gamma_4, \gamma_5, \psi_2, \psi_3, \psi_4, \psi_5$ (16)	$K_1, K_2, \Theta_{20}, \Theta_{30}, \Theta_{40}$ (5)	1
3	16+2+5=23	$Z_2, Z_4, Z_5, Z_6, \gamma_2, \gamma_3, \gamma_4, \gamma_5, \psi_2, \psi_3, \psi_4, \psi_5$ (16)	$" + K_3$ (6)	1
4	16+2+5=23	$Z_2, Z_4, Z_5, Z_6, \gamma_2, \gamma_3, \gamma_4, \gamma_5, \psi_2, \psi_3, \psi_4, \psi_5$ (16)	$" + K_4$ (7)	1

The solution obtained is as below:

$Z_1 = 2.875 + 3.019i$ $Z_2 = 0.479 + 5.479i$

$Z_3 = 5.355 + 3.884i$ $Z_4 = 2.958 + 6.344i$

$Z_5 = 4.652 + 6.397i$ $Z_6 = -0.703 + 2.537i$

$\psi_2 = 22.064°$ $\psi_3 = 36.74°$

$\gamma_2 = 9.286°$ $\gamma_3 = 14.613°$

$\Theta_{30} = 24.152°$ $\Theta_{40} = 43.921°$

$K_3 = 78.27 \text{ in} - \text{lb/rad}$ $K_4 = 78.27 \text{ in} - \text{lb/rad}$

The length of the fixed-guided segment is determined by using equation (23). Selecting input link R_4 as pseudo-rigid-body link, the compliant segment length L_4 comes out as 8.235 in. Using the equation, (16) as given below, the moment of inertia is obtained.

$$K_t = 2\gamma K_\Theta \frac{EI}{L} \tag{16}$$

where, E is the modulus of elasticity, I is the moment of inertia, L is the length of the compliant segment, γ is the characteristic radius factor, K_Θ is the stiffness coefficient and, K_t is the torsional spring stiffness. Using the thermoplastic polymer Polypropylene material, moment of inertia I comes out as $I = 7.154 \times 10^{-4}$ in^4. Selecting the rectangular cross-section for the compliant segment and assuming the width of 0.5 in, the thickness of the compliant segment is obtained by equation (24). The value of thickness obtained is 0.258 in. The resulting compliant mechanism is shown in Figure 4.5. In order to compare the precision positions from PRBM and FEA, the Y displacements of coupler point are compared for given X displacements. The comparison is shown in Table 4.7 for PRBM with two FEA software ABAQUS® and ANSYS®.

The mechanism is modeled in the same way and same boundary conditions are applied in two software and however the results obtained from those are varying as shown in Table 4.7. The energy comparison between pseudo-rigid-body model results and FEA results from both ABAQUS® and ANSYS® are shown in Table 4.8.

Table 4.7. Precision Positions Comparison PRBM vs. Compliant Mechanism (FEA)

Pseudo-rigid-body four-bar mechanism		Compliant mechanism				% Relative error in Y displacement between PRBM and	
		ABAQUS®		ANSYS®			
X disp.	Y disp.	X disp.	Y disp.	X disp.	Y disp.	ABAQUS®	ANSYS®
-2.6171	1.3978	-2.6171	1.3135	-2.6171	1.3135	0.255	0.162
-5.6174	1.898	-5.6174	1.7593	-5.6174	1.7593	0.462	0.285
-7.6176	1.6481	-7.6176	1.4818	-7.6176	1.4818	0.585	0.327

Table 4.8. Energy Comparison PRBM vs. Compliant Mechanism (FEA)

	Pseudo-rigid-body four-bar mechanism	Compliant mechanism (ABAQUS®)	Compliant mechanism (ANSYS®)	% Error in energy obtained using PRBM and	
				ABAQUS®	ANSYS®
E_1	6.3	5.678	5.9705	9.869	5.231
E_2	28	25.999	27.344	7.146	2.343
E_3	51.6	48.907	51.447	5.219	0.297

The coupler curve obtained from PRBM is plotted along with precision positions marked on it. The coupler curve for this example is shown in Figure 4.6.

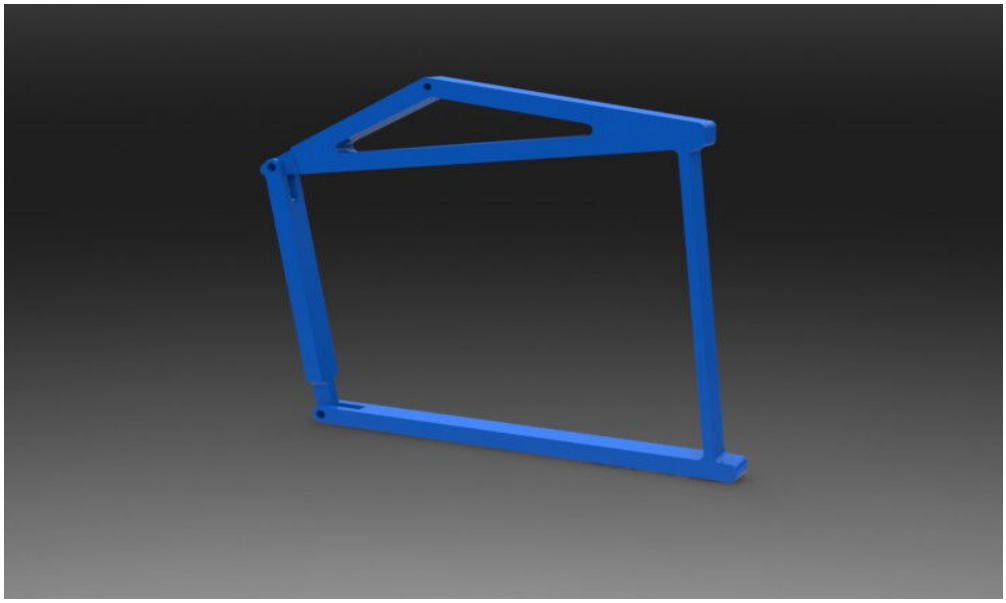

Figure 4.5. Solid Model of a Compliant Mechanism with One Fixed-Fixed Segment

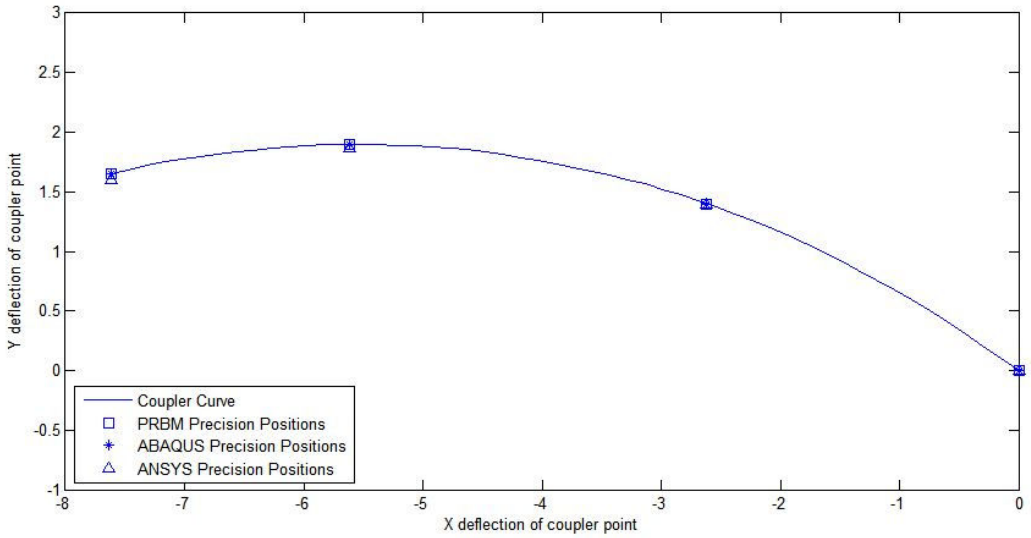

Figure 4.6. Coupler Curve Obtained from PRBM with Precision Positions

4.5.2. Case 2: Undeflected Position of the Mechanism to be one of the Specified Positions.

In this case, the energy-free state of the mechanism happens to be one of the specified precision positions. So the energy-free state loop-closure equation is not needed and reduced system of equations can be used. Thus, for the three precision

positions synthesis problem, two energies are specified and third energy is assumed to be zero.

e.g. A compliant mechanism with fully-compliant segments is to be designed for three-precision positions path generation with prescribed timing synthesis with energy specifications:

$\delta_2 = -3 + 0.5\mathrm{i}$ $\delta_3 = -5 + 0.25\mathrm{i}$

$\phi_2 = 20°$ $\phi_3 = 35°$

$E_1 = 0\ \text{in} - \text{lb}$ $E_2 = 15\ \text{in} - \text{lb}$ $E_3 = 44.8\ \text{in} - \text{lb}$

Assuming four torsional springs in the pseudo-rigid-body model four-bar mechanism, there are 8 kinematic loop-closure equations. As the energy at first precision position is zero, the energy equation for first precision position is not required, and so there are 2 energy equations. The energy-free state loop-closure equation is also not needed. Thus, there are total 10 equations with 16 unknowns giving 4 kinematic free choices. A compliant mechanism with two fixed-guided segments as shown in Figure 3.2 (A) is selected for synthesis. As the four springs in pseudo-rigid-body model generate two fixed-guided segments, two same spring constants for each compliant segment will be useful for sizing it.

$R_2, R_4, \theta_{21}, \theta_{41}$, are selected as free choices as given below for solving loop-closure equations.

$R_2 = 5.5\ \text{in}$ $R_4 = 7\ \text{in}$

$\theta_{21} = 85°$ $\theta_{41} = 65°$

The solution obtained from loop-closure equations is used as input to solve 2 energy equations by optimization approach. The coupler equation (37) and first precision

position loop-closure equation (39) are considered to determine remaining link lengths and angles. These add 4 scalar equations and 4 unknowns. The solution obtained is as below:

$Z_1 = 2.876 + 3.019i$ $Z_2 = 0.4794 + 5.479i$

$Z_3 = 5.355 + 3.885i$ $Z_4 = 2.958 + 4.110i$

$Z_5 = 4.652 + 6.422i$ $Z_6 = -0.703 + 2.537i$

$\gamma_2 = 9.286°$ $\gamma_3 = 14.613°$

$\psi_2 = 22.064°$ $\psi_3 = 36.74°$

$K_1 = 80.882 \text{ in} - \text{lb/rad}$ $K_2 = 80.882 \text{ in} - \text{lb/rad}$

$K_3 = 87.733 \text{ in} - \text{lb/rad}$ $K_4 = 87.733 \text{ in} - \text{lb/rad}$

The length of the fixed-guided segment is determined by using equation (23). Selecting input link R_2 pseudo-rigid-body link, the compliant segment length L_2 comes out as 7.0588 in. Using the equation (16), the moment of inertia is obtained. Using the thermoplastic polymer Polypropylene material, moment of inertia I comes out as $I = 5.808 \times 10^{-4} \text{ in}^4$. Similarly, for output pseudo-rigid-body link, R_4, the compliant segment length L_4 comes out as 8.235 in and moment of inertia as $I = 8.019 \times 10^{-4} \text{ in}^4$.Selecting the rectangular cross-section for the compliant segments and assuming the width of 0.5 in, the thickness of the compliant segment obtained for input link is 0.2406 in and for output link is 0.2679 in. The resulting compliant mechanism is shown in Figure 4.7. In order to compare the precision positions from PRBM and FEA, the Y displacements of coupler point are compared for given X displacements. The comparison is shown in Table 4.9 for PRBM with two FEA software ABAQUS® and ANSYS® .The mechanism is modeled in the same way and same

boundary conditions are applied in both software and however the results obtained from those are varying as shown in Table 4.9. The energy comparison between pseudo-rigid-body model results and FEA results from both ABAQUS® and ANSYS® are shown in Table 4.10.

Table 4.9. Precision Positions Comparison PRBM vs. Compliant Mechanism (FEA)

Pseudo-rigid-body four-bar mechanism		Compliant mechanism				% Relative error in Y displacement between PRBM and	
		ABAQUS®		ANSYS®			
X disp.	Y disp.	X disp.	Y disp.	X disp.	Y disp.	ABAQUS®	ANSYS®
0	0	0	0	0	0	0	0
-3	0.5	-3	0.4707	-3	0.4967	0.964	0.108
-5	0.25	-5	0.2479	-5	0.2516	0.0418	0.0308

Table 4.10. Energy Comparison PRBM vs. Compliant Mechanism (FEA)

	Pseudo-rigid-body four-bar mechanism	Compliant mechanism (ABAQUS®)	Compliant mechanism (ANSYS®)	% Error in energy obtained using PRBM and	
				ABAQUS®	ANSYS®
E_1	0	0	0	0	0
E_2	15	13.769	13.499	8.21	10
E_3	44.8	41.228	40.418	7.974	9.781

The coupler curve obtained from PRBM is plotted along with precision positions marked on it. The coupler curve for this example is shown in Figure 4.8.

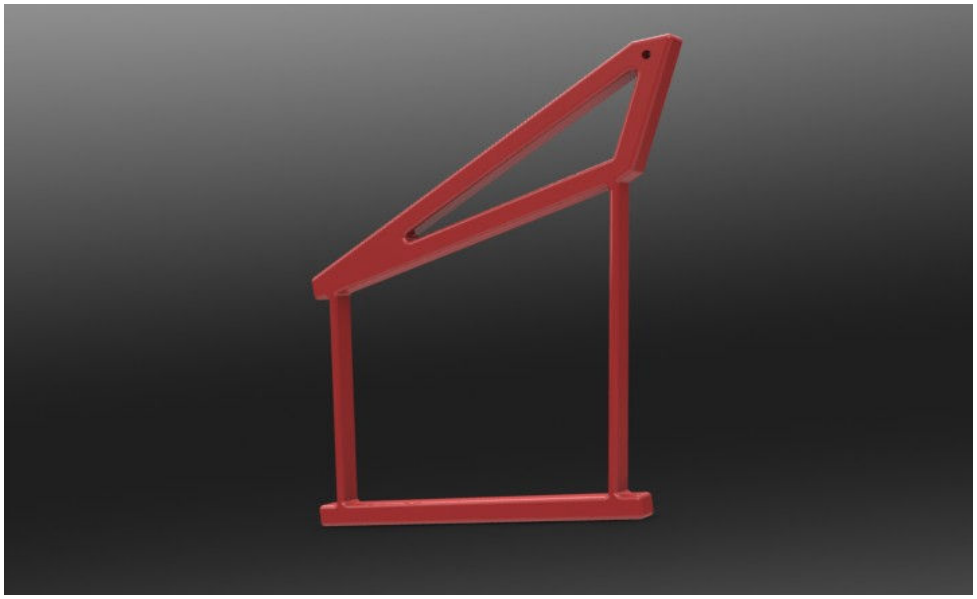

Figure 4.7. Solid Model of a Compliant Mechanism with Two Fixed-Fixed Segments

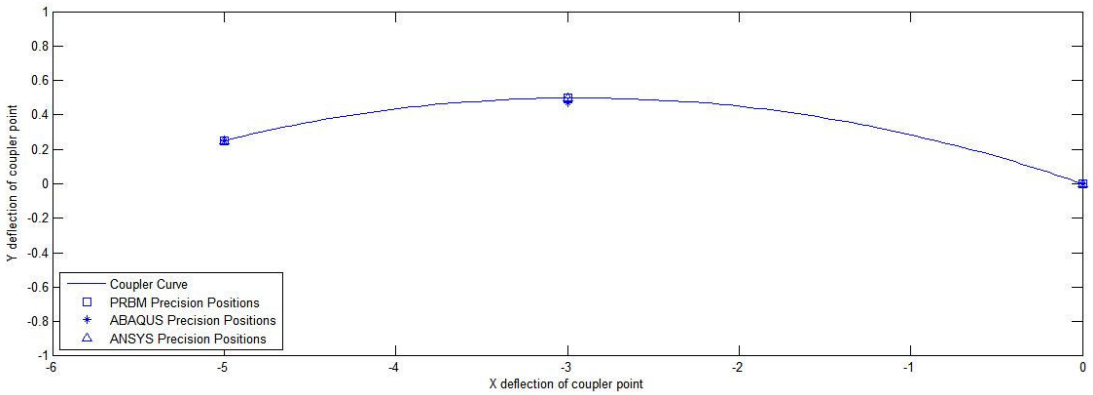

Figure 4.8. Coupler Curve Obtained from PRBM with Precision Positions

4.5.3. Case 3: All Four Torsional Spring Constants Same. This can be special case of compliant mechanism synthesis in which all the four torsional spring constants will be the same. This simplifies the sizing of the compliant segments. The optimization approach provides the simplified way to apply such kinds of restrictions on the spring constants. The addition of new such constraint equations in the conventional method may

cause over-constraining. Different types of constraints e.g. total stiffness of the mechanism to be under certain limit, individual spring stiffness values to be within certain lower and upper bounds etc. can be applied on the spring stiffness values using optimization approach.

e.g. A compliant mechanism with small-length flexural segments is to be designed for three-precision positions path generation synthesis with energy specifications:

$\delta_2 = -3 + 0.5\mathrm{i}$ $\delta_3 = -5 + 0.2\mathrm{i}$

$E_1 = 11.75 \text{ in} - \text{lb}$ $E_2 = 37.25 \text{ in} - \text{lb}$ $E_3 = 60 \text{ in} - \text{lb}$

Assuming four torsional springs in the pseudo-rigid-body model four-bar mechanism, there are 8 kinematic loop-closure equations, 3 energy equations and 2 scalar undeflected state loop-closure equations, having 21 unknowns giving 7 free choices (Table 4.4). A compliant mechanism with four small-length flexural pivots as shown in Figure 3.2 (C) is selected for synthesis. As the special case, all the torsional spring stiffness values are assumed to be same. $R_2, R_4, \theta_{21}, \theta_{41}, \gamma_2, \gamma_3$ are selected as free choices as given below for solving loop-closure equations.

$R_2 = 6 \text{ in}$ $R_4 = 7 \text{ in}$

$\theta_{21} = 60°$ $\theta_{41} = 40°$

$\gamma_2 = 9°$ $\gamma_3 = 15°$

$\Theta_{20} = 30°$

Two undeflected state loop-closure equations are solved by selecting Θ_{20} as free choice. The solutions obtained from these two sets of equations are used as input to solve 3 energy equations by optimization approach. The coupler equation (37) and first precision position loop-closure equation (39) are considered to determine remaining link

lengths and angles. These add 4 scalar equations and 4 unknowns. The solution obtained is as below:

$Z_1 = 3.479 - 1.537i$ $Z_2 = 3 + 5.196i$

$Z_3 = 5.841 + 5.196i$ $Z_4 = 5.362 + 4.499i$

$Z_5 = -1.464 + 3.809i$ $Z_6 = -7.305 + 6.042i$

$\phi_2 = 24.473°$ $\phi_3 = 40.214°$

$\psi_2 = 22.635°$ $\psi_3 = 36.136°$

$\Theta_{30} = -33.795°$ $\Theta_{40} = 8.7545°$

$K_1 = K_2 = K_3 = K_4 = 30.6878 \text{ in} - \text{lb/rad}$

The length of the small-length flexural pivot is taken as 5% of the longer rigid part. Thus, the pseudo-rigid-body link length obtained is addition of rigid part length, L and small-length flexural pivot length l . Selecting input link R_2 as pseudo-rigid-body link, the small-length flexural pivot length l_2 comes out as 0.2857 in and rigid part length, L_2 as 5.714 in. Using the equation, (17) as given below, the moment of inertia is obtained.

$$K_t = \frac{EI}{l} \tag{17}$$

where, E is the modulus of elasticity, I is the moment of inertia, l is the length of the small-length flexural pivot, K_t is the torsional spring stiffness. Using the thermoplastic polymer Polypropylene material, moment of inertia I comes out as $I = 4.383 \times 10^{-5} \text{ in}^4$. Selecting the rectangular cross-section for the compliant segment and assuming the width of 2 in, the thickness of the compliant segment is obtained. The value of thickness obtained is 0.06407 in. Similarly, for the output pseudo-rigid-body

link R_4, the small-length flexural pivot length l_4 and rigid part length, L_4 are as 0.3333 in and 6.667 in. The width is assumed to be 2 in and thickness value of 0.0675 in is obtained. The resulting compliant mechanism is shown in Figure 4.9. In order to compare the precision positions from PRBM and FEA, the Y displacements of coupler point are compared for given X displacements. The comparison between PRBM and FEA software ABAQUS® is shown in Table 4.11. The energy comparison between pseudo-rigid-body model and compliant mechanism obtained using ABAQUS® shown in Table 4.12.

Table 4.11. Precision Positions Comparison PRBM vs. Compliant Mechanism (FEA)

Pseudo-rigid-body four-bar mechanism		Compliant mechanism ABAQUS®		% Relative error in Y displacement
X displacement	Y displacement	X displacement	Y displacement	
-3.076	1.967	-3.076	1.9725	0.151
-6.076	2.467	-6.076	2.4893	0.339
-8.076	2.167	-8.076	2.2055	0.460

Table 4.12. Energy Comparison PRBM vs. Compliant Mechanism (FEA)

	Pseudo-rigid-body four-bar mechanism	Compliant mechanism (ABAQUS®)	% Error in energy obtained using PRBM and ABAQUS®
E_1	11.75	11.7682	0.155
E_2	37.25	37.4105	0.431
E_3	60	60.3288	0.548

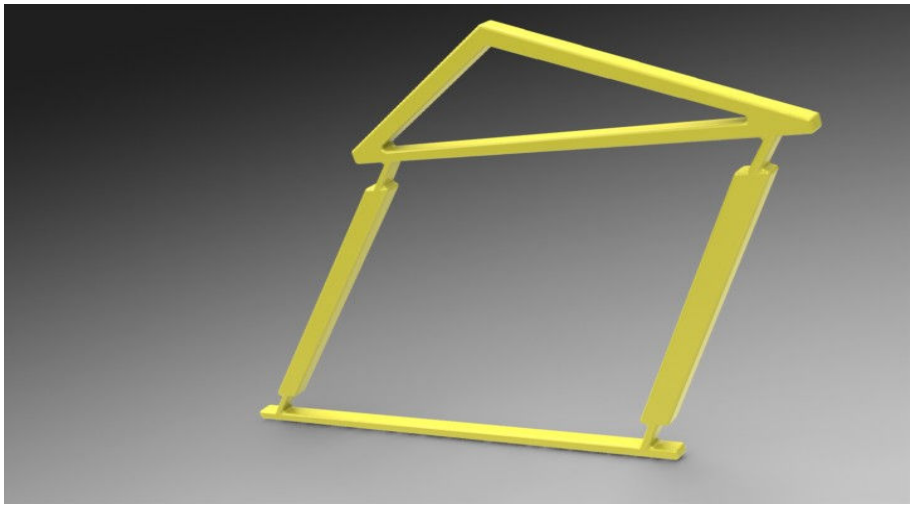

Figure 4.9. Solid Model of a Compliant Mechanism with Four Small-Length Flexural Pivots

The coupler curve obtained from PRBM is plotted along with precision positions marked on it. The coupler curve for this example is shown in Figure 4.10.

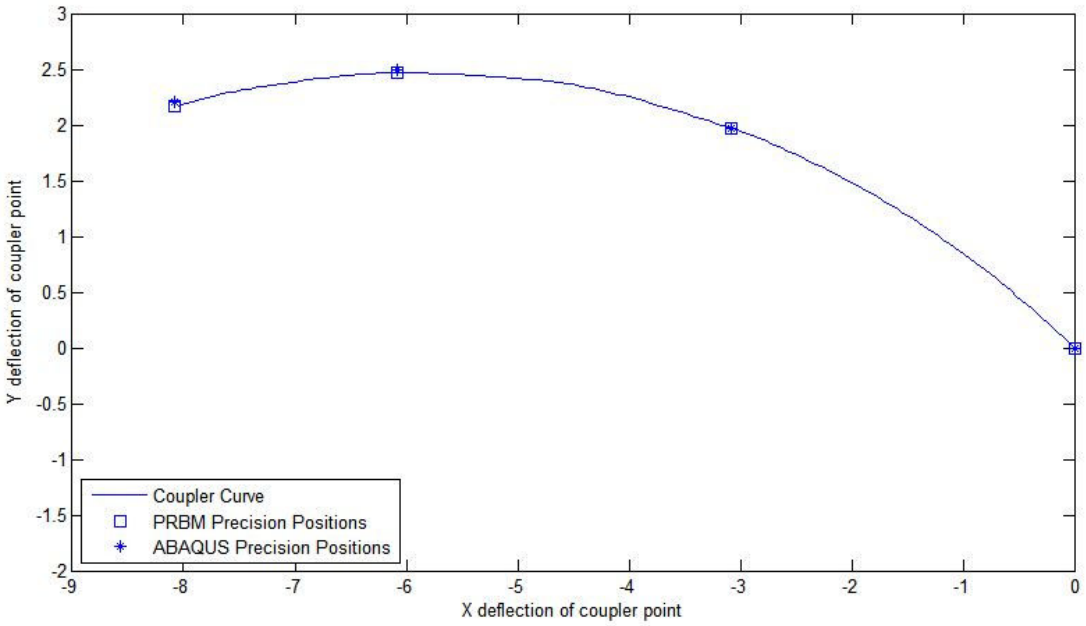

Figure 4.10. Coupler Curve Obtained from PRBM with Precision Positions

4.5.4. Case 4: Application of Straight-Line Generating Compliant Mechanism in Vehicle Suspension System.

The compliant mechanisms find numerous applications in real life such as in MEMS, precision instruments etc. The rigid-body straight-line mechanisms such as Watt's straight-line mechanism or Robert straight-line mechanism (Barlas, 2004) are used in vehicle suspension systems. The Chebyshev or Hoeken straight-line generating rigid-body mechanism has been designed for Mars Rover suspension mechanism (Barlas, 2004). Using this rigid-body straight-line generating mechanisms, the compliant straight-line generation mechanisms can be obtained using synthesis with compliance technique and these mechanisms can be used in suspension systems of small robotic vehicles. The compliant mechanism suspension system will have advantages like reduced weight, reduced number of parts etc. over rigid-body mechanisms. Figure 4.11 shows the rigid-body Hoeken straight-line mechanism with coupler point which almost follows straight line over much of its path (Howell, 2001). The link lengths in the mechanism can be specified as function of crank length R_2 as follows:

$$R_1 = 2R_2, \qquad R_3 = R_4 = 2.5R_2, \qquad a_3 = 5R_2, \qquad b_3 = 0$$

This rigid-body mechanism can be considered as the pseudo-rigid-body model for the compliant mechanism to be designed. A fully compliant mechanism can be obtained by using four small-length flexural pivots at four pin joints with energy storage considerations in compliant segments. But as the small-length flexural pivots can't rotate fully, the mechanism won't have full rotation; but it can move over much of the range of straight line path. The full rotation can be obtained by using two small-length flexural pivots.

The synthesis procedure for the Hoeken straight-line generating mechanism is given by example. e.g. It is desired to synthesize a compliant straight-line generating mechanism for three precision positions with energy specified as below:

$\delta_2 = -2 + 0\mathrm{i}$ $\delta_3 = -4 + 0\mathrm{i}$

$\mathrm{E}_1 = 2.15\ \mathrm{in-lb}$ $\mathrm{E}_2 = 49.5\ \mathrm{in-lb}$ $\mathrm{E}_3 = 66.1\ \mathrm{in-lb}$

For this, the rigid-body synthesis loop-closure equations are different from that of given by equations (13) for a four-bar mechanism. The link lengths in the mechanism can be expressed as function of crank length. The kinematic-loop closure equations are given below:

$$5\mathrm{R}_2(\cos(\Theta_{31}+\gamma_2)-\cos(\Theta_{31}))+\mathrm{R}_2(\cos(\Theta_{21}+\phi_2)-\cos(\Theta_{21}))=\mathrm{Re}(\delta_2) \quad 41(a)$$

$$5\mathrm{R}_2(\sin(\Theta_{31}+\gamma_2)-\sin(\Theta_{31}))+\mathrm{R}_2(\sin(\Theta_{21}+\phi_2)-\sin(\Theta_{21}))=\mathrm{Im}(\delta_2) \quad 41(b)$$

$$2.5\mathrm{R}_2(\cos(\Theta_{31}+\gamma_2)-\cos(\Theta_{31}))+\mathrm{R}_4(\cos(\Theta_{41}+\psi_2)-\cos(\Theta_{41}))=\mathrm{Re}(\delta_2) \quad 41(c)$$

$$2.5\mathrm{R}_2(\sin(\Theta_{31}+\gamma_2)-\cos(\Theta_{31}))+\mathrm{R}_4(\sin(\Theta_{41}+\psi_2)-\sin(\Theta_{41}))=\mathrm{Im}(\delta_2) \quad 41(d)$$

$$5\mathrm{R}_2(\cos(\Theta_{31}+\gamma_3)-\cos(\Theta_{31}))+\mathrm{R}_2(\cos(\Theta_{21}+\phi_3)-\cos(\Theta_{21}))=\mathrm{Re}(\delta_3) \quad 41(e)$$

$$5\mathrm{R}_2(\sin(\Theta_{31}+\gamma_3)-\sin(\Theta_{31}))+\mathrm{R}_2(\sin(\Theta_{21}+\phi_3)-\sin(\Theta_{21}))=\mathrm{Im}(\delta_3) \quad 41(f)$$

$$2.5\mathrm{R}_2(\cos(\Theta_{31}+\gamma_3)-\cos(\Theta_{31}))+\mathrm{R}_4(\cos(\Theta_{41}+\psi_3)-\cos(\Theta_{41}))=\mathrm{Re}(\delta_3) \quad 41(g)$$

$$2.5\mathrm{R}_2(\sin(\Theta_{31}+\gamma_3)-\cos(\Theta_{31}))+\mathrm{R}_4(\sin(\Theta_{41}+\psi_3)-\sin(\Theta_{41}))=\mathrm{Im}(\delta_3) \quad 41(h)$$

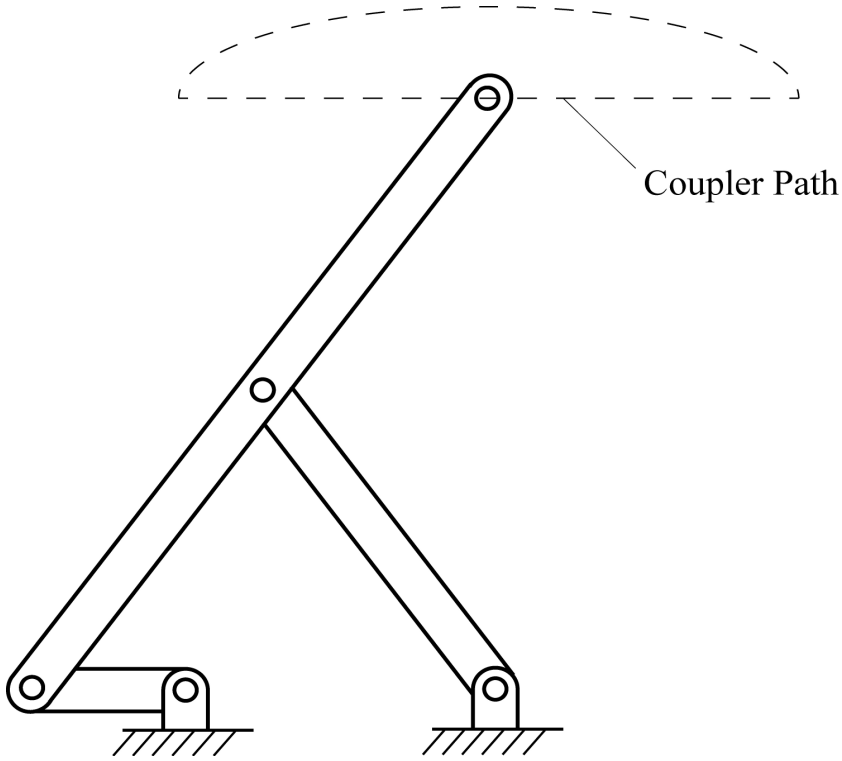

Figure 4.11. Rigid-body Hoeken Straight-Line Mechanism

The energy-free state loop-closure equation and energy equations are same as used in the previous synthesis examples. Assuming two torsional springs in the pseudo-rigid-body model four-bar mechanism, there are 8 kinematic loop-closure equations, 3 energy equations and 2 undeflected state loop-closure equations as discussed above, having 14 unknowns giving 3 free choices. A compliant mechanism with two small-length flexural pivots as shown in Figure 3.2 (K) is selected for synthesis. For convenience of sizing small-length flexural pivots, two spring stiffness values are restricted to be the same. R_2 and θ_{21} are selected as free choices as given below for solving kinematic loop-closure equations. Θ_{10} assumed to be as 0°.

$R_2 = 1$ in $\theta_{21} = 90°$

$\Theta_{20} = 70°$

Two undeflected state loop-closure equations are solved by selecting Θ_{20} as free choice. The solutions obtained from these two sets of equations are used as input to solve 3 energy equations by optimization approach. The solution obtained is as below:

$Z_1 = 2 + 0i$ $Z_2 = 0 + 1i$

$Z_3 = 2 + 1.499i$ $Z_4 = 0 + 2.5i$

$Z_5 = 2 + 1.499i$

$\phi_2 = 90°$ $\phi_3 = 180°$

$\psi_2 = 36.869°$ $\psi_3 = 53.130°$

$\gamma_2 = 16.26°$ $\gamma_3 = 53.130°$

$\Theta_{30} = 38.052°$ $\Theta_{40} = 82.862°$

$K_1 = 117.222\ \text{lb} - \text{in/rad}$ $K_2 = 117.222\ \text{lb} - \text{in/rad}$

The length of the small-length flexural pivot is taken as 5% of the longer rigid part. Selecting output link R_4 as pseudo-rigid-body link, the small-length flexural pivot length l_4 comes out as 0.1191 in and rigid part length, L_4 as 2.2809 in. Using the equation (17) and selecting thermoplastic polymer Polypropylene material, moment of inertia I comes out as $I = 6.9806 \times 10^{-5}\ \text{in}^4$. Selecting the rectangular cross-section for the compliant segment and assuming the width of 3 in. The value of thickness obtained is 0.06536 in. The resulting compliant mechanism is shown in Figure 4.12. The mechanism with crank length of 1 in generates a straight line of approximately 4.5 in for $270°$ crank rotation. In order to compare the precision positions from PRBM and FEA, the Y displacements of coupler point are compared for given X displacements. The comparison between PRBM and FEA software ABAQUS® is shown in Table 4.13.

Table 4.13. Precision Positions Comparison PRBM vs. Compliant Mechanism (FEA)

Pseudo-rigid-body four-bar mechanism		Compliant mechanism ABAQUS®		% Relative error in Y displacement
X displacement	Y displacement	X displacement	Y displacement	
-0.2793	-0.0215	-0.2793	-0.02038	0.399
-2.2793	-0.0215	-2.2793	-0.01045	0.484
-4.2793	-0.0215	-4.2793	-0.0213	0.005

The energy comparison between pseudo-rigid-body model and compliant mechanism obtained using ABAQUS® shown in Table 4.14.

Table 4.14. Energy Comparison PRBM vs. Compliant Mechanism (FEA)

	Pseudo-rigid-body four-bar mechanism	Compliant mechanism (ABAQUS®)	% Error in energy obtained using PRBM and ABAQUS®
E_1	2.15	2.1327	0.806
E_2	49.5	49.2079	0.590
E_3	66.1	66.915	1.233

Figure 4.12. Solid Model of Compliant Straight-Line Generating Mechanism with Two Small-Length Flexural Pivots

The coupler curve obtained from PRBM is plotted along with precision positions marked on it. The coupler curve for this example is shown in Figure 4.13.

A sample MATLAB® code for this example is provided in Appendix B.

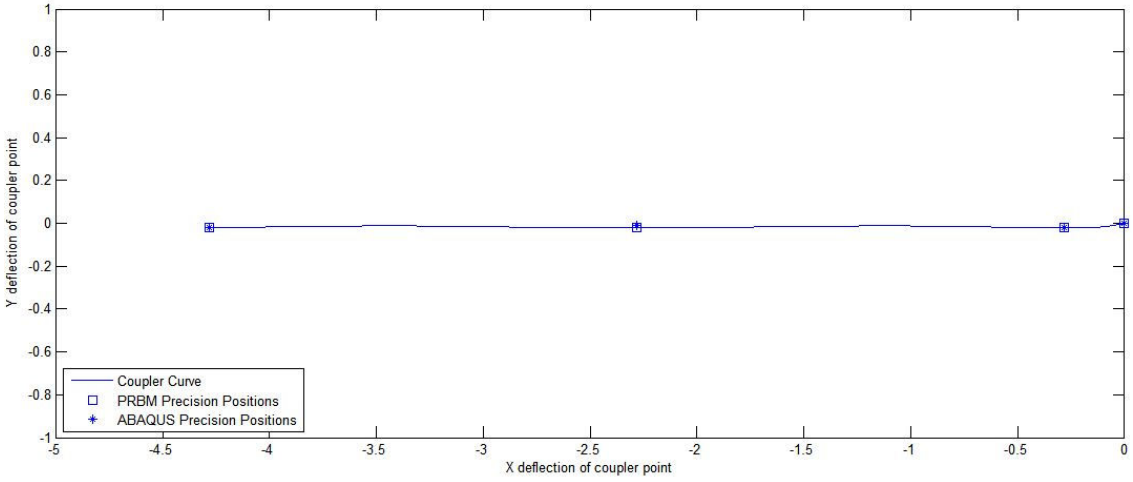

Figure 4.13. Coupler Curve Obtained from PRBM with Precision Positions

The pseudo-rigid-body model considered for fixed-guided segments in this work was tailored to work for fixed-guided segments with constant beam end angle. But it is observed that the PRBM considered here for fixed-guided segment works well for fixed-guided segments with varying beam end angles also. It has been observed that, the FEA software ABAQUS® and ANSYS® give different solutions of the precision position displacements and energies at precision positions for the problem modeled in the same way. The formula to calculate the percentage relative error in displacement can be found in Appendix A.

4.7. SUMMARY

In this Section, the optimization concept, types of optimization and design process are reviewed. The optimization routine developed for solving energy/torque equations is presented. The strongly coupling and weakly coupling of kinematic and energy/torque equations is studied and the results are explained with example. The energy equivalence between pseudo-rigid-body model and the corresponding compliant mechanism using FEA is discussed. The tables outlining the number of equations, number of variables, and number of free choices for different synthesis cases with different number of springs are presented. The different cases of synthesis based on number of torsional springs, types of compliant segments etc. are presented. The results obtained from pseudo-rigid-body model concept are compared with FEA. The new approach is used to synthesize the straight-line generating compliant mechanism which can be used in the suspension system of small robotic vehicles.

5. EXPERIMENTAL VALIDATION

In parallel with validation of results using finite element analysis software, the experimental setup is manufactured to validate the results practically. This Section discusses the experimental setup, and the testing procedure. The experiment is performed on pseudo-rigid-body model four-bar mechanism with one torsional spring. The compliant mechanism with one fixed-pinned segment is selected for synthesis.

5.1. EXPERIMENTAL SETUP

An experimental setup is made up of two parts i) upper part of the setup is used for testing cantilever beams ii) lower part can be used to test compliant mechanisms and is shown in Figure 5.1. The experimental setup is bolted to the wooden pieces, which are used to clamp the whole setup on table with four c-clamps. In this work, as the experiment is being done on compliant mechanisms, only lower part of the setup is discussed. The experimental setup is shown in Figure 5.1.

The input and output segments of the compliant mechanism are mounted in two separate jaws and fastened with bolts. The jaws are mounted on rotating bars so as rotate and hold the segment at any initial angle. The rotating bar can be fixed at particular required angle using vise and blocks lined with friction pads on inside. These rotating bars are in turn mounted on two bearings which are mounted on two sliding fixtures. These fixtures are free to move on horizontal guides so as to accommodate the mechanisms with varying ground link length. If the compliant segment, fixed at ground is placed in the jaw; the effective length of the compliant segment is measured from the top

end of the jaw. On the other hand, when the compliant or rigid segment is pinned to the ground, the effective length of the segment starts from center of the rotating bar.

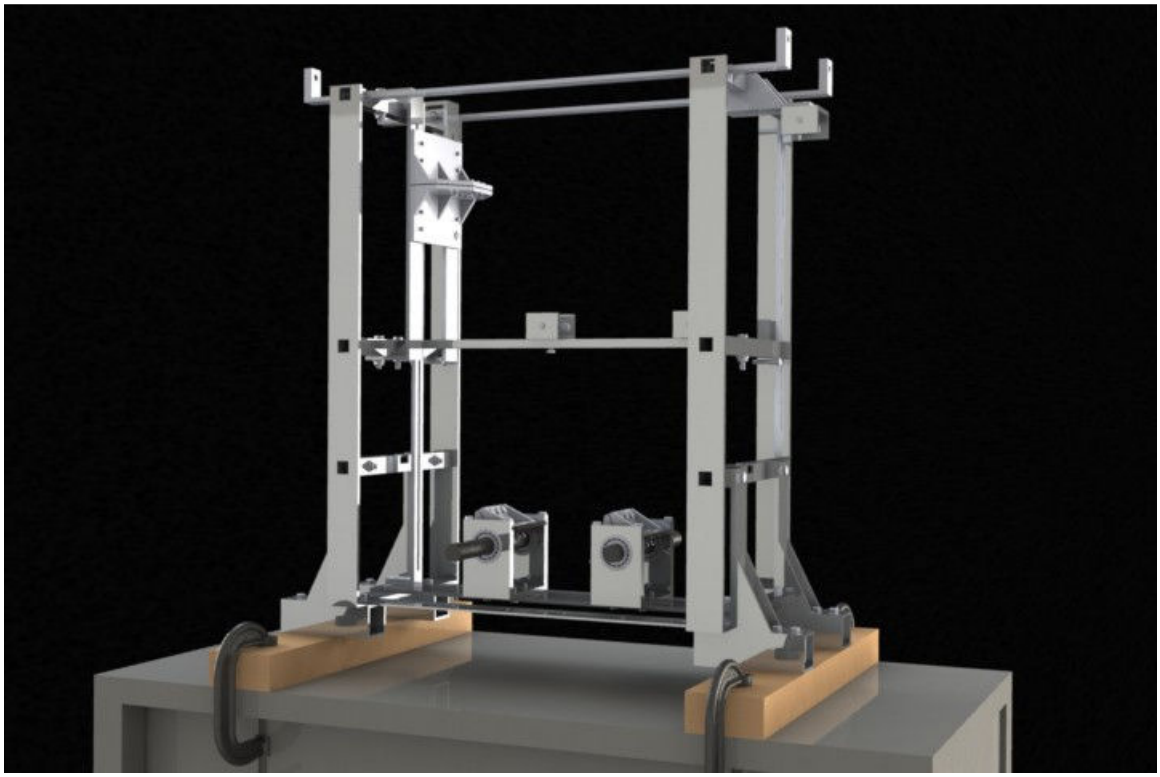

Figure 5.1. Experimental Setup CAD

The angle for the ground link varies with initial position angle of the input and output links. So in order to mount a compliant mechanism, the pseudo-rigid-body ground link angle should be adjusted. The experimental setup with compliant mechanism mounted is shown in Figure 5.2.

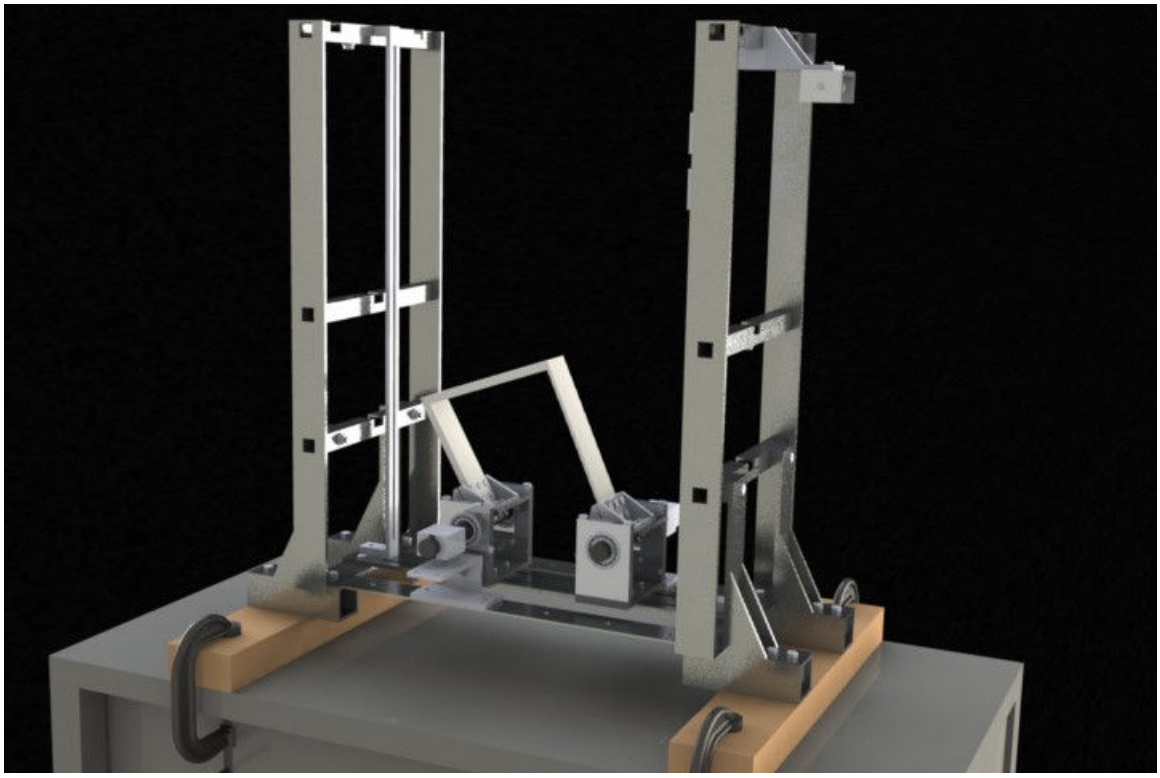

Figure 5.2. Experimental Setup with Compliant Mechanism

The load is applied using the light-weight string passing over the three frictionless pulleys A, B and C so as to have minimum frictional resistance. The pulley A is free to slide so as to adjust the loading angle. The loads are applied by using loading pan attached to the other end of the string. Figure 5.3 shows the mechanism loaded with light-weight string passing over three pulleys. One end of the string is attached to pinned end of the compliant segment, while the loading pan is attached to other hanging end. The following section presents an example in which the compliant mechanism is synthesized using synthesis with compliance technique and in latter section; the testing procedure and results are discussed.

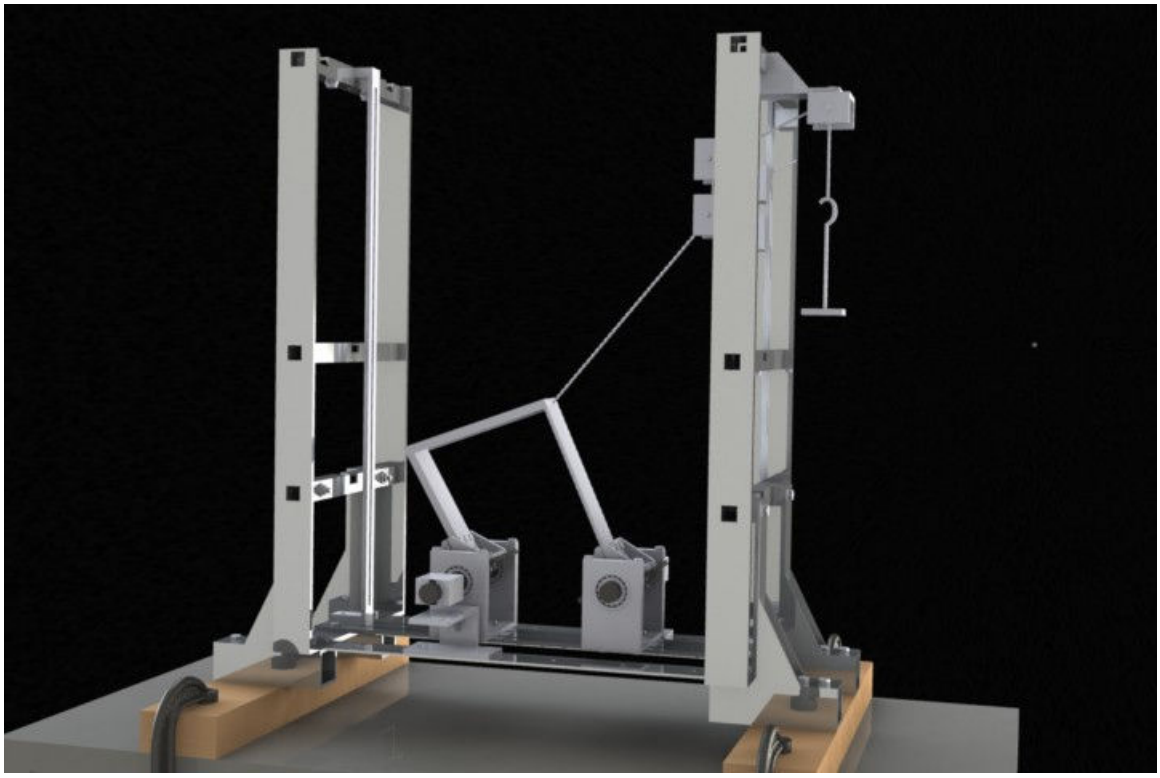

Figure 5.3. Experimental Setup with Compliant Mechanism and Loading Arrangement

5.2. EXAMPLE

The pseudo-rigid body four-bar mechanism with one torsional spring is selected for the experiment. For this mechanism, a compliant mechanism with one fixed-pinned segment is selected.

e.g. It is desired to synthesize a compliant mechanism for three precision positions path generation with prescribed timing synthesis, energy specified at these points as follows:

$\delta_2 = -0.646 + 1.58\mathrm{i}$ $\delta_3 = -1.227 + 2.54\mathrm{i}$

$\phi_2 = 11.20°$ $\phi_3 = 19.10°$

$E_1 = 1.207\ \text{in} - \text{lb}$ $E_2 = 3.828\ \text{in} - \text{lb}$ $E_3 = 6.563\ \text{in} - \text{lb}$

Assuming one torsional spring in the pseudo-rigid-body model four-bar mechanism, there are 8 kinematic loop-closure equations, 3 energy equations and 2 energy-free state loop-closure equations, having 19 unknowns giving 5 free choices (Table 4.3). A compliant mechanism with one fixed-pinned segment as shown in Figure 3.2 (R) is selected for synthesis. $R_2, R_4, \theta_{21}, \theta_{41}$, are selected as free choices as given below for solving loop-closure equations.

$R_2 = 5.5$ in $\quad\quad$ $R_4 = 7.25$ in

$\theta_{21} = 30.2°$ $\quad\quad$ $\theta_{41} = 11.71°$

$\Theta_{20} = 15.86°$

Two energy-free state loop-closure equations are solved by selecting Θ_{20} as free choice. The solutions obtained from these two sets of equations are used as input to solve 3 energy equations by optimization approach. The coupler equation (37) and first precision position loop-closure equation (39) are considered to determine remaining link lengths and angles. These add 4 scalar equations and 4 unknowns. The solution obtained is as below:

$Z_1 = 3.902 - 0.8802i$ $\quad\quad$ $Z_2 = 4.754 + 2.767i$

$Z_3 = 6.249 - 2.176i$ $\quad\quad$ $Z_4 = 7.099 + 1.471i$

$Z_5 = 7.929 - 0.148i$ $\quad\quad$ $Z_6 = 1.68 + 2.027i$

$\psi_2 = 11.948°$ $\quad\quad$ $\psi_3 = 19.825°$

$\Theta_{30} = -28.356°$ $\quad\quad$ $\Theta_{40} = -6.008°$

$K_1 = 38.536$ lb $-$ in/rad

The length of the fixed-pinned segment is determined by using equation (23). Selecting input link R_2 as pseudo-rigid-body link, the compliant segment length l_2 comes

out as 6.4706 in. Using the equation (15), the moment of inertia is obtained. Using the Delrin® as material, moment of inertia I comes out as $I = 2.212 \times 10^{-4}$ in^4. Selecting the rectangular cross-section for the compliant segment and assuming the width of 1.5 in, the thickness of the compliant segment is obtained as 0.121 in. The resulting compliant mechanism is shown in Figure 5.4.and individual links are shown in Figure 5.5.

An energy comparison between pseudo-rigid-body model and compliant mechanism, using commercial finite element software ABAQUS® is done to verify equivalence of the design and validate the solution. Given the dimensional and material properties of the compliant mechanism, the ABAQUS® is used to find out the energy stored in the mechanism at precision positions. The results are shown below in Table 5.1.

Table 5.1. Energy Comparison PRBM vs. Compliant Mechanism (FEA)

	Pseudo-rigid-body four-bar mechanism	Compliant mechanism (ABAQUS®)	% Error in Energy
E_1	1.207	1.149	4.82
E_2	3.829	3.636	5.04
E_3	6.563	6.231	5.07

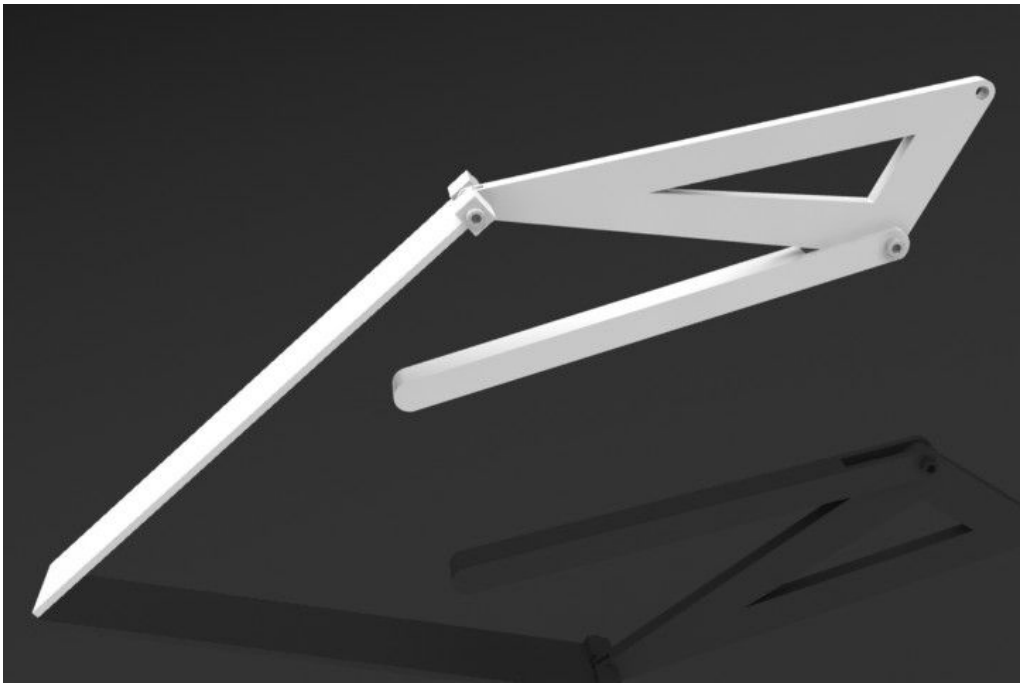

Figure 5.4. Solid Model of A Compliant Mechanism

The dimensions of the three links are as follows:

Input compliant link:

Length $L_2 = 6.4706$ in, width $b = 1.5$ in and thickness $h = 0.121$ in

Output link:

Length $R_4 = 7$ in, width $b = 0.6$ in and thickness $h = 0.5$ in

Coupler: It has three links rigidly joined.

$R_3 = 6.616$ in, $R_5 = 7.926$ in, and $R_6 = 2.633$ in, width $b = 2.491$in and thickness $h = 0.3$ in

Ground link:

Length $R_1 = 4.169$ in

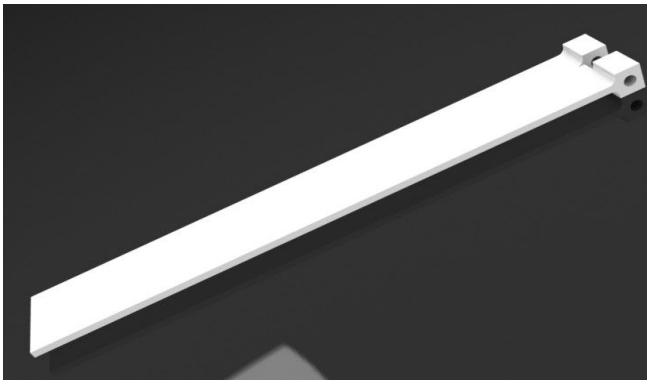

(a)

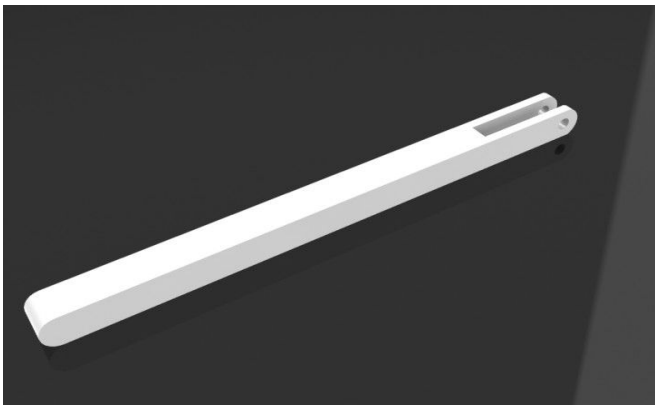

(b)

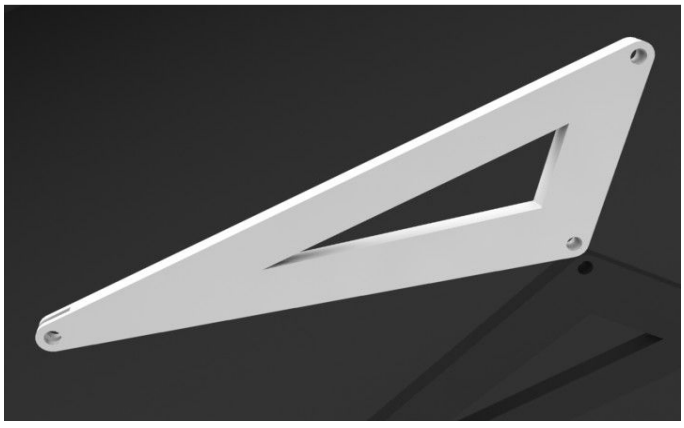

Figure 5.5. CAD Models (a) Input Compliant Link (b) Output Link (c) Coupler

5.3. TESTING AND RESULTS

The experimental setup described above is manufactured and assembled as shown in Figure 5.6. The whole setup is manufactured with Aluminum 6061.

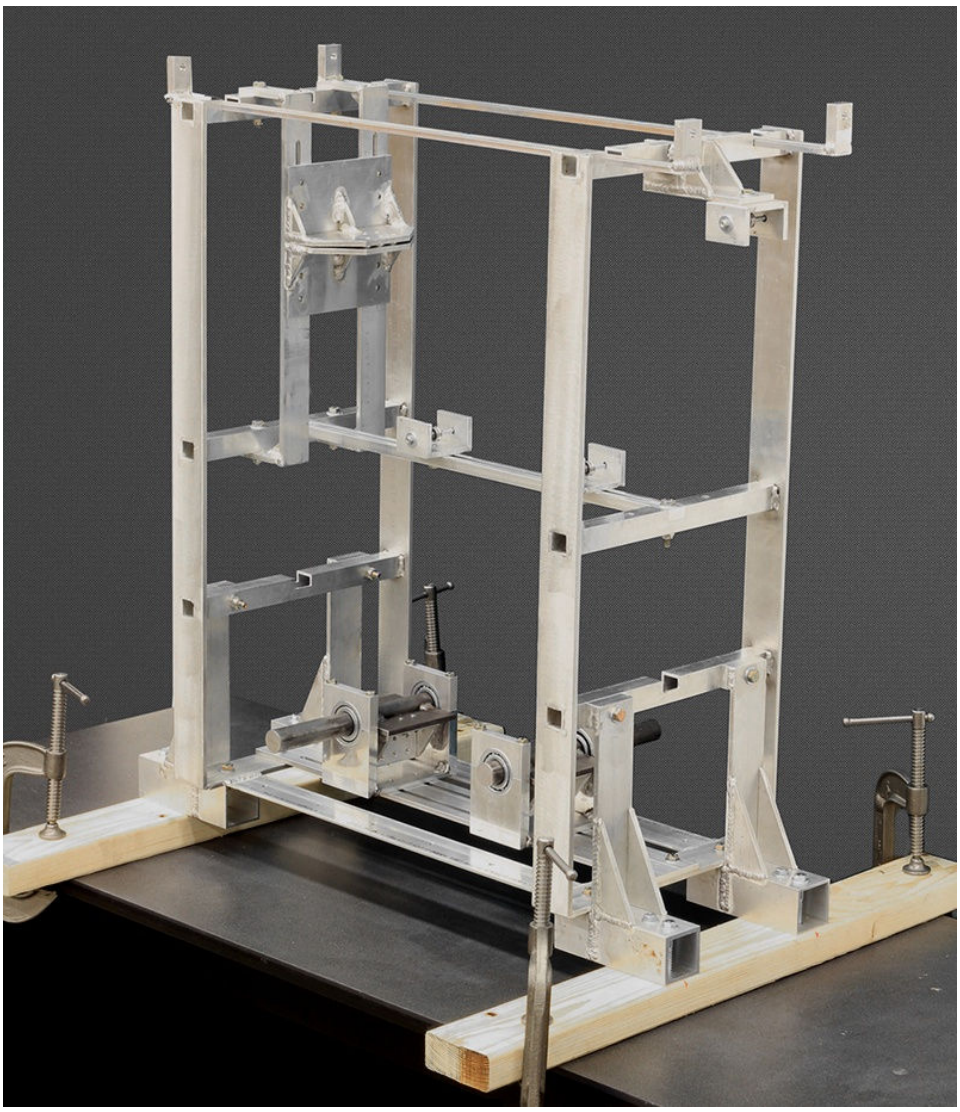

Figure 5.6. An Experimental Setup

After synthesizing the compliant mechanism using synthesis with compliance technique, the mechanism is analyzed using ABAQUS® for stresses and it is ensured that

stresses within the links are under yield strength of the material. The Delrin® is selected as the material for all the segments in the compliant mechanism due to its good machinability.

The thickness and width of all segments particularly the compliant fixed-pinned segment in the mechanism are adjusted so as not to exceed the yield strength of 8000 psi of the Delrin® material. The individual pieces are manufactured and assembled to generate compliant mechanism. The ground link is generated by maintaining the fixed distance between the centers of two rotating bars. The compliant link is fixed to the one jaw, of which the rotation is restricted by holding the rotating bar in a vise with two pieces which are inlined with friction material to ensure no rotation. The rotating rod, to which the rigid link attaches, is free to rotate and so it acts as pin joint. Both rotating bars are mounted on bearings to ensure smooth rotation. All the bearings and pulleys are lubricated to minimize the friction. The input, output link, coupler links and ground link are shown in Figure 5.7 (a), (b), (c) and (d). The loads to be applied are calculated from PRBM. Due to the few angle constraints in experimental setup, the loading angle is adjusted to 129° with the horizontal instead of 90°. The load values obtained from PRBM for three precision positions are as follows:

$F_1 = 1.7742$ lb, $F_2 = 3.1269$ lb $F_3 = 4.1589$ lb

(a)

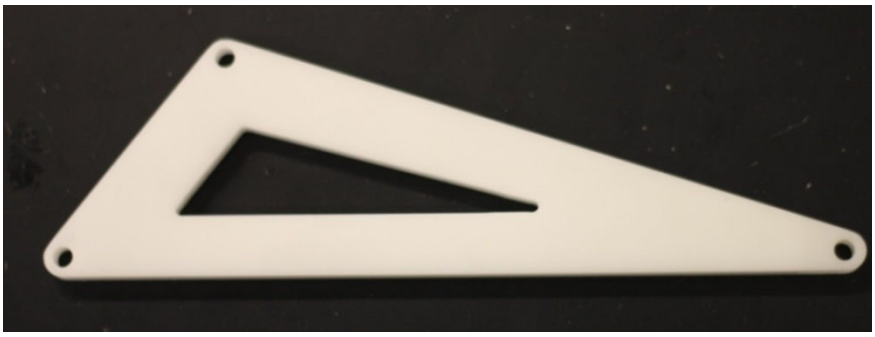

(b)

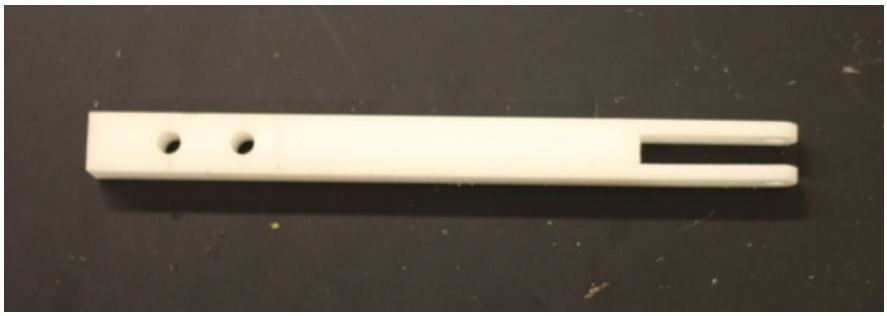

Figure 5.7. Compliant Mechanism for Experiment (a) Input Compliant Link (b) Output Link (c) Coupler (d) Ground Link

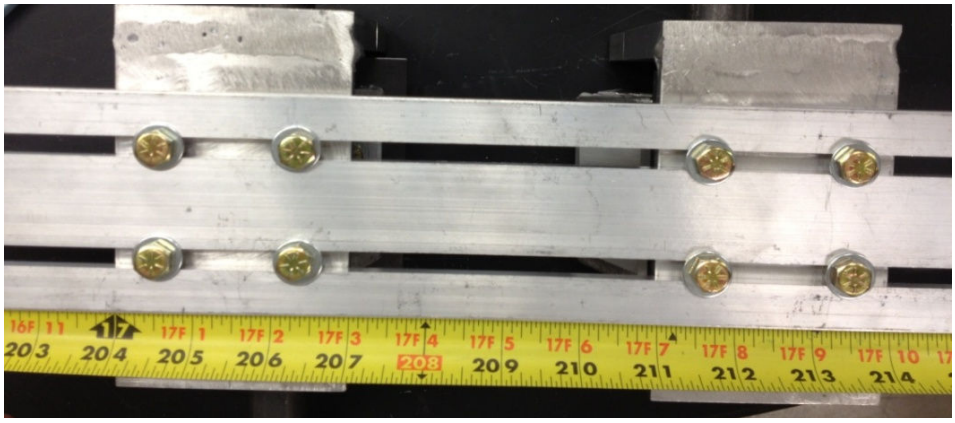

Figure 5.7. Compliant Mechanism for Experiment (a) Input Compliant Link (b) Output Link (c) Coupler (d) Ground Link (contd.)

The mechanism is mounted in energy-free state on the setup and is shown in Figure 5.8.

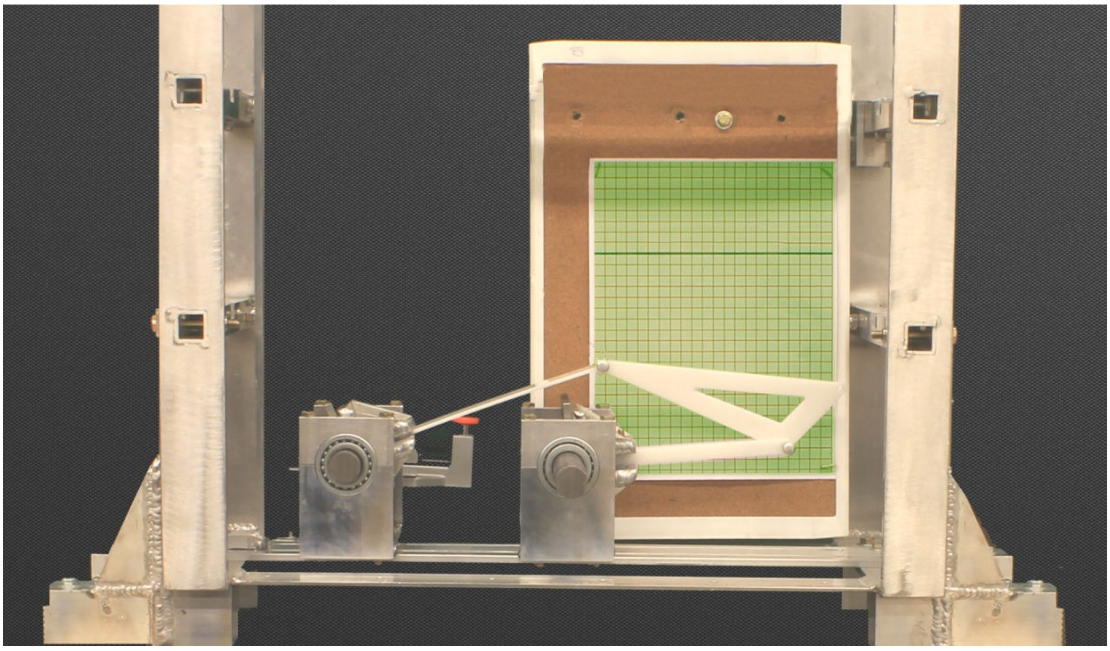

Figure 5.8. Compliant Mechanism in Energy-Free State

The load is applied to input compliant link with loading string fastened to pin passing through input and coupler link as shown in Figure 5.9. As there are three pulleys and one bearing used, the frictional force has to be considered while applying the loads to the mechanism. The loading pan used to hold the weights is found to be of 0.34 lb.

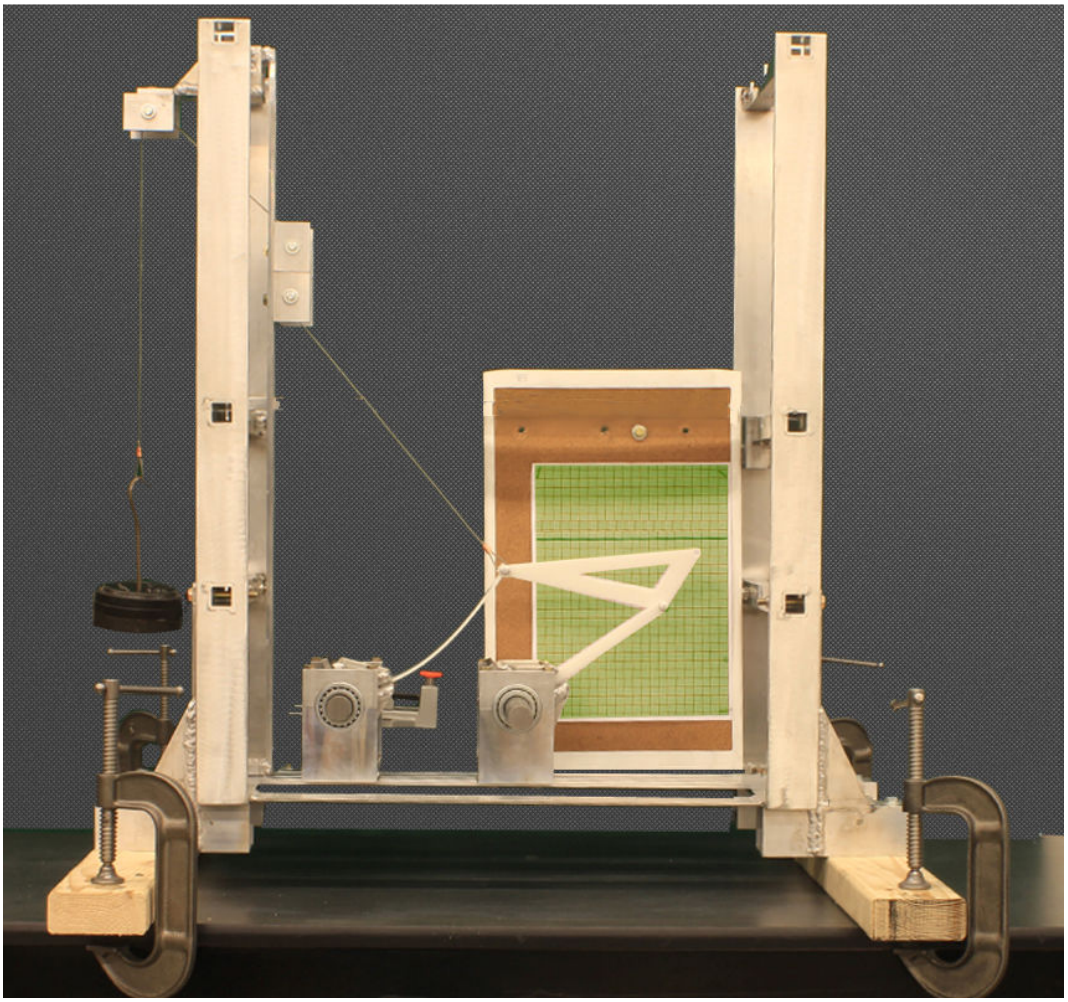

Figure 5.9. A Compliant Mechanism Loaded

The frictional forces between the rope and pulley is calculated by a simple experiment as shown in Figure 5.10 and using the Capstan friction equation (Meriam, 1978) as mentioned below.

$$T_2 = T_1 e^{\mu\beta} \tag{42}$$

where, T_1 is the tension force in the low tension rope and T_2 is the tension force in the high tension rope, μ is the coefficient of friction and β is the angle of contact between the rope and pulley.

From the experiment, the coefficient of friction between rope and pulley is found to be 0.01. This is used to calculate the frictional forces at the pulleys and final load to be applied is determined by adding these frictional forces at three pulleys to the loads calculated by PRBM for precision positions. The final loads to be applied are obtained as below:

$F_1 = 1.8407$ lb, $F_2 = 3.2427$lb $F_3 = 4.3115$ lb

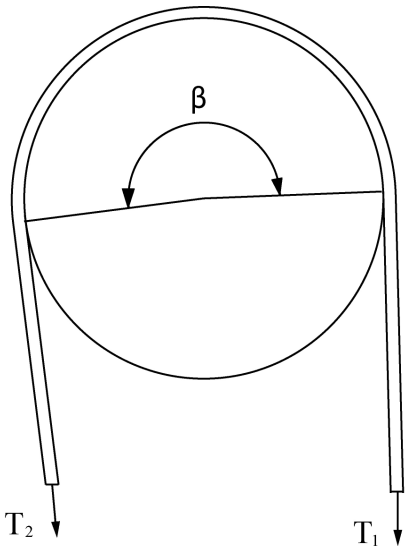

Figure 5.10. The Capstan Friction Equation Experiment

It was difficult to get and apply such accurate loads. So the nearest available loads 1.84 lb, 3.34 lb, 4.34 lb are applied. With each load applied, the X and Y co-ordinates of the coupler point are recorded on the graph paper attached to the cork board. A coupler curve is obtained from PRBM. The precision positions obtained from ABAQUS® and experiment are plotted on the same curve as shown in Figure 5.11. In order to get the precision positions from ABAQUS®, the X displacements are given to the coupler point and Y displacements are obtained. All the length measurements are done using vernier caliper.

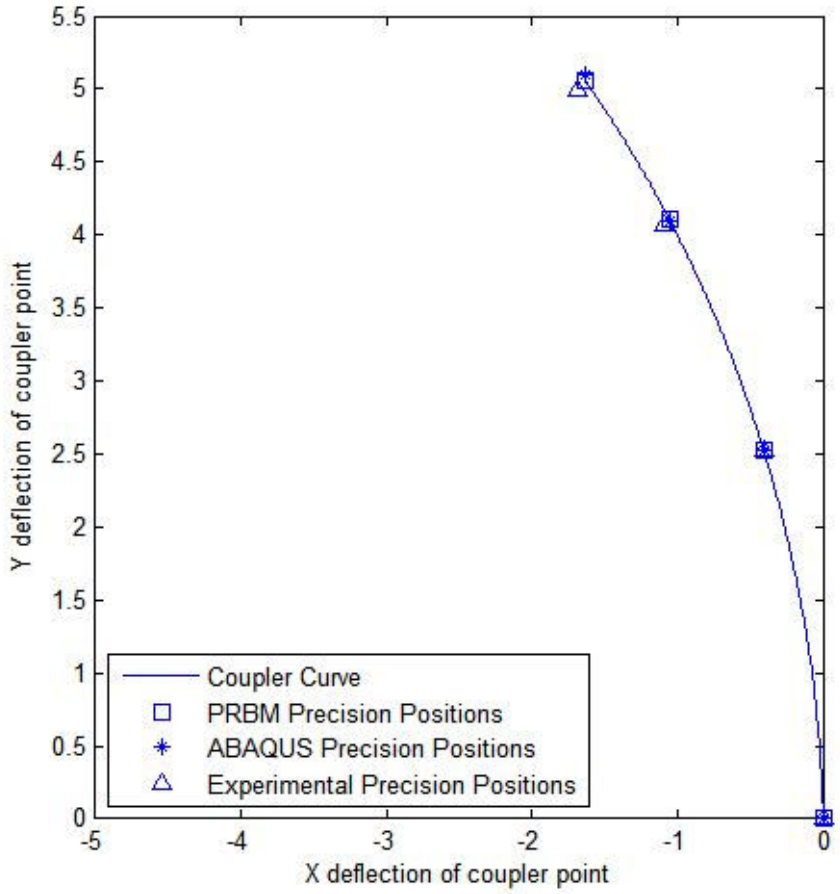

Figure 5.11. Coupler Curve Obtained from PRBM with Precision Positions

5.4. DISCUSSION OF RESULTS

The measured data points are plotted and a smooth coupler curve passing through those points is drawn. Figure 5.11 shows the coupler curve comparison obtained from PRBM, FEA and experiment. There are many sources of errors which cause the deviations in precision positions. Some of them are listed below:

- The loads applied are little higher than the obtained from theoretical calculation. This may have induced some errors in the deflection,
- All the theoretical calculations are done considering link length and angle dimensions up to third digit after the decimal point. But while manufacturing it was very difficult to manufacture the parts with that precision. e.g. The length of coupler links used in theoretical calculations are $R_3 = 7.926$ in, $R_5 = 6.616$ in , $R_6 = 2.633$ in; but the actual parts are manufactured with the dimensions $R_3 = 7.9$ in, $R_5 = 6.6$ in, $R_6 = 2.6$ in.
- The Young's modulus of the beam's material is not provided by the manufacturer. The value of E is calculated in the lab using PRBM formulae by applying load of 0.84 lb and measuring deflection.
- Errors in measurement
- The average values of PRBM parameters such as γ and K_θ are considered. This assumption contributed to some extent in the errors.

With these many sources of the error, the results obtained are fairly accurate and the relative error in the precision position displacements is below 1.58%. With the more research work in this direction, the errors may be further reduced and accuracy of the results can be improved.

5.5. SUMMARY

In this Section, the experimental setup designed, and manufactured to perform experiments on compliant cantilever beam and mechanism is presented. The testing procedure and mechanism synthesized for an experiment are explained with CAD models and photographs. The path generation with prescribed timing synthesis for three precision positions with energy specifications synthesis example is provided and the results are validated by comparing precision positions and energies at precision positions. The possible sources of error are briefly discussed at the end.

6. CONCLUSIONS AND FUTURE WORK

6.1. CONCLUSIONS

The pseudo-rigid-body model (PRBM) naturally enables the use of the vast body of existing knowledge of rigid-body mechanism synthesis and analysis techniques for compliant mechanism synthesis and analysis, and vice versa. The synthesis with compliance technique uses the PRBM concept to synthesize compliant mechanisms for conventional rigid-body mechanism tasks, e.g. path generation, motion generation, etc. with energy/torque considerations at the precision positions. The existing synthesis with compliance technique is reviewed and its limitations in the current form of usage are discussed with examples. A methodology for synthesis with compliance technique, using an optimization approach, is developed which overcomes the limitations such as negative or unrealistic solutions for the critical spring stiffness values. It provides a way to guide the user as to how the values of the initial estimates should be changed in order to obtain realistic solutions in fewer number of iterations. This methodology makes the synthesis procedure computationally simple, expedient and less cumbersome by separating the set of kinematic equations from the energy/torque equations.

Many of the synthesis cases for the compliant mechanisms, with a four-bar PRBM, which were not easily solvable by the synthesis with compliance technique, now were readily solved with the new method. The design tables providing information about the number of equations, number of unknowns and number of free choices for a pseudo-rigid-body four-bar mechanism, with varying number of torsional springs for different synthesis types, may be readily used for synthesis. Recommendations for energy/torque specifications at the precision positions are given so as to make the solution procedure

easy. The strongly coupled and weakly coupled system of kinematic and energy/torque equations have been studied. It is demonstrated that even solving the synthesis cases which are characterized as strongly coupled, by treating and solving them as weakly coupled systems, also readily provide solutions. These solutions are likely subsets from the entire set of possible solutions to the nonlinear system of equations. The new approach, for solving equations by treating them as a weakly coupled system, has certain advantages such as computationally simple, fast and more stable. The user has to assign reasonable values to a relatively smaller number of variables, as compared to a strongly coupled system, solved in the conventional way.

Different cases of synthesis have been presented using the proposed technique for various synthesis tasks of a pseudo-rigid-body four-bar mechanism, for three precision positions with energy/torque specifications. These include a general synthesis case where the undeflected state of the mechanism is different from the prescribed precision positions. The synthesis case, where the undeflected state of the mechanism is coincident with one of the precision positions, will require a reduced system of equations to be solved. Different compliant segments have been used in examples to validate the synthesis technique and the PRBMs. A straight-line generating compliant mechanism, which could be used in the suspension system of a small robotic vehicle, is synthesized. The finite element analysis software ABAQUS® and/or ANSYS® are used to analyze the synthesized compliant mechanism, for the purpose of validation. The experiment was conducted using a designed compliant mechanism containing one fixed-free segment; the PRBM results are satisfactorily verified using the FEA and experimental results.

6.2. RECOMMENDATIONS

This work presents the use of synthesis with compliance technique, augmented by incorporating an optimization approach for a pseudo-rigid-body four-bar mechanism for three precision positions synthesis problems. This method is also applicable to synthesis cases with more than three precision positions. A distinct possibility exists, since the kinematic and energy/torque equations are separated from each other (treated as a weakly coupled system), that we should be able to use the proposed technique to synthesize compliant mechanisms which have PRBMs other than four-bar mechanisms, e.g. five-bar mechanisms, etc.

The PRBMs used in this work, for the fixed-free compliant segment and the fixed-guided compliant segment, assumes the average values of the PRBM parameters, such as characteristic radius factor and stiffness coefficient. This assumption introduces some errors in the results. More accurate results may be obtained by the use of variable PRBM parameters as functions of the load factor.

The experiment has been performed on a compliant mechanism synthesized for three precision positions with energy specifications, and consisting of one fixed-free compliant segment. The results go a long way to validate the usefulness of the proposed method as well as the PRBM concept. In future work, extensive experimental validation should be conducted involving more complex compliant mechanisms, with different compliant segment types, for different synthesis tasks and with more precision positions, and for torque specification cases also.

Metallic inserts could be used in the segments to synthesize compliant mechanisms with low creep and higher strength properties.

BIBLIOGRAPHY

Albanesi, A. E., Fachinotti, V. D., and Pucheta, M. A., 2010, "A Review on Design Methods for Compliant Mechanisms," *Asociación Argentina de Mecánica Computacional, Mecánica Computacional* Vol. XXIX, pp. 59-72.

Anantsuresh, G. K., 1994, "A New Design Paradigm for Micro-Electro-Mechanical Systems and Investigation on the Compliant Mechanism Synthesis," Ph.D. Thesis, University of Michigan, Ann Arbor.

Annamalai, Y., 2003, "Compliant Mechanism Synthesis for Energy and Torque Specifications," M.S. Thesis, University of Missouri-Rolla.

Bisshopp, K.E., and Drucker, D.C., 1945, "Large Deflection of Cantilever Beams," *Quarterly of Applied Mathematics*, Vol. 3, No. 3, pp. 272-275.

Barlas, F., 2004, "Design of a mars Rover Suspension Mechanism," M.S. Thesis, Izmir Institute of Technology, Turkey.

Burns, R. H., 1964, "The Kinenostatic Synthesis of Flexible Link Mechanisms," Ph.D. Dissertation, Yale University.

Burns, R. H., and Crossley, F. R. E., 1968, "Kinetostatic Synthesis of Flexible Link Mechanisms," ASME Paper 68-Mech-36.

Dado, M. H., 2000, "Variable Parametric Pseudo-Rigid-Body Model for Large-Deflection Beams with End Loads," *International Journal of Non-Linear Mechanics*, Vol. 36 pp. 1123-1133.

Dado, M. H., 2005, "Limit Position Synthesis and Analysis of Compliant 4-Bar Mechanisms with Specified Energy Levels Using Variable Parametric Pseudo-Rigid-Body Model," *Mechanism and Machine Theory* Vol. 40, No.8 pp. 977-992.

Erdman, A. G., and Sandor, G. N., 1997, *Mechanism Design and Analysis*, Vol.1, 3rd Ed., Prentice Hall, Upper Saddle River, NJ.

Frecker, M. I., Ananthasuresh, G. K., Nishiwaki, S., Kikuchi, N., and Kota, S., 1997, " Topological Synthesis of Compliant Mechanisms Using Multi-Criteria Optimization," *Journal of Mechanisms, Transmissions, and Automation in Design*, Trans. ASME, Vol. 119, pp. 238-245.

Frish-Fay, R., 1962, *Flexible Bars,* Butterworths, London.

Harrison, H.B., 1973, "Post-Buckling Analysis of Non-Uniform Elastic Columns," *International Journal for Numerical Methods in Engineering*, Vol. 7, pp. 196-210.

Her, I., 1986, “Methodology for Compliant Mechanism Design,” Ph.D. Dissertation, Purdue University.

Her, I., and Midha, A., 1987, “A Compliance Number Concept for Compliant Mechanism, and Type Synthesis,” *Journal of Mechanisms, Transmissions, and Automation in Design*, Trans. ASME, Vol. 109, No. 3, pp. 348-355.

Her, I., Midha, A., and Salamon, B. A., 1992, "A Methodology for Compliant Mechanisms Design: Part II - Shooting Method and Application", *Advances in design Automation*, (Ed.: D. A. Hoeltzel), DE-Vol. 44-2, 18th ASME Design Automation Conference, pp. 39-45.

Hill, T.C., and Midha, A., 1990, “A Graphical User-Driven Newton-Raphson Technique for the use in the Analysis and Design of Compliant Mechanisms,” *Journal of Mechanisms, Transmissions, and Automation in Design*, Trans. ASME, Vol. 112, No. 1, pp. 123-130.

Howell, L. L., and A. Midha, 1994, "A Method for the Design of Compliant Mechanisms with Small-Length Flexural Pivots," *Journal of Mechanisms, Transmissions, and Automation in Design*, Trans. ASME, Vol. 116, No. 1, pp. 280-290.

Howell, L. L., and Midha, A., 1995, "Parametric Deflection Approximations for End Loaded, Large-Deflection Beams in Compliant Mechanisms," *Journal of Mechanisms, Transmissions, and Automation in Design*, Trans. ASME, Vol.117, No.1, pp. 156-165.

Howell, L. L., 2001, *Compliant Mechanisms*, John Wiley and Sons, Inc., New York, New York.

Howell, L. L., and Midha, A., 1996, "A Loop-Closure Theory for the Analysis and Synthesis of Compliant Mechanisms," *Journal of Mechanisms, Transmissions, and Automation in Design*, Trans. ASME, Vol. 118, No.1, pp. 121-125.

Howell, L. L., 1991, "The Design and Analysis of Large-Deflection Members in Compliant Mechanisms," M.S. Thesis, Purdue University.

Howell, L. L., and Midha, A., 1994, "A Generalized Loop-Closure Theory for the Analysis and Synthesis of Compliant Mechanisms, "*Machine Elements and Machine Dynamics*, (Eds.: G. R. Pennock et al.), D E-Vol. 71, 23rd Biennial ASME Mechanisms Conference, pp. 491-500.

Howell, L. L., 1993, "A Generalized Loop-Closure Theory for the Analysis and Synthesis of Compliant Mechanisms," Ph.D. Dissertation, Purdue University.

Kolachalam, S. K., 2003, "Synthesis of Compliant Single-Strip Mechanisms that may be Represented by a Dyad," M.S. Thesis, University of Missouri-Rolla.

Krovi, V., Ananthsuresh, G. K., and Kumar, V., 2002, "Kinematic and Kinetostatic Synthesis of Planar coupled Serial Chain Mechanisms," *Journal of Mechanisms, Transmissions, and Automation in Design*, Trans. ASME, Vol. 124, No.2, pp. 301-312.

Lu, K. J., and Kota, S., 2003, "Design of Compliant Mechanisms for Morphing Structural Shapes," *Journal of Intelligent Systems and Structures*, Vol. 14, pp. 379-391.

Mallik, A. K., Ghosh, A., Dittrich, G., 1994, *Kinematic Analysis and Synthesis of Mechanisms*, CRC Press Inc., Boca Reton, Florida.

Mattiason, K., 1981, "Numerical Resukts from Large Deflection Beam and Frame Problmes Analyzed by means of Elliptic Integrals," *International Journal for Numerical Methods in Engineering*, pp. 145-153.

Meriam, J. L., 1978, *Engineering Mechanics Volume 1, STATICS*, J. Wiley & Sons, pp. 301-302.

Mettlach, G. A., and Midha, A., 1995, "Four-Precision-Point-Synthesis of Compliant Mechanisms using Burmester Theory," *Proceedings of the 4th National Applied Mechanisms and Robotics Conference*, Vol. II, Cincinnati, Ohio, pp. 63-01 - 63-08.

Mettlach, G. A., 1996, "Analysis and Design of Compliant Mechanisms using Analytical and Graphical Techniques," Ph.D. Dissertation, Purdue University.

Mettlach, G.A., and Midha, A., 1999, "Characteristic Deflection Domain Concept in Compliant Mechanism Design and Analysis," *Proceedings of the 6th National Applied Mechanisms and Robotics Conference,* Cincinnati, Ohio, pp. 27-1 – 27-6.

Midha, A., Her, I., and Salamon, B.A., 1992, "A Methodology for Compliant Mechanisms Design: Part I – Introduction and Large Deflection Analysis," *Advances in Design Automation,* (Ed.: D.A. Hoeltzel), DE-Vol. 44-2, 18th ASME Design Automation Conference, pp. 29-38.

Midha, A., Her, I., and Salamon, B.A., 1992a, "On the Nomenclature and Classification of Compliant Mechanisms: The Components of Mechanisms," *Flexible Mechanisms, Dynamics and Analysis*, (Eds.: G. Kinzel et al.), DE-Vol. 47, 22nd Biennial ASME Mechanisms Conference, pp. 237-245.

Midha, A., Her, I., and Salamon, B.A., 1992b, "On the Nomenclature and Classification of Compliant Mechanisms: Abstractions of Mechanisms, and Mechanism Synthesis Problems," *Flexible Mechanisms, Dynamics and Analysis*, (Eds.: G. Kinzel et al.), DE-Vol. 47, 22nd Biennial ASME Mechanisms Conference, pp. 222-235.

Midha, A., Norton T. W. and Howell, L. L. 1994 "On the Nomenclature, Classification, and Abstractions of Compliant Mechanisms," *Journal of Mechanisms, Transmissions, and Automation in Design*, Trans. ASME, Vol. 116, No. 1, pp. 270-279.

Midha, A., Christensen, M. N., and Erickson, M. J., 1997, "On the Enumeration and Synthesis of Compliant Mechanisms using Pseudo-Rigid-Body Four-Bar Mechanism," *Proceedings of the 5th National Applied Mechanisms & Robotics Conference,* Vol. 2, Cincinnati, Ohio, pp. 93-01 - 93-08.

Midha, A., Howell, L. L., and Norton T. W.2000 "Limit Positions of Compliant Mechanisms Using the Pseudo-Rigid-Body-Model Concept," *Mechanism and Machine Theory,* Vol. 35, No. 1, pp. 99-115.

Midha, A., Annamalai, Y., and Kolachalam, S. K., 2004, "A Compliant Mechanism Design Methodology for Coupled and Uncoupled Systems, and Governing Free Choice Selection Considerations" *Proceedings of DETC'04 ASME Design Engineering Technical Conferences and Computers and Information in Engineering Conference*, Salt Lake City, Utah, pp. 57579-1-9.

Midha, A., Kolachalam, S. K., and Annamalai, Y., 2011, "On the Classification of Compliant Mechanisms and Synthesis Compliant of Single-Strip Mechanisms" *Proceedings of the ASME 2011 International Design Engineering Technical Conferences & Computers and Information in Engineering Conference,* Washington, DC pp. 71400-1-10.

Midha, A., Bapat, S., Mavanthoor, A., and Chinta V., 2012, "Analysis of a Fixed-Guided Compliant Beam with an Inflection Point Using the Pseudo-Rigid-Body Model (PRBM) Concept," *Proceedings of the ASME 2012 International Design Engineering Technical Conferences & Computers and Information in Engineering Conference,* Chicago, IL, pp. 71400-1-10

Miller, R.E., 1980, "Numerical Analysis of a Generalized Plane Elastica," *International Journal for Numerical Methods in Engineering,* Vol. 15, pp. 325-332.

Murphy, M.D., 1993, "A Generalized Theory for the Type Synthesis and Design of Compliant Mechanisms," Ph.D. Dissertation, Purdue University.

Murphy, M. D., Midha, A., and Howell, L. L., 1994, "The Topological Synthesis of Compliant Mechanisms," *Machine Elements and machine Dynamics: Proceedings of the 1994 ASME Mechanisms Conference*, DE-Vol. 71, pp. 475-479.

Nocedal, J., Wright S.J., 2006, *Numerical Optimization*, Second Edition, Springer Science + Business Media, LLC, New York.

Norton, R. L., 1999, *Design of Machinery*, McGraw-Hill, Boston, Massachusetts.

Norton, T.W., 1991, “On the Nomenclature, Classification, and Mobility of Compliant Mechanisms,” M.S. Thesis, Purdue University.

Norton, T. W., Howell, L. L., and Midha, A., 1993, "On the Graphical Synthesis Techniques for Planar Four-Bar Mechanisms: Limit Positions and High Performance,' Section 4.5, *Modern Kinematics: Developments in the Last Forty Years,* (Ed.: A. G. Erdman), John Wiley and Sons, Inc, New York, New York.

Pauly, J., 2002, "Analysis of Compliant Mechanisms with Complex-Shaped Segments," M.S. Thesis, University of Missouri - Rolla.

Rao, S. S., *Engineering Optimization: Theory and Practice*, John Wiley and Sons, Inc., Fourth Edition, New Jersey.

Saggere, L., and Kota, S., 2001, "Synthesis of Planar, Compliant Four-Bar Mechanisms for Compliant-Segment Motion Generation," *Journal of Mechanisms, Transmissions, and Automation in Design*, Trans. ASME, Vol. 123, No. 4, pp. 535-541.

Sandor, G.N., and Erdman, A.G., 1984, *Mechanism Design: Analysis and Synthesis*, Vol. 2, Prentice Hall, Upper Saddle River, NJ.

Sevak, N. M., and McLarnan, C. W., 1974, "Optimal Synthesis of Flexible Link Mechanisms with Large Static Deflections," *Journal of Engineering for Industry*, Trans. ASME, Vol.97,No. 2, pp. 520-526.

Shoup, T.E., and Mclarnan, C.W. 1971, “On the Use of the Undulating Elastica for the Analysis of Flexible Link Devices,” *Journal of Engineering for Industry*, Trans. ASME, pp. 263-267.

Shoup, T.E., 1972, “On the Use of Nodal Elastica for the Analysis of Flexible Link Devices,” *Journal of Engineering Industry*, Trans. ASME, Vol. 94, No. 3, pp. 871-875.

Su, H-J., and McCarthy, J. M., 2007, "Synthesis of Bistable Compliant Four-Bar Mechanisms Using Polynomial Homotopy," *Journal of Mechanisms, Transmissions, and Automation in Design*, Trans. ASME, Vol. 129, No.10, pp. 1094-1098.

Tari, H., and Su H-J., 2011, "A Complex Solution Framework for the Kinetostatic Synthesis of a Compliant Four-Bar Mechanism," *Mechanism and Machine Theory*, Vol. 46, pp. 1137-1152.

Zhang, A., and Chen, G., 2012, "A Comprehensive Elliptic Integral Solution to the Large Deflection Problem in Compliant Mechanisms," *Proceedings of the ASME 2012 International Design Engineering Technical Conferences & Computers and Information in Engineering Conference*, August 12-15, 2012, Chicago, pp. 70239-1-10.

APPENDIX A

RELATIVE ERROR CALCULATION

The errors in the coupler point displacement are calculated using the relative error formula used to calculate relative error in deflection obtained using PRBM and elliptic integrals (Howell, 2001). Figure A.1 shows the approach used to calculate the relative error.

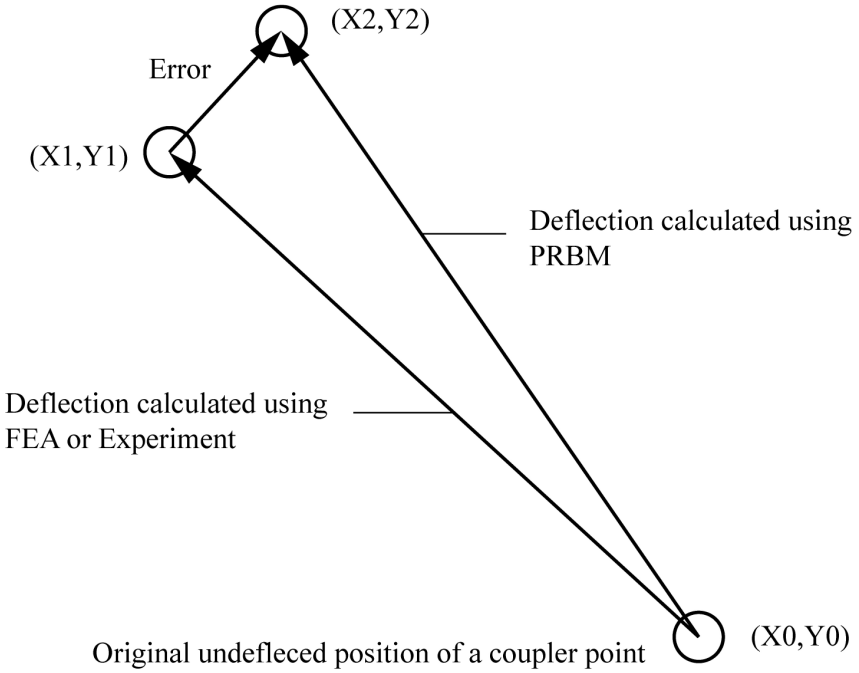

Figure A.1. Calculation of Relative Error in Coupler Point Displacement

Relative error is calculated as

$$\text{Relative Error} = \frac{\sqrt{((X2 - X1)^2 + (Y2 - Y1)^2)}}{\sqrt{((X2 - X0)^2 + (Y2 - Y0)^2)}}$$

APPENDIX B

MATLAB® CODES

MATLAB® Code for Rigid Body Synthesis:

Main function:

```
clc;clear all;

%Initial Estimates
y0=[37*(pi/180),24*(pi/180),45*(pi/180),2*(pi/180),6*(pi/180),10*(pi/18
0),19*(pi/180),94*(pi/180)];

options=optimset('display','iter');
options.MaxFunEvals=100000;
options.MaxIter = 4000;
y=fsolve(@myfun,y0);

theta31=y(1); ph2=y(2); ph3=y(3); gamma2=y(4); gamma3=y(5);  ps2=y(6);
ps3=y(7); theta41=y(8);

%Given
Redelta2=-0.5; Imgdelta2=0; Redelta3=-1; Imgdelta3=0;

% Free Choices
theta21=100*(pi/180); R2=1;

% Loop-closure Equations

f(1)=2.5*R2*(cos(theta31+gamma2)-
cos(theta31))+2.5*R2*(cos(theta31+gamma2)-
cos(theta31))+R2*(cos(theta21+ph2)-cos(theta21))-Redelta2;
f(2)=2.5*R2*(sin(theta31+gamma2)-
sin(theta31))+2.5*R2*(sin(theta31+gamma2)-
sin(theta31))+R2*(sin(theta21+ph2)-sin(theta21))-Imgdelta2;
f(3)=2.5*R2*(cos(theta31+gamma2)-
cos(theta31))+2.5*R2*(cos(theta41+ps2)-cos(theta41))-Redelta2;
f(4)=2.5*R2*(sin(theta31+gamma2)-
sin(theta31))+2.5*R2*(sin(theta41+ps2)-sin(theta41))-Imgdelta2;
f(5)=2.5*R2*(cos(theta31+gamma3)-
cos(theta31))+2.5*R2*(cos(theta31+gamma3)-
cos(theta31))+R2*(cos(theta21+ph3)-cos(theta21))-Redelta3;
f(6)=2.5*R2*(sin(theta31+gamma3)-
sin(theta31))+2.5*R2*(sin(theta31+gamma3)-
sin(theta31))+R2*(sin(theta21+ph3)-sin(theta21))-Imgdelta3;
f(7)=2.5*R2*(cos(theta31+gamma3)-
cos(theta31))+2.5*R2*(cos(theta41+ps3)-cos(theta41))-Redelta3;
f(8)=2.5*R2*(sin(theta31+gamma3)-
sin(theta31))+2.5*R2*(sin(theta41+ps3)-sin(theta41))-Imgdelta3;
```

Objective function:

```
function f=myfun(y)

theta31=y(1); ph2=y(2); ph3=y(3); gamma2=y(4); gamma3=y(5);  ps2=y(6);
ps3=y(7); theta41=y(8);

%Given
Redelta2=-0.5; Imgdelta2=0; Redelta3=-1; Imgdelta3=0;

% Free Choices
theta21=100*(pi/180); R2=1;

%Loop Closure Eqautions
f(1)=2.5*R2*(cos(theta31+gamma2)-
cos(theta31))+2.5*R2*(cos(theta31+gamma2)-
cos(theta31))+R2*(cos(theta21+ph2)-cos(theta21))-Redelta2;
f(2)=2.5*R2*(sin(theta31+gamma2)-
sin(theta31))+2.5*R2*(sin(theta31+gamma2)-
sin(theta31))+R2*(sin(theta21+ph2)-sin(theta21))-Imgdelta2;
f(3)=2.5*R2*(cos(theta31+gamma2)-
cos(theta31))+2.5*R2*(cos(theta41+ps2)-cos(theta41))-Redelta2;
f(4)=2.5*R2*(sin(theta31+gamma2)-
sin(theta31))+2.5*R2*(sin(theta41+ps2)-sin(theta41))-Imgdelta2;
f(5)=2.5*R2*(cos(theta31+gamma3)-
cos(theta31))+2.5*R2*(cos(theta31+gamma3)-
cos(theta31))+R2*(cos(theta21+ph3)-cos(theta21))-Redelta3;
f(6)=2.5*R2*(sin(theta31+gamma3)-
sin(theta31))+2.5*R2*(sin(theta31+gamma3)-
sin(theta31))+R2*(sin(theta21+ph3)-sin(theta21))-Imgdelta3;
f(7)=2.5*R2*(cos(theta31+gamma3)-
cos(theta31))+2.5*R2*(cos(theta41+ps3)-cos(theta41))-Redelta3;
f(8)=2.5*R2*(sin(theta31+gamma3)-
sin(theta31))+2.5*R2*(sin(theta41+ps3)-sin(theta41))-Imgdelta3;
end
```

MATLAB® Code for Energy Free State Loop-Closure Equations:

Main function:

```
clc;clear all;
% Initial Estimates
y0=[50*(pi/180),125*(pi/180)];
y=fsolve('myfun',y0);

theta30=y(1); theta40=y(2);
%Results from Rigid Body Synthesis
R1=2; R2=1; R3=2.5; R4=2.5;
theta10=0*(pi/180);

%Free Choice
theta20=70*(pi/180);
```

```
% Energy Free State Loop-Closure equations
f(1)=R1*cos(theta10)+R4*cos(theta40)-R3*cos(theta30)-R2*cos(theta20);
f(2)=R1*sin(theta10)+R4*sin(theta40)-R3*sin(theta30)-R2*sin(theta20);

Objective function:

function f=myfun(y)

theta30=y(1); theta40=y(2);

%Results from Rigid Body Synthesis
R1=2; R2=1; R3=2.5; R4=2.5;
theta10=0*(pi/180);

%Free Choice
theta20=70*(pi/180);

% Energy Free State Loop-Closure equations
f(1)=R1*cos(theta10)+R4*cos(theta40)-R3*cos(theta30)-R2*cos(theta20);
f(2)=R1*sin(theta10)+R4*sin(theta40)-R3*sin(theta30)-R2*sin(theta20);
```

MATLAB® Code for Energy Equations using Optimization:

Main function:

```
clear all; clc;
%*********************************************************************
*

x0=[60;60]; %Initial values
lb=[10,10,10,10]; % lower bounds
ub=[]; % upper bounds
options=optimset('display','iter');

options.MaxFunEvals=100000;
options.MaxIter = 4000;
%options = optimset(options,'Algorithm','interior-point');
x=fmincon(@objfun,x0,[],[],[],[],lb,ub,@confuneq,options); %
Optimization function

% Evaluation of K values
K3=x(1); K4=x(2);

% Evaluation of Objective Function
%R1=2; R2=1; R3=2.5; R4=2.5;
%theta10=0*(pi/180);theta20=70;
theta30=38.052; theta40=82.862;
%theta21=90;
theta31=36.869; theta41=90;
%phi2=90; phi3=170;
```

```
tsai2=36.869; tsai3=53.130; gamma2=16.26; gamma3=53.130;

%theta22=theta21+phi2; theta23=theta21+phi3;
theta32=theta31+gamma2; theta33=theta31+gamma3;
theta42=theta41+tsai2; theta43=theta41+tsai3;

%b10=theta20; b20=180-(theta20-theta30);
b30=theta40-theta30; b40=theta40;
%b11=theta21; b21=180-(theta21-theta31);
b31=theta41-theta31; b41=theta41;
%b12=theta22; b22=180-(theta22-theta32);
b32=theta42-theta32; b42=theta42;
%b13=theta23; b23=180-(theta23-theta33);
b33=theta43-theta33; b43=theta43;

%db11=(b11-b10)*pi/180; db21=(b21-b20)*pi/180;
db31=(b31-b30)*pi/180; db41=(b41-b40)*pi/180;
%db12=(b12-b10)*pi/180; db22=(b22-b20)*pi/180;
db32=(b32-b30)*pi/180; db42=(b42-b40)*pi/180;
%db13=(b13-b10)*pi/180; db23=(b23-b20)*pi/180;
db33=(b33-b30)*pi/180; db43=(b43-b40)*pi/180;

E1=2.15; E2=49.5; E3=66.1;
fn=(E1-(1/2*K3*db31^2+1/2*K4*db41^2))^2+(E2-
(1/2*K3*db32^2+1/2*K4*db42^2))^2+(E3-(1/2*K3*db33^2+1/2*K4*db43^2))^2;
%Displaying Solution
disp('*****************************************************');
disp('Solution is');disp(x');
disp('Function value at the solution');disp(fn);
disp('*****************************************************');
```

Objective function

```
function fn= objfun(x)
K3=x(1); K4=x(2);

%Objective Function
%R1=2; R2=1; R3=2.5; R4=2.5;
%theta10=0*(pi/180); theta20=70;
theta30=38.052; theta40=82.862;
%theta21=90;
theta31=36.869; theta41=90;
%phi2=90; phi3=170;
tsai2=36.869; tsai3=53.130; gamma2=16.26; gamma3=53.130;

%theta22=theta21+phi2; theta23=theta21+phi3;
theta32=theta31+gamma2; theta33=theta31+gamma3;
theta42=theta41+tsai2; theta43=theta41+tsai3;

%b10=theta20; b20=180-(theta20-theta30);
b30=theta40-theta30; b40=theta40;
%b11=theta21; b21=180-(theta21-theta31);
b31=theta41-theta31; b41=theta41;
```

```
%b12=theta22; b22=180-(theta22-theta32);
b32=theta42-theta32; b42=theta42;
%b13=theta23; b23=180-(theta23-theta33);
b33=theta43-theta33; b43=theta43;

%db11=(b11-b10)*pi/180; db21=(b21-b20)*pi/180;
db31=(b31-b30)*pi/180; db41=(b41-b40)*pi/180;
%db12=(b12-b10)*pi/180; db22=(b22-b20)*pi/180;
db32=(b32-b30)*pi/180; db42=(b42-b40)*pi/180;
%db13=(b13-b10)*pi/180; db23=(b23-b20)*pi/180;
db33=(b33-b30)*pi/180; db43=(b43-b40)*pi/180;

E1=2.15; E2=49.5; E3=64.1;  % Energy values should be co-related with
the PRBM angles
fn=(E1-(1/2*K3*db31^2+1/2*K4*db41^2))^2+(E2-
(1/2*K3*db32^2+1/2*K4*db42^2))^2+(E3-(1/2*K3*db33^2+1/2*K4*db43^2))^2;
```

Constraint function

```
function [c,ceq]= confuneq(x)
K3=x(1); K4=x(2);
c =[];
ceq=[K3-K4];
```

VITA

Ashish Bharat Koli was born in 1987 in India. He received his Bachelor's degree in Mechanical Engineering from Walchand College of Engineering in Sangli, India, in June 2008. After undergraduate school, he worked in Hindustan Petroleum Corporation Ltd. for two years. He was admitted to a Master of Science degree program in Mechanical Engineering at Missouri University of Science and Technology, Rolla, MO, in the Fall semester, 2010, and graduated in May 2013.